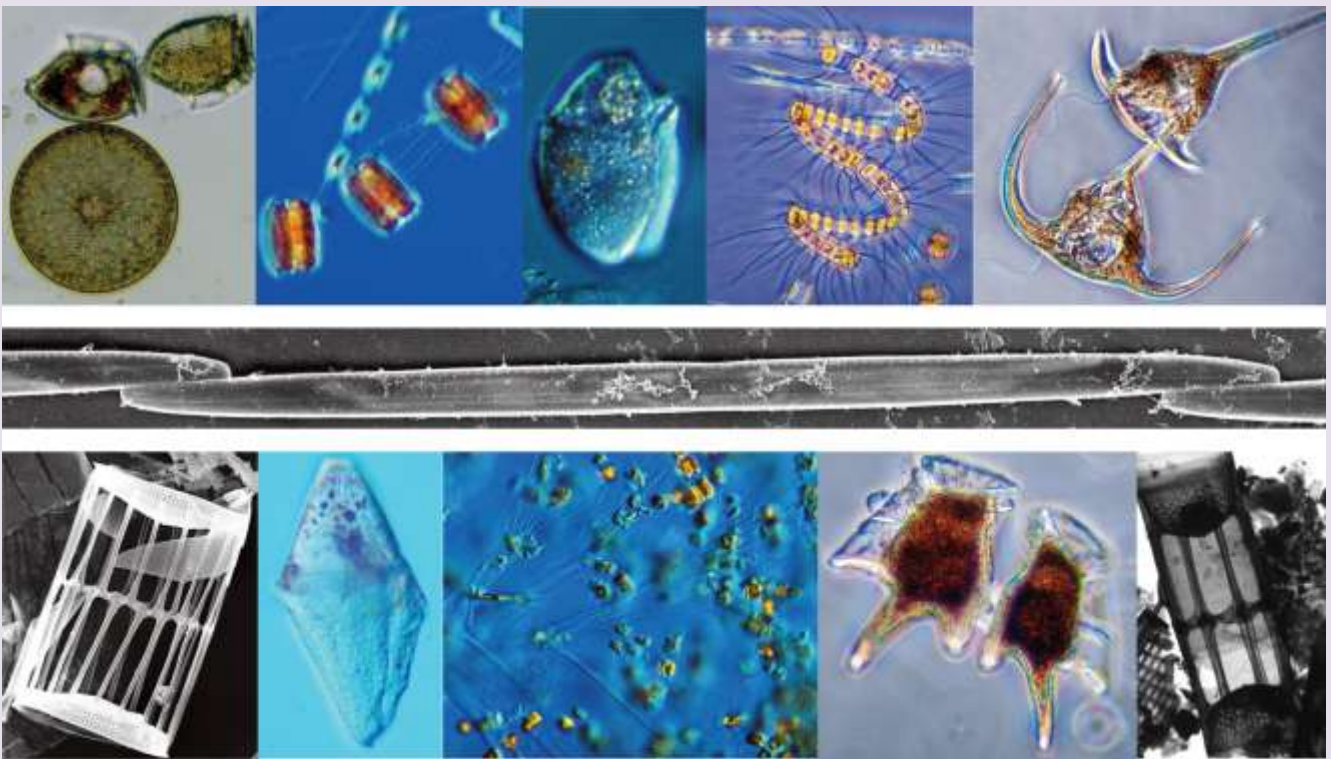


Seasonal Cycle of Phytoplankton in Outer Oslofjorden with Emphasis on *Pseudo-nitzschia* Species

Vladyslava Hostyeva



Master Thesis in Marine Biology

Department of Biology



UNIVERSITY OF OSLO

Spring 2011

Denne oppgaven er gjennomført i perioden 2009-2011 ved Biologisk institutt, Universitet i Oslo. Oppgaven ble til under hoved-veiledning av Wenche Eikrem og med-veiledning av Bente Edvardsen.

Jeg vil gjerne få takke mine veiledere, **Wenche** og **Bente**, for kompetente råd, oppmuntrende støtte, toleranse og mulighet til faglig utvikling. Wenche for at jeg fikk mulighet til å være med til Kreta og delta i ICHA konferansen, det var uforglemmelig ☺!

Mange personer har bidratt til arbeidet med denne masteroppgaven og jeg ønsker å takke alle de som frivillig og ufrivillig har bidratt til å virkeliggjøre denne oppgaven:

- ✓ Elliane Egge, Simone Dittami og Andrea Gerecht
- ✓ Rita Amundsen og Sissel Irene Brubak
- ✓ Mannskapet på R/V "Trygve Braarud"
- ✓ Grethe R. Hasle, Jahn Throndsen, Tom Andersen, Nina Lundholm og Lars Edler

Hvert og ett av bidragene har styrket kvaliteten i forskningen og gjort denne utfordrende prosessen lettere for meg.

Videre ønsker jeg å takke mine venner. En siste, men ikke minste, takk til mine foreldre: *Огромное спасибо за поддержку и безграничную помощь, внимание и терпение, любовь и заботу! Спасибо вам, мои дорогие!*

My dear Begi, thank you for your unconditional love and moral support...

Abstract

Seasonal dynamics and composition of the phytoplankton community, with a special emphasis on *Pseudo-nitzschia* species were studied during the period June 2009-June 2010. Samples were collected monthly at station OF2 (59.18N, 10.69E) located in the outer part of Oslofjorden. Vertical net hauls (17-0 m) and surface seawater (1 m) were collected and hydrographical (light, temperature, salinity, density) and chlorophyll (*in vivo* and *in vitro*) measurements were carried out. Bottle samples from the surface water layer were analysed using the Uthermöhl method for quantitative evaluations of the phytoplankton community. Live and preserved vertical net hauls were analysed qualitatively in light microscopy (LM). In addition scanning (SEM) and transmission (TEM) electron microscopy of acid cleaned vertical net hauls were carried out to identify *Pseudo-nitzschia* species

The outer part of Oslofjorden is known as a heterogeneous area with regards to phytoplankton and hydrographical conditions. During the sampling year, the hydrographical and biological data showed seasonal diversity in accordance with previously reported trends. Several seasonal peaks of phytoplankton with maximum concentrations of 1.15×10^6 cells L⁻¹, 1.29×10^6 cells L⁻¹, and 3.78×10^6 cells L⁻¹, were recorded in June 2009, September 2009 and January 2010, respectively.

During the sampling year, more than 88 taxa of planktonic organisms were identified and enumerated. In terms of individual phytoplankton taxa, the most common bloom-forming diatoms included: *Chaetoceros* spp., *Skeletonema* spp., *Leptocylindrus* spp., *Dactyliosolen fragilissimus*, *Proboscia alata*, *Pseudo-nitzschia* spp., *Rhizosolenia* spp. and *Thalassionema nitzschoides*. The dinoflagellate taxa dominated during the spring/summer of 2010 included: *Ceratium* spp., *Dinophysis* spp., *Protoperidinium* spp. and small unidentified dinoflagellates. Among other phytoplankton, the most common taxa were *Eutreptiella* spp., *Dinobryon* sp., *Dictyocha speculum* and small unidentified monads.

Analysis of the phytoplankton community showed that most of the identified species are common in Outer Oslofjorden, except *Prorocentrum gracile*, *Dinophysis tripos*, *Dinophysis odiosa*, *Pseudo-nitzschia pseudodelicatissima*, and *P. cf. cuspidata*.

The succession of *Pseudo-nitzschia* species was recorded in live and preserved material using LM, SEM, and TEM. Morphological features were analysed and compared with data available in the literature. Earlier investigations from Norwegian waters have shown a considerable variation in the species composition of the genus, both geographically and seasonally.

Pseudo-nitzschia species were present in every sample collected during the year. In general, occurrence and diversity of *Pseudo-nitzschia* species varied through the seasons, with a more or less gradual increase from June 2009 until January 2010 followed by a subsequent decrease. The highest concentration of *Pseudo-nitzschia* spp. was recorded in January 2010 with 1.61×10^6 cells L⁻¹. A total of ten species were observed, nine of them were identified: *P. delicatissima*, *P. calliantha*, *P. cf. cuspidata*, *P. pseudodelicatissima*, *P. fraudulenta*, *P. pungens*, *P. multiseriata*, *P. seriata*, and *P. americana*. Previously reported *Pseudo-nitzschia heimii* was not observed in the present study, while *P. pseudodelicatissima* and *P. cf. cuspidata* were recorded for the first time. *Pseudo-nitzschia calliantha* and *P. delicatissima* were the most frequently observed and present in 9 out of 11 samples.

Of the 9 *Pseudo-nitzschia* species identified in the present study 8 are potentially toxic: *Pseudo-nitzschia delicatissima*, *P. pseudodelicatissima*, *P. calliantha*, *P. cf. cuspidata*, *P. pungens*, *P. multiseriata*, *P. fraudulenta*, and *P. seriata*. Potentially toxic *Pseudo-nitzschia* species were observed in all samples examined. The ability to produce domoic acid varies between *Pseudo-nitzschia* species, thus a precise identification and knowledge about their geographical and seasonal occurrence at the species level is important to early warning systems serving the aquaculture industry.

Table of Contents

| | | |
|----------|---|-----------|
| 1 | Introduction..... | 1 |
| 1.1 | Outer Oslofjorden and Skagerrak: physical conditions and water properties | 1 |
| 1.2 | Phytoplankton seasonal cycle | 4 |
| 1.3 | Genus <i>Pseudo-nitzschia</i> | 7 |
| 1.3.1 | Taxonomy and morphological features | 7 |
| 1.3.2 | Distribution and toxicity of <i>Pseudo-nitzschia</i> | 10 |
| 1.4 | Background, aims, and questions | 12 |
| 2 | Materials and Methods | 14 |
| 2.1 | Study area and sampling | 14 |
| 2.2 | Physical and chemical conditions | 15 |
| 2.2.1 | Hydrography and fluorescence <i>in vivo</i> | 15 |
| 2.2.2 | Irradiance | 15 |
| 2.2.3 | Chlorophyll <i>a in vitro</i> | 16 |
| 2.3 | Phytoplankton material..... | 16 |
| 2.3.1 | Qualitative examination | 17 |
| 2.3.2 | Quantitative examination | 17 |
| 2.3.3 | Species identification | 18 |
| 2.4 | Preparation of <i>Pseudo-nitzschia</i> for electron microscopy | 19 |
| 2.4.1 | Scanning electron microscopy (SEM) | 19 |
| 2.4.2 | Transmission electron microscopy (TEM) | 19 |
| 2.5 | Statistical approach | 20 |
| 3 | Results | 21 |
| 3.1 | Hydrographical conditions..... | 21 |
| 3.1.1 | Physical parameters | 21 |
| 3.1.1 | Temporal variability in chlorophyll <i>a</i> | 26 |
| 3.2 | Phytoplankton composition and seasonality | 26 |

| | | |
|----------|--|-----------|
| 3.2.1 | Total phytoplankton composition..... | 27 |
| 3.2.2 | Species composition and seasonal occurrence | 29 |
| 3.3 | Abundance of phytoplankton species in the surface layer..... | 38 |
| 3.3.1 | Cell counts | 38 |
| 3.3.2 | Species diversity | 43 |
| 3.4 | <i>Pseudo-nitzschia</i> species..... | 47 |
| 3.4.1 | Species composition and seasonal occurrence | 47 |
| 3.4.2 | Morphology | 48 |
| 4 | Discussion..... | 72 |
| 4.1 | Evaluation of methods and materials..... | 72 |
| 4.2 | Phytoplankton seasonal cycle..... | 74 |
| 4.3 | Genus <i>Pseudo-nitzschia</i> | 77 |
| 4.3.1 | Identification and morphology..... | 77 |
| 4.3.2 | Seasonal cycle | 82 |
| 4.4 | Conclusions..... | 85 |
| | Appendix..... | 87 |
| | Reference list | 93 |

1 Introduction

1.1 Outer Oslofjorden and Skagerrak: physical conditions and water properties

Topographically, the 100 kilometres long Oslofjorden can be subdivided into an inner, middle, and outer part, separated from each other by a sill (Alve and Nagy 1990). The outer part of Oslofjorden is located south of the 17 kilometres long and 1 kilometre narrow Drøbaksundet (with a threshold depth of 19 meters). It stretches down to Færder fyr and west to Tjøme; at Fulehuk-Missingen it has a topographical border with the inner part of the Skagerrak. The depth in the outer part of Oslofjorden ranges from 200 to 350 meters, while the greatest depth in the Skagerrak is about 700 meters. The boundary between the Skagerrak and the main part of the North Sea runs from Hanstholm on Jutland, the west coast of Denmark, to Lindenes, on the south coast of Norway (Anon. 1993).

From the North Sea and the Kattegat, water bodies of different origin enter the Outer Oslofjorden through the Skagerrak, influencing the area by transporting waters with different levels of salinity, temperature, and nutrients (Sætre 2007). These water masses can be separated into different surface currents according to their path through the North Sea to the Skagerrak and according to their dilutions by fresh water from different sources (Baalsrud and Magnusson 2002). The simplified patterns of the main surface currents in the North Sea and adjacent waters are shown in Figure 1.1.

On the way from Florida towards the north, the Gulf Stream (or the North Atlantic Current) passes the British Islands and from the Norwegian Sea it sends a small branch of Atlantic Water to the North Sea. The Atlantic Water, which is mainly forced into the North Sea by wind and differences in air pressure, transports warm water masses with salinity above 35 psu at a depth of ca. 70 m. At the north-west coast of Denmark, the

North Atlantic Current meets the Jutland Current which, flowing from the German Bight, transports water masses from the English Channel and the west coast of Jutland. These two currents unite and continue transporting water masses with salinity of 32-35 psu at approximately 30m depth. Another branch of the Jutland Current flows eastwards along the northern coast of Denmark, and meets the Baltic Current in the northern Kattegat. The Baltic Current carries brackish water from the Baltic Sea through the Kattegat where it forms a surface layer less than 20 m deep and with a salinity of 25-32 psu. Then the mixture of these currents moves northwards along the Swedish west coast. In the eastern Skagerrak they meet the water from the central and southern North Sea and continue westwards as the Norwegian Coastal Current (NCC).

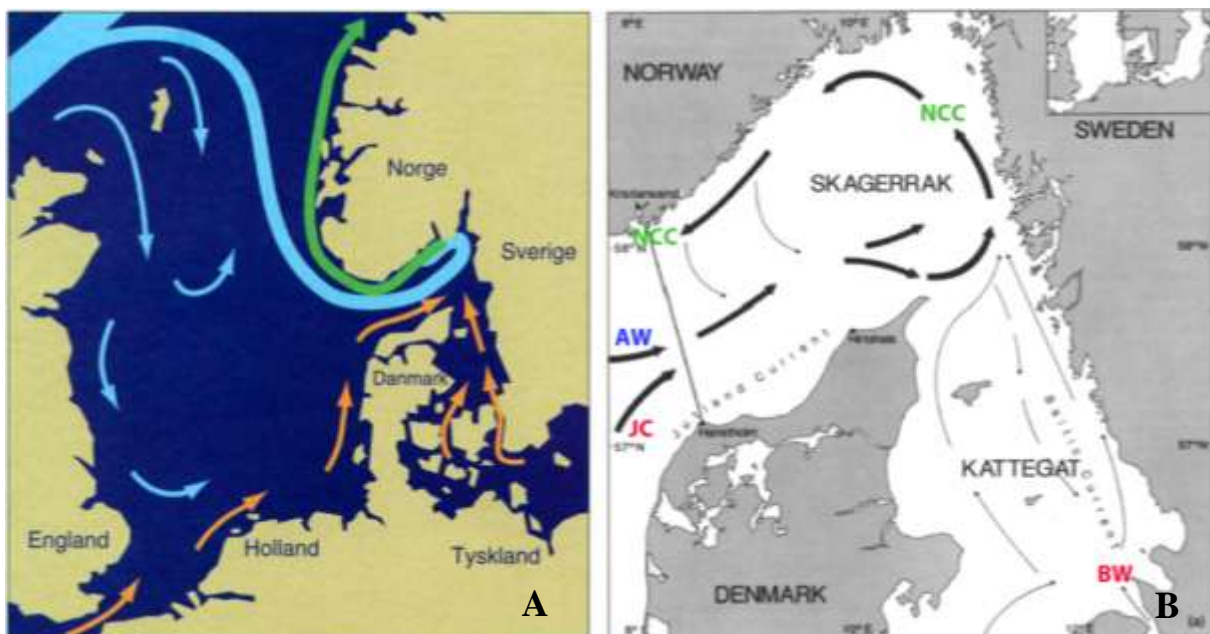


Figure 1.1: Surface circulations in the North Sea (A) and adjacent area (B); fig. 1.1 A modified from Baalsrud and Magnusson, 2002 (The Atlantic Waters: blue arrows, AW; The Jutland Current: red arrow, JC; The Baltic Waters: red arrow, BW; The Norwegian Coastal Current: green arrow, NCC); fig. 1.1 B from Svanson, 1975.

The Atlantic Water and the Norwegian Coastal Water are the two dominant water masses in the Skagerrak and along the Norwegian coast. A number of factors may influence the general circulation patterns and physicochemical properties of the coastal water masses; these include the input of freshwater and Atlantic water, tidal forces, and wind conditions (Sætre 2007). The NCC is driven by its density structure and originates primarily from local freshwater runoff and brackish water from the Baltic Sea; it

gradually increases in salinity and its stratification decreases as it mixes with Atlantic Water. While the current system in the North Sea is controlled mainly by tides, water circulation in the Skagerrak is mostly determined by meteorological forces and the outflow of the Baltic Sea. Winds from the east accelerate and force the NCC closer to the southern Norwegian coast, whereas winds from the west slow the NCC down and force it off the coast. As a result, these forces create the wind-driven anticlockwise recirculation in the upper layers of the Skagerrak (Aure 1979) (Figure 1.1B). The anticlockwise circulation favours upwelling of deeper, nutrient-rich water in the central part of the Skagerrak (Svansson 1975), a process of great importance for the primary productivity of this area.

The stratification in the northern Skagerrak is mainly influenced by freshwater, the latter creating a surface layer that is much less saline than the underlying Atlantic Waters. According to Sætre (2007), the Skagerrak area on average receives approximately 2,100 m³/s of freshwater, of which nearly 75% can be accounted for by the Baltic outflow, 15% come from the North Sea, and 10% are coastal runoff from Sweden and Norway. Although the outflow from the Baltic Sea is a dominant contributor to the NCC formation and a major source of freshwater, it does not account for most of the nutrients found in Norwegian coastal waters. The nutrient-enriched waters are transported into the Skagerrak mostly by the Jutland Current, which on the way mixes with water masses from the central and southern parts of the North Sea.

A large part of southern Norway is drained via the outer part of Oslofjorden into the Skagerrak. The water masses of Oslofjorden have an estuarine distribution pattern: brackish water from coastal runoff flows out as a surface current, and an underlying counter-current of inflowing saline water flows into the fjord. The deeper water layers are quite stable and uniform, with salinities ranging from 33 to 34 psu. In the inner part of Oslofjorden, the estuarine circulation is often restricted to the upper layers of the water column. From previous observations it is known that in the inner Oslofjorden water masses are more or less stagnant and separated from the central and outer parts of the fjord (Gade 1968). In the Outer Oslofjorden, as well as in the northern Skagerrak, the stratification level is controlled by the discharge of the rivers Skienselva, Glomma and the brackish water supplied by the Göta River and the Baltic current. The fresh

water discharge has a seasonal character with a peak in spring-summer. As reported by Aure et al. (2010), in the winter-spring time the waters from the German Bight are the main source of nutrient supply in Outer Oslofjorden (Aure et al. 2010). In the summer period, however, the dominant contributors of nutrients are local sources. In addition to their strong impact on abiotic factors within Oslofjorden (most importantly nutrients), river discharge and ocean currents may import characteristic phytoplankton species. As an example, the Jutland Current carries large numbers of marine diatoms into the Skagerrak, while the less saline Baltic Current carries brackish water species into the Kattegat (Hui 1996).

1.2 Phytoplankton seasonal cycle

The composition of phytoplankton species in Norwegian coastal waters has been examined in several taxonomic studies and field surveys over more than a century. As a result, a number of species from various algal groups were originally described from these waters. In regard to species composition the Norwegian coastal waters are heterogeneous. In fact, more than 700 species from different algal groups can be found (Thronsen et al. 2007). The phytoplankton community of the Skagerrak area is rich in species due to the supply of water from the Baltic and Atlantic regions. According to “Checklist of phytoplankton in the Skagerrak-Kattegat” (see http://www.smhi.se/oceanografi/oce_info_data/plankton_checklist/ssshome.htm), the Skagerrak alone was found to be the home of 58 species of diatoms, 152 species of dinoflagellates, and 291 species belonging to the other algal groups (haptophytes, cryptophytes, chlorophytes).

Numerous studies have been carried out on the succession of phytoplankton in the North Sea, the Skagerrak, and Oslofjorden. The phytoplankton community of the Inner Oslofjorden was thoroughly studied in the 1930s by Braarud and Bursa, in the 1960s by Hasle and Smayda, Braarud and Nygaard, and in the 1980s by Paasche and Østergren. In the North Sea and adjacent waters, major investigations were made by Braarud and co-workers in 1948 (Braarud et al. 1953). Since then, a number of monitoring programs have been carried out in the area by the Norwegian Institute for Water Research,

Institute of Marine Research, Skagerrak Forum, a.o. (see <http://algeinfo.imr.no/>, <http://www.smhi.se>, <http://www.bvvf.se>).

The previous investigations have shown that the phytoplankton production in the area is subject to seasonal variations and that several factors may influence plankton growth and abundance. In the marine environment the seasonal pattern of freshwater discharge is known to influence both primary production and species composition (Mann and Lazier 1991). The relationship between meteorological conditions (wind) and phytoplankton dynamics in Oslofjorden was described by Braarud (1945) and Wiull (1948) (Braarud 1945; Wiull 1948). According to a survey published by Braarud et al. in 1953, phytoplankton growth is highly dependent on hydrographical and physical conditions, such as temperature, salinity, density, light, and nutrient supply in the water masses. The stability factor plays an important role, which influences the turbulence process and thereby indirectly affects the supply of inorganic nutrients (nitrate, phosphate, and silicate) from the underlying nutrient-rich waters to the euphotic layer. Stratification of the upper layers, either by low salinity or high temperatures (or a combination), and shallow areas are the most important factors in keeping phytoplankton in the upper eutrophic layer, where they receive sufficient light to grow. The same work also followed phytoplankton development in the North Sea and adjacent waters throughout a seasonal cycle, which comprised poor plankton vegetation in the winter months, followed by rapid growth of diatoms in spring (a phenomenon known as the spring diatom bloom) with a succession of *Thalassiosira-Chaetoceros* species. During the spring months the diatom population gradually decreases, as the nutrient supply is depleted, and dinoflagellates increase in number and become dominant towards the beginning of summer; a second diatom-bloom may occur in the autumn period, as a result of nutrient input due to vertical mixing of water masses.

In the Outer part of Oslofjorden the phytoplankton succession follows the same seasonal cycle, with some events characteristic for this particular area. In the dark winter months, primary production is limited mainly by poor light conditions, and the biomass of phytoplankton consequently is low. At the same time cooling and wind facilitates vertical mixing, leading to an enrichment of the upper layer with essential nutrients. As a result, the first spring-bloom in the outer Oslofjorden may occur already in February-March and is normally dominated by diatoms that are able to multiply rapidly at low

temperatures, such as species of the centric diatom genera *Chaetoceros*, *Thalassiosira*, *Skeletonema*, and *Coscinodiscus*, but flagellates are also common. In April-May, when nutrients are depleted and cell numbers are relatively low, another spring-bloom may occur in the outer Oslofjorden. This second bloom can be initiated by freshwater runoff from land and input from the local Glomma and Drammen rivers, as well as by vertical mixing of unstable waters. Together these factors may lead to the formation of a brackish layer and a renewing of the nutrient supply. At this time of the year, the phytoplankton community can be dominated by a single diatom species. Large inter-annual variations have been observed in this area and spring-bloom initiation may vary from the middle of January to the middle of April. In the following summer months, reduced phytoplankton vegetation can be found in the central parts of Outer Oslofjorden. The water column is highly stratified with a well-defined pycnocline at approximately 10-30 m depth. In summer, the coastal phytoplankton community is rich and variable; the main dominant species are dinoflagellates and other flagellates. Nevertheless, local blooms can sporadically occur in the area. The September-October period is characterized by continuing good light conditions and changes in the stability of the water column. Increasing winds lead to the weakening of the pycnocline and to vertical mixing, resulting in the introduction of new nutrients into the euphotic zone. These processes may initiate an autumn-bloom, which usually is dominated by dinoflagellates of the genera *Ceratium*, *Dinophysis*, and *Proto-peridinium*. Overall, the seasonal bloom patterns exhibit noticeable inter-annual variations, which are largely regulated by variations in meteorological and hydrodynamic processes, as well as by nutrient availability and grazing pressure (Braarud et al. 1953; <http://kvina.niva.no/fryo/Temasider/Planktonalger/tabid/64/Default.aspx>).

Occasionally, among the regular blooms harmful algal blooms (HABs) can occur, which in large concentration may have a negative impact on the environment, as well as human and aquatic animal health. Harmful algae are assumed to be a natural part of the phytoplankton community. Between the 1960s and 1990s, *Karenia mikimotoi* ((Miyake & Kominami ex Oda) G. Hansen & Ø. Moestrup 2000), previously known as *Gyrodinium aureolum* E. M. Hulbert, was one of the most common bloom-forming dinoflagellates in Norwegian and European waters (Jones et al. 1982; Dahl and Yndestad 1985; Gentien 1998). In May-June 1988 a toxic bloom of a nanoflagellate *Chrysochromulina polylepis*

Manton & Parke extended over most parts of the Skagerrak-Kattegat and spread along the Norwegian coast (Underdal et al. 1989). During the last decade several toxic and potentially toxic species (e.g. *Prorocentrum minimum* (Pavillard) J. Schiller 1933; *Chrysochromulina leadbeateri* Estep 1984; *Prymnesium parvum* N. Carter 1937) have made their appearance in Norwegian Coastal Waters (Dahl and Yndestad 1985; Edvardsen 1993; Johnsen et al. 2010). By 1999, the recorded number of potentially harmful algae in Norwegian waters comprised approximately 20-30 different species representing several algal groups including haptophytes, dinoflagellates, diatoms, and dictyochophytes (Tangen and Dahl 1999). The planktonic diatoms that presently have been reported as potentially toxic are all marine species and most of them belong to the genus *Pseudo-nitzschia* H. Peragallo 1900.

1.3 Genus *Pseudo-nitzschia*

1.3.1 Taxonomy and morphological features

The genus *Pseudo-nitzschia* is a genus of marine, pennate diatoms in the class Bacillariophyceae Haeckel 1878, division Ochrophyta Cavalier-Smith 1995. The taxonomic position of the genus was a topic of debate for many decades. The genus *Pseudo-nitzschia* (as *Pseudo-Nitzschia*) was proposed by H. Peragallo (1897-1908) for some species morphologically different from the other members of the genus *Nitzschia* Hassall, 1845. However, because of other “imperfect” morphological features compared to the genus *Fragilariopsis* Hustedt, 1913 (such as a partially reduced raphe and retained capability of movement), Hustedt reduced *Pseudo-nitzschia* to a section of *Nitzschia* in 1958. *Pseudo-nitzschia* was reinstated as a genus by Hasle in 1994, based on specific morphological features of the cells (chains formed colonies with overlapping cell tips, eccentric raphe system) and re-examination of *Nitzschia* and *Pseudo-nitzschia* lectotypes (Hasle 1994). Later, Hasle’s proposal was supported by analysis of the small subunit of rRNA from *Pseudo-nitzschia*, *Nitzschia*, and other diatom species (Douglas et al. 1994).

Pseudo-nitzschia is a relatively small genus of diatoms containing approximately 35 species; many of them share similar morphological features. During the last decade, molecular analyses and sexual compatibility were used to define cryptic, semi-cryptic, and pseudo-cryptic diversity among *Pseudo-nitzschia* species, resulting in the description of several new taxa (Lundholm et al. 2002; Lundholm and Moestrup 2002; Lundholm et al. 2003; Lundholm et al. 2003; Amato and Montresor 2008; Churro et al. 2009; Quijano-Scheggia et al. 2009).

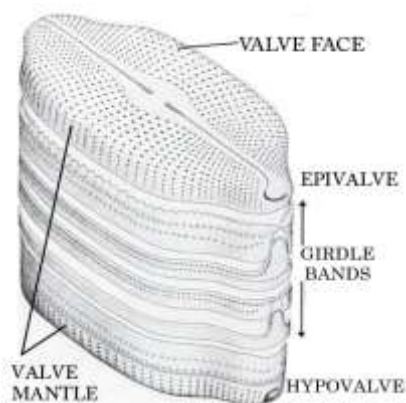


Figure 1.2: Diagram of a pennate diatom cell showing the frustule structure; modified from Round et al. 1980 (Round et al. 1990).

Pseudo-nitzschia cells, like the cells of all diatoms, have a silicified cell wall comprised of two separate valves (epi- and hypotheca) that fit together like a petri dish. The valves include a flat valve face and a sloping mantle. The two valves are combined by several thinner linking elements called cingulum or girdle bands, forming a structure called frustule (Figure 1.2). Cells of pennate diatoms are bilaterally symmetric and can be positioned along three axes: apical (length), pervalvar (height), and transapical (width) (Figure 1.3).

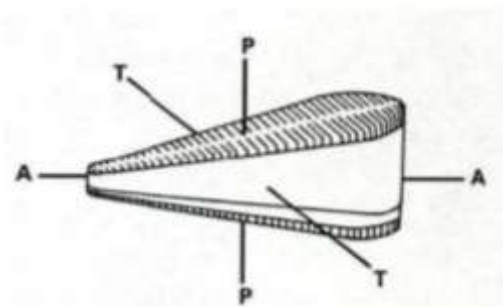


Figure 1.3: Diagram showing axes used in the description of pennate diatoms (AA-apical axis; PP-perivalvar axis; TT-transapical axis); from Throndsen et al. 2007.

Species of *Pseudo-nitzschia* form characteristic stepped colonies with long, needle-shaped cells connected by an overlap (Figure 1.4, A and B). Both single cells and colonies are motile; by excreting a polysaccharide from the raphe slit, they are capable of sliding longitudinally. Each cell has two plate-like chloroplasts, with a typical golden brown colour due to the pigment fucoxanthin, located along the girdle, one in each cell half. Most of the *Pseudo-nitzschia* cells

are strongly elongated, linear to lanceolate in girdle view, mostly linear to lanceolate in valve view (some valves are asymmetric with respect to the apical axis); cell ends are pointed or rounded in valve view. The cells have a strongly eccentric canal raphe, not

elevated above the valve surface; the raphe can be interrupted in the middle by a central nodule forming a larger interspace between the central fibulae (Figure 1.4 C). The valve surface has transapical ribs called interstriae, the silicified non-perforated structure between two striae (Figure 1.4, A and B). The number of interstriae is equal to or twice the number of the fibulae. The striae have one or more rows of perforated poroids. In addition, the majority of *Pseudo-nitzschia* cells have three girdle bands; the band closest to the valve is often termed the valvocopula. Girdle bands may have perforated poroids. Specific terminology used in the description of *Pseudo-nitzschia* species can be found in Hasle et al. 1996, Skov et al. 1999, and Thronsen et al. 2007.

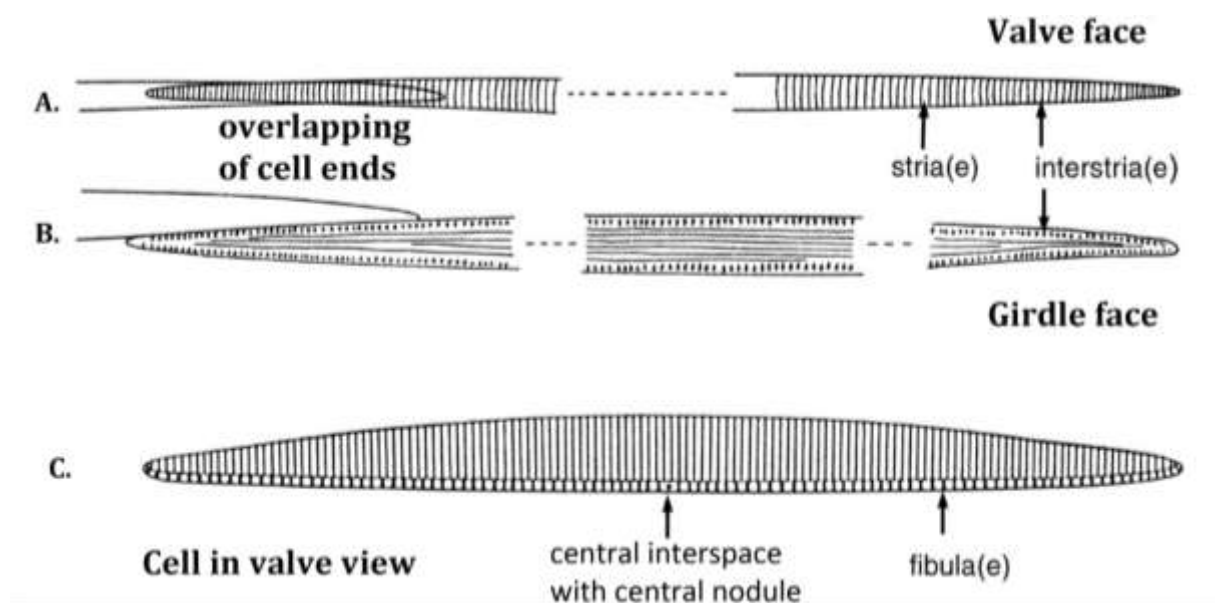


Figure 1.4: *Pseudo-nitzschia* cells in valve view (A and C), girdle view (B), and terminology used in this study; modified from Thronsen et al. 2007.

The genus is relatively easy to recognise under the light microscope, while species identification is often troublesome. A light microscopy observation on uncleaned material in water mounts provides only general information about the valve outline, the length of the cell overlap in the chain, and of some heavily silicified valve surface structures. By applying acid treatment, the organic material covering the diatom cells and obscuring morphological details of the valve can be removed. The fine valve structures become visible in both light and electron microscopes, although the resolution of the electron microscopes (transmission and scanning) is much higher and reveals more specific morphological details.

The differences in valve width (transapical axis) are traditionally used for the separation of *Pseudo-nitzschia* into two complexes or groups: the *seriata*-group (gathers species with a transapical axis of more than 3 μm) and the *delicatissima*-group (combines species with a transapical axis of less than 3 μm) (Proschkina-Lavrenko 1955; Hasle and Syvertsen 1997). Recently, two additional complexes of morphologically similar species were added: the *americana*-complex (combines three species with short and wide valves) and the *pseudodelicatissima / cuspidata* complex (combines about six species with long and narrow valves) (Lundholm et al. 2002; Lundholm et al. 2003). However, the morphological features of the cells often show considerable overlap and variation among the *Pseudo-nitzschia* species, making species determination difficult and requiring verification by electron microscopy.

1.3.2 Distribution and toxicity of *Pseudo-nitzschia*

Species of the genus *Pseudo-nitzschia* are a regular component of the marine phytoplankton worldwide and appear to have a cosmopolitan distribution (Hasle 2002). However, some species occur only in temperate, tropical or polar regions (Hasle and Syvertsen 1997; Fryxell and Hasle 2003). Blooms of *Pseudo-nitzschia* are most common in nutrient rich waters such as up-welling areas and in locations with a high terrestrial run-off (Smith et al. 1990; Trainer et al. 2002).

During the last two decades *Pseudo-nitzschia* species have received much attention because some members of the genus have the potential to produce the phycotoxin domoic acid (DA). Domoic acid is a neurotoxic amino acid that accumulates in pelagic and benthic organisms that filter feed directly on harmful *Pseudo-nitzschia* cells and through the food web may affect birds, marine mammals, and humans consuming the shellfish. Domoic acid causes amnesic shellfish poisoning (ASP) in humans that eat contaminated shellfish. The main symptoms of ASP are nausea, vomiting, diarrhea, and abdominal cramps; the neurological symptoms can in severe cases include headache, hallucinations, loss of short term memory, respiratory malfunction, and sometimes even coma and death. Domoic acid was identified as the causative toxin in an episode of ASP in late autumn 1987, when over 100 people became intoxicated, and three people died after consuming blue mussels cultivated in Cardigan Bay, Prince Edward Island, Eastern Canada (Wright et al. 1989). At the time of the toxic outbreak, *Pseudo-nitzschia*

multiseriis (Hasle) Hasle (then called *Nitzschia pungens* or *Pseudo-nitzschia pungens* f. *multiseriis*) was a dominant organism in the bloom and contributed 98-100% to the total cell number in the phytoplankton (Bates et al. 1989).

Since the Canadian toxic outbreak in 1987, several more species of the genus have been associated with DA intoxications worldwide. *Pseudo-nitzschia calliantha* Lundholm, Moestrup & Hasle (then called *P. pseudodelicatissima* (Hasle) Hasle) was the second member of the genus reported to produce DA in the Bay of Fundy in 1988 (Martin et al. 1990). *Pseudo-nitzschia australis* Frenguelli 1939 was identified as the source of DA that killed Brandt's cormorants and brown pelicans in Monterey Bay, California in the autumn of 1991, which had fed on DA-contaminated anchovies (Fritz et al. 1992). In 1993 and in 1994, *P. australis* was suspected to be the source of DA in New Zealand scallops (Rhodes 1998), and later in 1999 this species was found to be responsible for the deaths of over 400 Californian sea lions (Scholin et al. 2000). There has been an increasing number of reports from around the world where domoic acid has been detected in the water but the causative organism was not identified, as in the case of the death of hundreds of sea birds in Baja, Mexico in 1996 (Sierra Beltran et al. 1997).

More recently, the presence of DA-producing *Pseudo-nitzschia* species was reported from several European coasts: *P. multiseriis* from the Netherlands (Vrieling et al. 1996); *P. australis*, *P. multiseriis*, and *P. pseudodelicatissima* from French waters (Amzil et al. 2001; Nezan et al. 2006), *P. australis* from Irish waters (Cusack et al. 2002), and *P. seriata* from Scottish and Danish waters (Fehling et al. 2004; Lundholm et al. 2005). Cases of ASP have never been reported from European waters, though. Not all members of the genus *Pseudo-nitzschia* are able to produce DA and even the toxic species do not synthesize domoic acid all the time. Presently, a total of twelve *Pseudo-nitzschia* species is classified as potentially toxic (Lundholm and Moestrup 2007).

In Norwegian coastal waters species of the genus *Pseudo-nitzschia* are common and regularly observed. In fact, the first diatom reported to produce DA, *Pseudo-nitzschia multiseriis* (then called *P. pungens* f. *multiseriis* Hasle), was originally described from Oslofjorden. In 1996 Hasle, Lange, and Syvertsen published a review of *Pseudo-nitzschia* species' seasonal and long-term distributional patterns in the Skagerrak and adjacent waters (Hasle et al. 1996). During the sampling period (October 1978 through

September 1993) they identified several *Pseudo-nitzschia* species: *P. delicatissima*, *P. fraudulenta*, *P. heimii*, *P. pungens*, *P. calliantha* (then called *P. pseudodelicatissima*), *P. multiseriata*, and *P. seriata*. Despite that all observed *Pseudo-nitzschia* species, except for *P. heimii*, were known to be potentially toxic, no outbreak of ASP in the area was reported. The most abundant species in the spring was *P. seriata*, whereas *P. pungens*, *P. multiseriata*, and *P. calliantha* were more frequently observed during the autumn. This long-term examination also revealed that the abundance of *P. multiseriata* seems to have decreased in the 1990s, while that of *P. calliantha* has apparently increased.

1.4 Background, aims, and questions

Microalgae are major primary producers in the sea and knowledge about their diversity, succession, and seasonal cycle is of great importance. Also, biological diversity of microalgae may reveal changes that take place in marine ecosystems in general.

Most phytoplankton monitoring programs carried out in the outer part of Oslofjorden are based on bulk measurements of chlorophyll or total biomass, and on general observations of the phytoplankton with a special emphasis on potentially toxic microalgae. Thorough investigations of total phytoplankton composition and abundance in Outer Oslofjorden are rare, especially in the case of taxa requiring electron microscopy for species identification. The last detailed examination of the *Pseudo-nitzschia* species in the area was performed in 1996 (Hasle et al. 1996). To date, most of our knowledge of the occurrence, seasonal dynamics, and potential toxicity of *Pseudo-nitzschia* in the outer Oslofjorden has been obtained from general phytoplankton observations with light microscope (LM). Frustule details are essential for identification and only visible with electron microscope (EM), but EM analysis is not routinely used during phytoplankton monitoring programs and the presence of *Pseudo-nitzschia* species could have been overlooked during the LM examination.

The location of a permanent sampling station is an important factor in any monitoring network which investigates the water quality in a particular area. Since the outer Oslofjorden covers approximately 2200 km², selection of the sampling station for this

study was mainly based on quality of the water masses (origin, exposure to currents, and freshwater discharge) and accessibility, with further consideration of time and economic issues. According to investigations made by Det Norske Veritas during a period of five years (2001-2005), station OF2 was found to be similar in hydrographical and biological conditions to more exposed and more distant stations in the coastal current (Dragsund et al. 2006) and was therefore chosen for this project. The sampling has been carried out in connection with the EU projects MIDTAL (<http://www.midtal.com/>) and BioMarKs (<http://www.biomarks.eu/>) and the NRC project HAPTODIV (Diversity and dynamics of marine haptophytes, 2009-2011).

The aim of the present thesis was to study the seasonal change of phytoplankton composition and abundance in the outer part of Oslofjorden, with a special emphasis on *Pseudo-nitzschia* species, during one year period from June 2009 through June 2010.

Questions addressed concerning the seasonal cycle of phytoplankton were: (1) Are there any changes in seasonal patterns compared to previous observations? (2) How is the seasonal variation of the phytoplankton taxa in the outer part of the Oslofjorden? (3) Are there any new species present?

Questions addressed concerning *Pseudo-nitzschia* species were: (1) What is the pattern of the seasonal cycle? (2) Are there differences in the species composition compared to previous observations? (3) Are there any new species present? (4) Which of the potentially toxic *Pseudo-nitzschia* species occur and when are they present?

The following approaches were used: I identified and quantified the dominant phytoplankton taxa throughout a year with special emphasis on *Pseudo-nitzschia* species. Because the identification of the *Pseudo-nitzschia* to species level requires a high resolution, electron microscopy was included in this study. In addition, a level of taxonomic knowledge is needed to detect the morphological differences between members of this genus.

2 Materials and Methods

2.1 Study area and sampling

The area of study is situated in the outer part of Oslofjorden, adjacent to the Northern Skagerrak (Figure 2.1). Sampling was performed at monitoring station OF2 (59.186668°N, 10.691667°E; depth 358 m). It is located south of the group of islands Missingene (Fredrikstad Kommune, Østfold) within Ytre Hvaler nasjonalpark (see <http://www.thefullwiki.org/>) and is exposed to the Norwegian Coastal Current (NCC) and wind from western and southern directions.



Figure 2.1: Map of the outer part of Oslofjorden and Skagerrak with surrounding seas, picture at top left; Oslofjorden with indicated sampling station OF2, picture at right (maps are from www.thefullwiki.org); R/V *Trygve Braarud*, picture at bottom left (photo: UIO).

Water samples were collected on a monthly basis from June 2009 to June 2010. Sampling was carried out on board of the UIO R/V *Trygve Braarud*, departing from the harbour of Engelsviken (Østfold County) at 09.00 on each occasion. Eleven cruises were conducted over the sampling period.

Deviations in research plans occurred due to unforeseen force majeure. On two occasions, 22 of September 2009 and 22 of June 2010, samplings were performed in collaboration with the EU project BioMARks. Due to meteorological conditions, the initial sampling station was changed to a station located north east of Rauøy at position 59.253735°N, 10.710908°E. In February 2010 the outer part of Oslofjorden was covered with ice, which made it impossible for R/V *Trygve Braarud* to reach OF2. Consequently, February 2010 was excluded from further analysis.

2.2 Physical and chemical conditions

In order to obtain information about the seasonal changes in physical and chemical properties of the sea water, the following parameters were measured on each cruise.

2.2.1 Hydrography and fluorescence *in vivo*

Conductivity, temperature, depth, and fluorescence were measured *in situ* with a CTD (Falmouth Scientific Inc., USA) at different depths (0-100 m). The instrument transformed conductivity into salinity and determined density of the sea water; a fluorometer Q300 (Dansk Havteknikk, Denmark), with a sensor attached to the CTD rosette, measured fluorescence from chlorophyll *a in vivo* as a relative estimate of chlorophyll *a* concentrations in the water. Salinity values were given in psu (practical salinity unit) describing the concentration of dissolved salts in water (milligrams of salt per kg solution). Temperature of the sea water was measured in degrees Celsius (°C).

2.2.2 Irradiance

Irradiance or photosynthetically active radiation (PAR, the irradiance between 350-700 nm) was measured using a LI-192 Underwater Quantum Sensor (underwater sensor) and a LI-190 Quantum Sensor (deck sensor), both connected to a LI-250A light meter

(Li-Cor® Biosciences). The underwater sensor measured the irradiance every meter from 0-18 m; the deck sensor monitored surface irradiance. The irradiance measurements were used to calculate normalized underwater irradiance by dividing the highest deck value with each deck value and multiplying each of these with the respective underwater value. The irradiance values were measured in $\mu\text{E m}^{-2}\text{s}^{-1}$ (or $\mu\text{mol photons m}^{-2}\text{s}^{-1}$). Irradiance measurements were used to determine the vertical attenuation coefficients and the 1% “light depth” (the depth where 1% of the irradiance at the surface remains; this can be considered the lower level of the euphotic zone).

2.2.3 Chlorophyll *a in vitro*

Water samples for determination of fluorometric chlorophyll *a* were collected from 1, 2, 4, 8, 12, 16, and 20 m depth with 1 L Niskin bottles attached to the CTD-rosette. The water was transferred into 1 L plastic bottles which had been prewashed with the samples. A volume ranging from 100-500 mL (depending on the amount of phytoplankton present) was filtered on Whatman glass-fibre filters (GF/F 25mm, 0.7 μm mesh size) in two replicates from each depth. Filters were transferred into cryo vials and immediately frozen in liquid N_2 on board. The samples were taken to UIO and stored at -80°C until analysis at the Marine Biology Program, Department of Biology (UIO). In the laboratory, chlorophyll *a* concentration *in vitro* was measured in 90% acetone extracts (30-60 minutes extraction time) with a Turner Designs fluorometer TD-700 (Turner Designs, Sunnyvale, CA) calibrated against a chlorophyll *a* standard ($\mu\text{g L}^{-1}$).

2.3 Phytoplankton material

In order to obtain information about phytoplankton composition in the study area, both qualitative and quantitative methods were applied. Diversity and seasonal cycle of phytoplankton, including *Pseudo-nitzschia* species, were studied in the samples collected with vertical net tows. Water samples collected from 1 m depth (surface) were used to study diversity and cell density. Samples were fixed on board shortly after collection and kept in the refrigerator; after transportation to UIO they were stored in a dark room at

4 °C until further examination. During the sampling period, all flasks with water samples were marked with the cruise date, station, depth, and means of preservation.

2.3.1 Qualitative examination

Vertical net hauls (20 µm mesh size) were collected from 17-0 m towing vertically with a speed of 0.2 m s⁻¹ or slower. Collected material was divided into three aliquots: 100 mL was fixed with 1 mL of neutral Lugol's-solution (10g KI₂ and 5g I₂ per 100 mL) in medicine bottles (Thronsdén 1978), 100 mL was fixed with 2 mL of formalin (40% HCHO water solution) in medicine bottles, and 100 mL was kept alive for observation under the light microscope. At UIO live material was kept in a climate room at a temperature corresponding to the sea temperature and examined shortly after sampling (the same or the next day). Both live and preserved samples were studied with a Nikon ELIPSE E6000 light microscope, equipped with an attached camera, under phase and differential interference contrasts (DIC) and photographed with a Nikon digital camera D 80.

2.3.2 Quantitative examination

A CTD-rosette with attached 1 L Niskin bottles was used to collect water samples from 1 m depth (surface). Hundred mL of seawater was drawn directly from the Niskin bottles into medicine flasks and preserved with 1 mL neutral Lugol's-solution (Thronsdén 1978). The samples were examined using Utermöhl's sedimentation technique (Utermöhl 1958; Hasle 1978) under a Nikon Eclipse TE300 inverted microscope (Figure 2.2). Subsamples of 10 mL were analysed after ca. 24 hours of sedimentation. On three occasions when cell densities were high (June 2009, September 2009, and January 2010), the 10 mL volume was divided into smaller subsamples before counting (a 5 mL subsample was diluted with 5 mL of sterile seawater). Phytoplankton enumeration was carried out using phase contrast and magnifications of 400, 200, and 100 times. The entire bottom of a Hydro-Bios tubular plankton chamber (Kiel-Holtenau, Germany) was always counted. The phytoplankton species were counted in several stages: first, the whole chamber bottom was scanned at lowest magnification and species >30 µm were counted; then the smaller phytoplankton species (5-20µm) were counted at 200x and 400x magnifications. Empty cells were not included in the results. Many flagellate

species generally lose their flagella as a result of fixation; unidentified flagellates and round-shaped organisms with or without flagella were gathered in groups and classified according to their sizes. The number of phytoplankton species counted in 10 mL was transformed to concentration in one liter (cells L^{-1}).



Figure 2.2: A 10 mL Hydro-Bios tubular plankton chamber with coverslips, picture at the left; a Nikon Elipse TE300 inverted microscope, picture at the right (pers. photos).

2.3.3 Species identification

During qualitative and quantitative examinations, it was attempted to identify the phytoplankton species to the lowest taxonomic level. Identification of phytoplankton species was mostly based on Thronsdon et al. (2007), Tomas (1996; 1997), Hoppenrath et al. (2009), and Cupp (1943). To achieve precise identification of the *Pseudo-nitzschia* species, light and electron microscopy were combined. *Pseudo-nitzschia* species identification was performed in accordance with Hasle (1965), Hasle and Lange (1996), Skov et al. (1999), Lundholm et al (2002, 2003), and Quijano-Scheggia (2009) (Cupp 1943; Hasle 1965; Hasle et al. 1996; Tomas 1996; Tomas 1997; Skov et al. 1999; Lundholm et al. 2002; Lundholm et al. 2003; Thronsdon et al. 2007; Hoppenrath et al. 2009; Quijano-Scheggia et al. 2009).

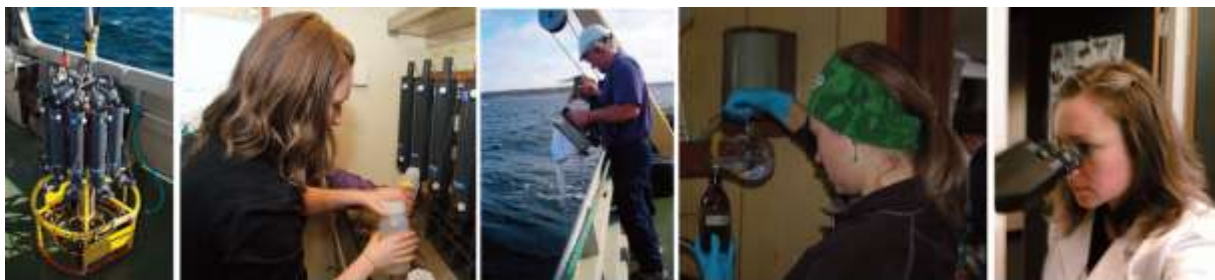


Figure 2.3: Pictures from the field and lab work; from left to right: CTD with attached 1L Niskin bottles; wet lab; sampling with plankton net; water sampling before fixation; examination with light microscope.

2.4 Preparation of *Pseudo-nitzschia* for electron microscopy

Scanning (SEM) and transmission (TEM) electron microscopy were used to perform detailed analyses of the fine structures of *Pseudo-nitzschia* frustules. Net tows fixed with formaldehyde were prepared for examinations with TEM and SEM. The organic matter around frustules was removed by using concentrated HNO₃ and H₂SO₄, the cleaning method described by Thronsen et al. (2007). Specimens for TEM and SEM were prepared at the same time and the rest of the acid-cleaned material was transferred into glass jars and preserved with 96% ethanol (Kemetyl).

2.4.1 Scanning electron microscopy (SEM)

A circular glass coverslip, with drops of acid-cleaned material dissolved in distilled water was mounted on aluminium stubs using double-sided carbon tape (Electron Microscopy Sciences, USA). Stubs were air dried and before SEM examination sputter-coated with ca. 3 nm of platinum in a Cressington 308 UHR sputter coater (Ted Pella, Inc., USA). From each sample 3 replicates were prepared and studied. Examination of the material was performed using a Hitachi FEG S-4800 scanning electron microscope, at 9-15 KV acceleration voltage and 8.4 mm working distance. Quartz PCI (Digital Imaging and Slow-Scan) software was used to capture and analyse images.

2.4.2 Transmission electron microscopy (TEM)

For TEM observations, a small drop of acid-cleaned material was placed onto Formvar (a polyvinyl resin support film) and carbon coated copper grids (150 µm mesh), air dried, and kept in a box until further examination. For each month a total of five grids were prepared. The grids were studied under a Philips CM-100; the Soft Imaging System (SIS) software was used to analyse and enhance captured images.

2.5 Statistical approach

The R statistical computing program (R Development Core Team, 2008) was used to process results. The hydrographical data collected during the sampling period are presented in a series of contour plots. Visualization of physico-chemical and biological water properties (figures 3.1, 3.2, and 3.4) was performed by interpolating discrete data with a R akima-package (interpolation of irregularly spaced data) (Akima et al. 2006). Nonmetric Multidimensional Scaling (NMDS, meta MDS function from the vegan package (Oksanen Jari et al. 2010) with the default Bray-Curtis index as a dissimilarity measure), was used to analyse the results from qualitative examination of the vertical net hauls by generating a geometric configuration of distances between sampling months. Two-dimensional scatter plots were used to illustrate changes in the phytoplankton composition and *Pseudo-nitschia* species over the seasons (figures 3.6, 3.9, and 3.10). The rarefaction method (Heck et al. 1975), from the vegan package (Oksanen Jari et al. 2010) in R, was used to compare the species diversity (as number of species) in the counted samples (quantitative examination). The rarefaction method allows to “thin-trim” samples of unequal sizes to the same standardized sample size by producing estimates that are comparable among differently sized samples (figure 3.8).

3 Results

3.1 Hydrographical conditions

3.1.1 Physical parameters

The temporal development of salinity, temperature, and density in the upper 40 meters of the sampling station OF2 are shown in contour plots 3.1 (A and B) and 3.2 (A). During the sampling period the salinity showed certain seasonal variations (Figure 3.1 A). The relatively low salinity values in the surface layers were observed several times, the first time in late summer (10-24 psu in August 2009 in the upper 5 meters) and the second time in late autumn (18-21 psu in November 2009 in the upper 5 meters). A continuous increase in salinity was observed from September through November 2009 (with the highest value of 30 psu in surface layers during October) and January through April 2010 (with the highest value of 32 psu in surface layers during March). In general, salinity was increasing with depth, showing relatively uniform distribution (28-34 psu at 10-40 meters) all through the sampling period with only small fluctuations observed in November-December 2009 (21-29 psu at 10-40 meters). Seasonal variations in water temperature in the upper 40 meters are shown in the figure 3.1 B. The highest temperature values were observed during summer 2009, with a maximum of 19 °C in the surface layers and 16 °C at 35 meters in August 2009. Low temperatures were observed during winter, with a minimum of -1.2-4 °C in the upper 15 meters and 5-9 °C below 15 meters in January 2010. Below 20 meters, temperature varied between 16 °C and 6 °C during the sampling period. Temperature and salinity are the two key factors that determine water density and stratification. The temporal development of density in the upper 40 meters was similar to that of salinity in its main features (Figures 3.1 A and 3.2 A), which indicated that density was mainly determined by salinity. The late summer 2009 was characterised by low density (5.1-10 δ_t) in the upper 5 meters of the water column, while during late autumn 2009 low density was observed from the surface layer

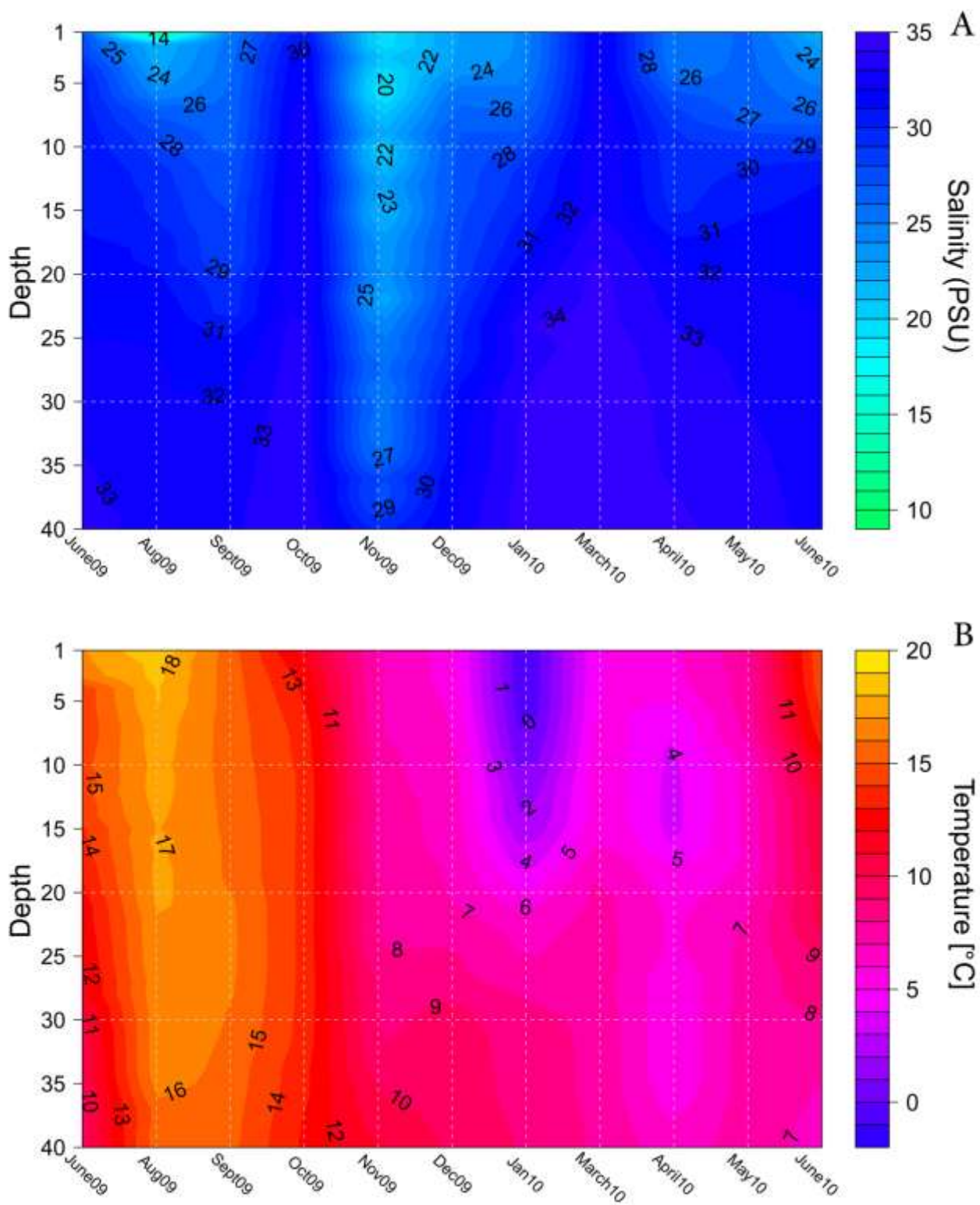


Figure 3.1: Contour plot showing the temporal development of salinity (A) and temperature (B) by time and depth during the sampling period (June 2009-June 2010) in outer Oslofjorden. Figures made by Elianne Egge.

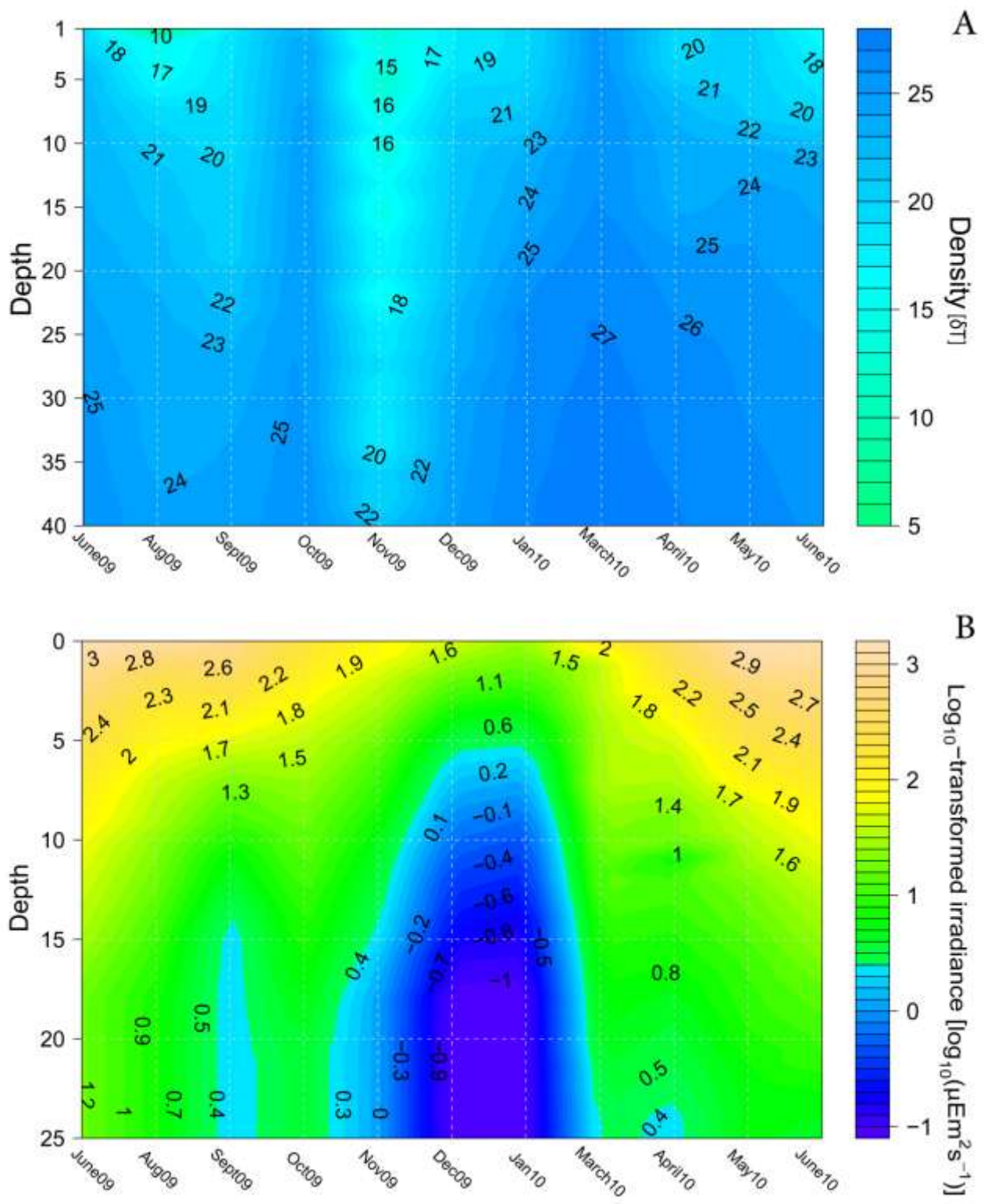


Figure 3.2: Contour plot showing the temporal development of density (A) and irradiance (B) by time and depth during the sampling period (June 2009-June 2010) in outer Oslofjorden. Figures made by Elianne Egge.

down to 35 meters (13-17 δ_t). Stratification of the water column was observed in June 2009, with a strong pycnocline in August 2009 at 5-7 meters that persisted throughout the rest of the summer. The pycnocline became weaker in the beginning of autumn and had disappeared by November 2009 when vertical mixing was observed. A pycnocline was formed again during the winter period (December 2009 and January 2010), but was almost broken down by the beginning of spring and only a weak pycnocline was located at approximately 25-30 meters (March 2010). The vertical stratification of the water column increased steadily towards the summer with a pycnocline at 5-15 meters in June 2010.

Seasonal variations of log-transformed irradiation measurements (photosynthetically active radiation, PAR) by depth through the upper 25 meters are presented in Figure 3.2 B. In general, the solar irradiation was strongest in the summer and spring period (maximum PAR at 0 meter was measured in June-August 2009), while it was weakest during the autumn and winter period (minimum PAR at 0 meter was measured in December 2009 and January 2010). The vertical attenuation coefficient varied from 0.13 (March 2010) to 0.41 (September 2009). The depth at which irradiance corresponded to 1% of surface light was determined for each sampling (Figure 3.3). The 1% light depth was at 19 meters in June and rose to 11 meters in September 2009; it dropped to 26 meters in October 2009 and then rose steadily towards the winter (13-14 meters in December 2009 and January 2010). The deepest 1% light depth was recorded in March 2010 at approximately 34 meters, while towards summer 2010 the 1% light depth rose to approximately 20 meters.

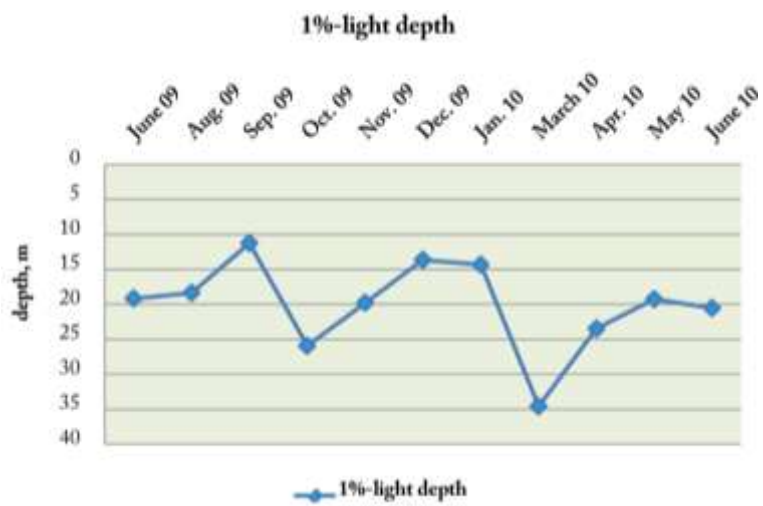


Figure 3.3: Seasonal variations in the 1% light depth of the water column during the sampling period (June 2009-June 2010).

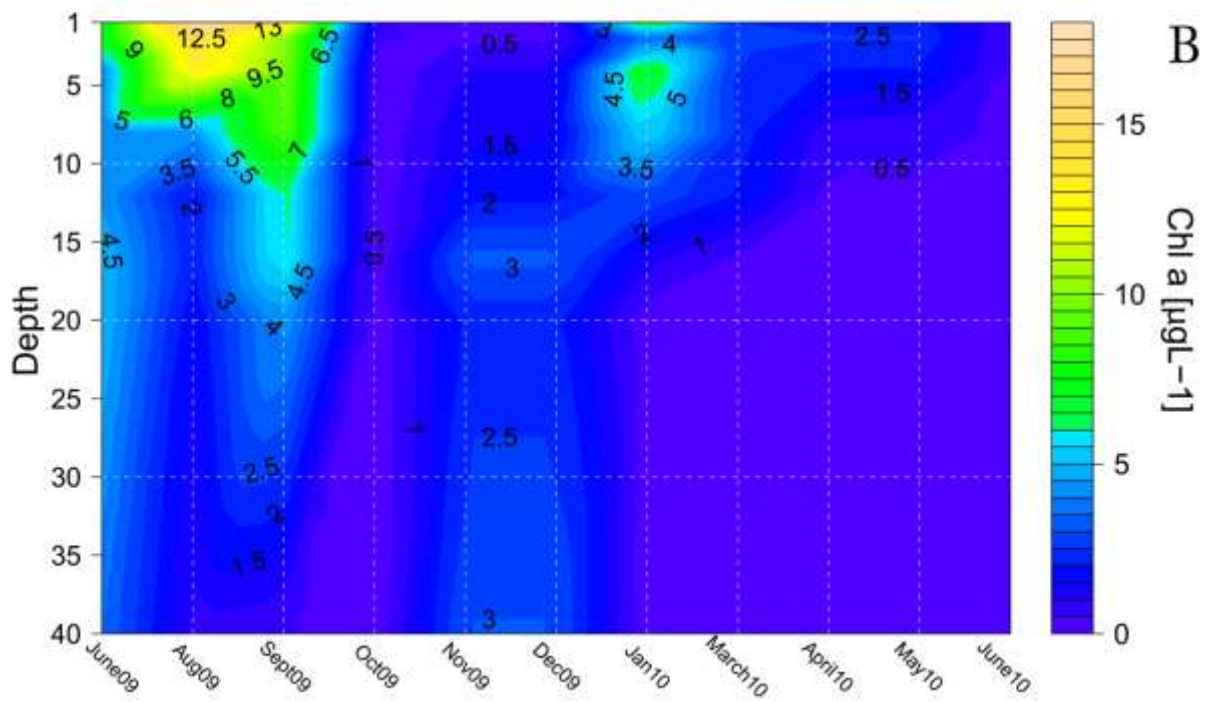
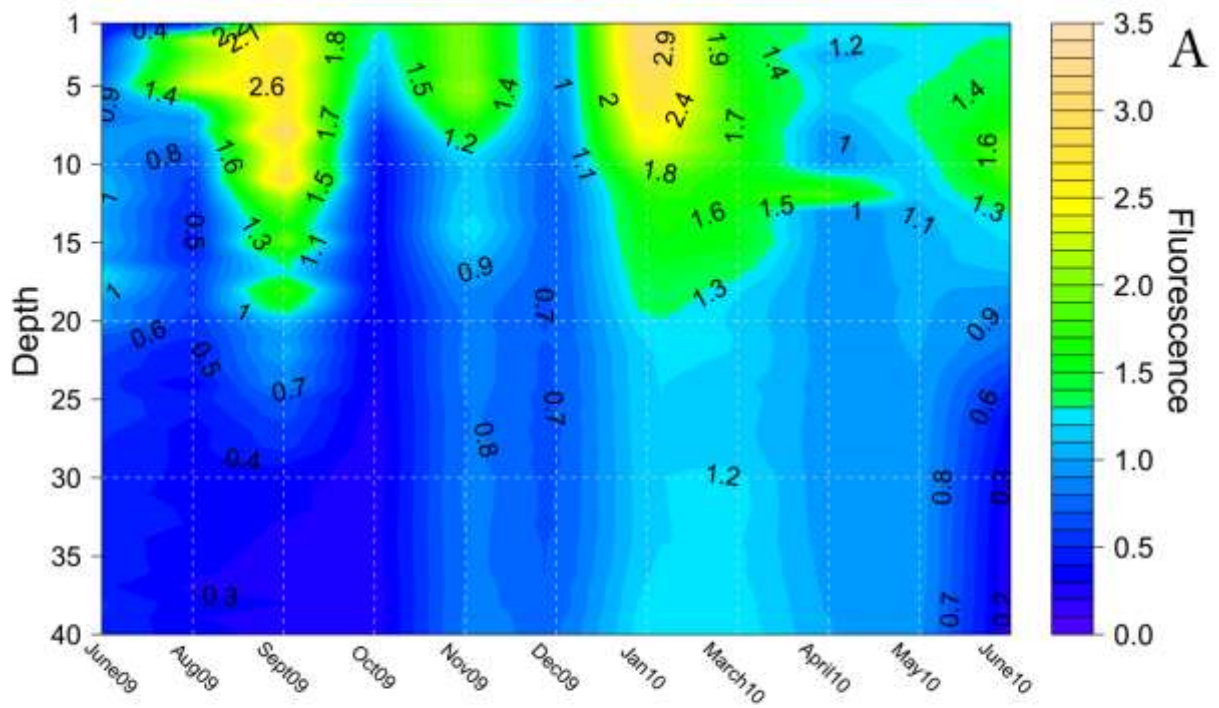


Figure 3.4: Contour plot showing temporal variations of chlorophyll in the upper 40 meters, (A) fluorescence *in vivo* and (B) chlorophyll *a* *in vitro* during the sampling period (June 2009-June 2010) in outer Oslofjorden. Figures made by Elianne Egge.

3.1.1 Temporal variability in chlorophyll *a*

The temporal fluctuations in chlorophyll *a* by depth, based on *in vivo* fluorescence measurements and *in vitro* chlorophyll *a* measurements, are presented in figure 3.4, A and B respectively. Fluorescence measurements showed relatively high values in the upper 20 meters in June and September 2009 as well as in January and March 2010; in the upper 2-11 meters in November 2009 and May, June 2010 (Figure 3.4 A). The contour plot of chlorophyll *a in vitro* (Figure 3.4 B), showed varying values and distribution of chlorophyll concentrations. The highest chlorophyll *a* values were measured in the surface layer during summer and the beginning of autumn, with maximum concentrations of 18 $\mu\text{g L}^{-1}$ in August 2009 and 13.7 $\mu\text{g L}^{-1}$ in September 2009 (Figure 3.4 B). Minor, but still noticeable, chlorophyll *a* maxima were observed in June 2009 and January 2010 with chlorophyll *a* concentrations of approximately 7 $\mu\text{g L}^{-1}$ at 1 and 4 meters.

3.2 Phytoplankton composition and seasonality

Composition and seasonal cycle of the phytoplankton community in the outer part of Oslofjorden were studied from natural water samples collected with net hauls; both live and preserved material from a total of eleven months were examined. A taxonomic list of the phytoplankton species identified in this study is presented in table 3.1 (potentially toxic and toxic species are marked with red colour).

The two major algal groups that contributed most to the phytoplankton diversity were the diatoms and dinoflagellates. Less variety was seen in the species composition of other groups. Identified phytoplankton species comprised more than 125 taxa, including 62 diatoms, 52 dinoflagellates, 2 haptophytes, 2 euglenophytes, 1 choanoflagellate, 2 chrysophytes, 2 dictyochophytes, and 1 ebridian. In this study prasinophytes, cryptophytes, and small members (<20 microns) of the haptophytes were not identified to the species level and grouped together as monads. Other organisms such as ciliates and tintinnids were noted, but generally not identified to species level. In addition, some species were identified only to the genus level. Phytoplankton in the pico- and nano -

size fractions (0.2–10 µm), which are difficult to identify under the light microscope, were not included in the taxonomic list.

3.2.1 Total phytoplankton composition

The diatoms were widely represented in the samples, most of the identified genera and species were radial, bi- or multipolar centric diatoms, just a few genera and species were pennate diatoms. Among the diatoms the greatest species diversity was observed within the genus *Chaetoceros* Ehrenberg 1844 (20 species were identified), followed by *Pseudonitzschia* H. Peragallo in H. & M. Peragallo 1900 (9 identified and 1 unidentified species were observed during electron microscopy of acid cleaned vertical net hauls). Less species variety was observed in the genus *Thalassiosira* Cleve 1873 (4 species) and the genus *Rhizosolenia* Brightwell 1858 (4 species). Of the genera *Guinardia* H. Peragallo 1892, *Leptocylindrus* Cleve 1889, and *Skeletonema* Greville 1865 only two species were identified for each genus. Several genera were represented by only 1 species (e.g. *Pleurosigma normanii*, *Thalassionema nitzschioides*, *Cylindrotheca closterium*). For some genera the number of species was difficult to establish as species delimitation is problematic. Even genus identification may be impossible in organisms with few distinguishing characters and many organisms could not even be assigned to a genus or species such as many boat shaped pennate diatoms that resemble *Navicula* Bory de Saint-Vincent 1822 and in this study they were termed naviculoids.

The dinoflagellates were as the diatoms widely represented all through the sampling period. Both thecate and naked dinoflagellates were observed in the examined vertical net hauls. Regarding species diversity, the genus *Protoperidinium* Bergh 1882 (12 species) was most diverse, followed by the genera *Ceratium* Schrank 1793 (seven species; in 2010 F.Gómez, D.Moreira, and P.López-García proposed a new genus name *Neoceratium* for the marine species of the genus *Ceratium*, this new genus name is currently recognized as a distinct genus (see <http://www.algaebase.org>), but is regarded as illegitimate (Calado and Huisman 2010) and in this study the genus name *Ceratium* will be used), *Dinophysis* Ehrenberg 1839 (six species), and *Prorocentrum* Ehrenberg 1834 (three species). Whenever it was difficult to make precise taxonomic identifications, the observed taxa were gathered into groups with morphologically similar species (e.g. *Diplopsalis*- and *Scrippsiella*-groups). Several genera such as

Amphidinium Claperède & Lachmann 1859; *Gymnodinium* Stein, 1878 and *Gyrodinium* Kofoid & Swezy 1921 were regular components of the phytoplankton. Other genera such as *Katodinium* Fott 1957 and *Oxytoxum* Stein, 1883, were less diverse and occurred only sporadically in the samples. *Amylax triacantha*, *Karlodinium* cf. *veneficum*, *Micracanthodinium* cf. *claytoni*, *Polykrikos* cf. *schwartzii*, *Dinophysis odiosa*, and *Dinophysis tripos* were rarest and each of them was observed on only one occasion (see Table 3.1).

In addition to diatoms and dinoflagellates, other algal groups were regularly observed during the sampling period. The haptophytes were represented by two taxa (*Phaeocystis globosa* and *P. pouchetii*); within the euglenophytes two taxa were identified (*Eutreptiella* cf. *braarudii*, *Eutreptiella* sp.). *Dictyocha speculum* and *Dictyocha fibula* were the only silicoflagellates (Dictyochophyceae) recorded from the studied samples. The chrysophyte *Dinobryon* sp. and ebridian *Ebria tripartia* were also found on several occasions. Other groups and species were observed on a few occasions (e.g. the chrysophyte *Meringosphaera* sp. and choanoflagellates). Ciliates (except *Myrionecta rubra*) and monades/unidentified (not identified) were regular components of the phytoplankton community.

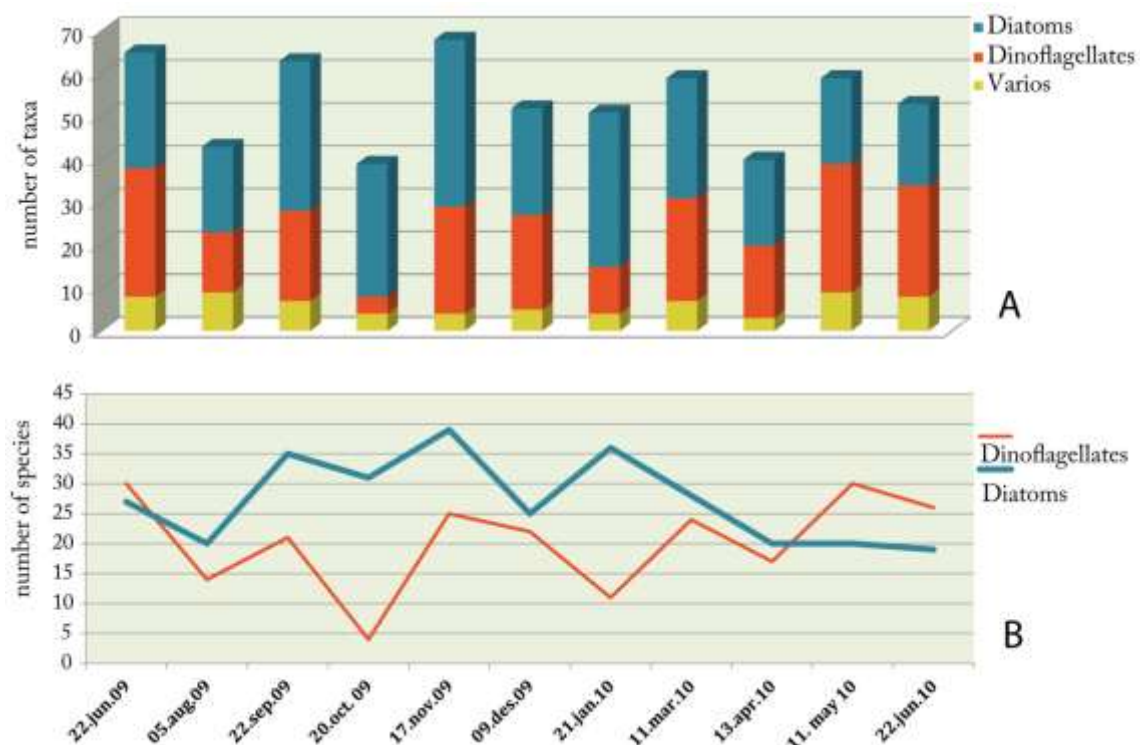


Figure 3.5: Seasonal changes in numbers of identified taxa of the major phytoplankton groups (A) and diatoms vs. dinoflagellates (B) during the sampling period.

The results obtained from the examined vertical net hauls showed that general taxa richness within these phytoplankton groups varied seasonally (Figure 3.5 A). Numbers of observed taxa were lowest in October 2009 and April 2010 with 39 and 40 identified taxa respectively and highest in November 2009 when 68 different phytoplankton taxa were observed. The number of identified diatom species was dominant most of the year, except in June 2009 and May and June 2010, when the dinoflagellates had higher species diversity (Figure 3.5 B).

3.2.2 Species composition and seasonal occurrence

In June 2009 dinoflagellates had the highest number of species with the greatest individual contribution of species from the genera *Ceratium* (with seven species), *Protoperidinium* (with ten species), and *Dinophysis* (with three species), followed by diatom species of the genera *Pseudo-nitzschia* (with 10 species), *Chaetoceros* (represented by five species) and *Rhizosolenia* (four species). Additional taxa such as *Dinobryon* sp., *Ebria tripartita*, *Eutreptiella* sp., and monads, contributed to the phytoplankton composition as well. Towards September 2009, the genus *Chaetoceros* reached its highest diversity, with 16 identified species in the samples, while the genus *Pseudo-nitzschia* became less diverse and was represented by only two species: *P. calliantha* and *P. pungens*. Other diatoms, *Cerataulina pelagica*, *Coscinodiscus* spp., *Skeletonema* sp., *Dactyliosolen fragilissimus*, and *Ditylum brightwellii* together with species of the genera *Guinardia* and *Leptocylindrus* were also detected. In the same period the thecate dinoflagellates *Ceratium* spp. and *Protoperidinium* spp. were replaced by species of the genus *Prorocentrum* and by naked dinoflagellates of the genera *Amphidinium* and *Gyrodinium*. The haptophyte *Phaeocystis globosa*, together with *Eutreptiella* sp., *Dictyocha speculum*, and *Ebria tripartita* was an important component of the phytoplankton community. In October 2009, the dinoflagellates reached their lowest numbers of species and were represented by *Gymnodinium* sp., *Gyrodinium* sp., *Ceratium furca*, and *C. tripos*. The assemblage of diatoms consisted mainly of species from the genera *Chaetoceros* (with seven species), *Pseudo-nitzschia* (with seven species), and the newly arrived species *Pseudosolenia calcar-avis*, *Pleurosigma normanii*, *Thalassionema nitzschoides*, and *Thalassiosira anguste-lineate*. In November 2009 the highest species variety in the phytoplankton community was recorded. The diversity of dinoflagellates increased again and the observed assemblage consisted of *Ceratium* spp., *Dinophysis*

spp., *Protoperidinium* spp., and *Akashiwo sanguinea*. The diatom community was the dominating component, represented by *Cerataulina pelagica*, *Chaetoceros curvicetus*, *C. debilis*, *C. decipiens*, *C. socialis*, *Pseudo-nitzschia* spp. (five species), *Dactyliosolen fragilissimus*, *Ditylum brightwellii*, *Leptocylindrus danicus*, *Skeletonema* sp., *Thalassiosira anguste-lineata*, and *T. nordenskoieldii*. The solitary diatom, *Attheya septentrionalis* was regularly observed during the autumn–winter period. Together with monads, the silicoflagellates *Dictyocha fibula* and *D. speculum* were also important components of the phytoplankton.

In winter samples, the phytoplankton community remained similar with diatom assemblages resembling those detected in late autumn. However, more variety was observed within the genera *Chaetoceros* (eleven species) and *Thalassiosira* (four species). The species diversity of the genus *Pseudo-nitzschia* became reduced throughout the winter, from five representatives in December 2009 to three in January 2010. Dinoflagellate diversity decreased towards January 2010 and was represented by species of the genera *Ceratium*, *Dinophysis*, *Protoperedinium*, *Gymnodinium*, and *Gyrodinium*. Monads, ciliates, and *Dictyocha speculum* were still present.

In March and April 2010, the diversity of both diatoms and dinoflagellates declined. Examined samples contained *Coscinodiscus* spp., *Dactyliosolen fragilissimus*, *Ditylum brightwellii*, *Guinardia delicatula*, *Leptocylindrus danicus*, *Rhizosolenia* spp., *Thalassionema nitzschoides*, and rest of the *Pseudo-nitzschia*, *Thalassiosira*, and *Chaetoceros* species from the winter. Diversity of dinoflagellates was greater in March 2010 and consisted of *Ceratium* and *Dinophysis* species, followed by *Protoperidinium* spp. and several species of naked dinoflagellates. For the first time the haptophyte *Phaeocystis pouchetii* was detected in the samples. Other species such as *Eutr*

eptiella cf. *braarudii*, *Dinobryon* sp., *Dictyocha speculum*, and choanoflagelletes were also observed.

In the late spring and further towards summer 2010 (May – June), diatoms were gradually replaced by dinoflagellates. In May, members of the genera *Ceratium*, *Dinophysis*, *Protoperidinium*, *Prorocentrum*, *Heterocapsa*, *Scripsiella*, *Amphidinium*, *Gymnodinium*, and *Gyrodinium* contributed greatly to the phytoplankton community.

The genus *Pseudo-nitzschia* was represented by an assemblage of five species; among other observed diatoms were *Cerataulina pelagica*, solitary *Chaetoceros thronsenii*, *Coscinodiscus* sp., *Guinardia flaccida*, *Rhizosolenia* spp., *Thalassionema nitzschioides*, *Leptocylindrus danicus*, and *L. minimus*. In the June samples, the members of previously present diatom genera, such as *Rhizosolenia* and *Thalassiosira*, were not observed. Only one species of the *Pseudo-nitzschia*, *P. delicatissima*, was detected in June. The other algal groups were represented by the haptophyte *Phaeocystis pouchetii*, the chrysophytes *Dinobryon* sp. and *Meringosphaera* sp., *Ebria tripartita*, and by colonies of choanoflagellates.

All through the sampling year the most frequently observed phytoplankton were the diatoms *Proboscia alata*, *Cylindroteca closterium*, *Chaetoceros* spp., *Skeletonema* spp., *Dactyliosolen fragilissimus*, *Leptocylindrus danicus*, navicoloids, *Thalassionema nitzschioides*, *Pseudo-nitzschia delicatissima*, *P. calliantha*, and *Coscinodiscus* spp; followed by the dinoflagellates *Ceratium tripos*, *C. furca*, *C. horridum*, *Gymnodinium* sp., as well as *Dinophysis acuminata* and *D. norvegica*. In addition, *Dictyocha speculum*, *D. fibula*, *Dinobryon* sp. together with ciliates and monads occurred regularly in the samples.

The examination of the vertical net haul samples revealed that species composition varies throughout the year. To determine relationships between phytoplankton community and different seasons, the species composition from eleven months was compared by using a non-metric multidimensional scaling (NMDS) method with a Bray-Curtis index of dissimilarity. The NMDS ordination diagram (Figure 3.6) illustrates how the phytoplankton composition changed over the sampling year, where the relative distance between the dates indicates the amount of similarity or difference between the sampling months. The spreading pattern of the eleven sampling months shows a certain degree of dissimilarity according to their distributions along the ordination axes. However, the sampling months can be separated into several seasonal groups according to their clustering, which outlines the seasonal cycle within the phytoplankton community.

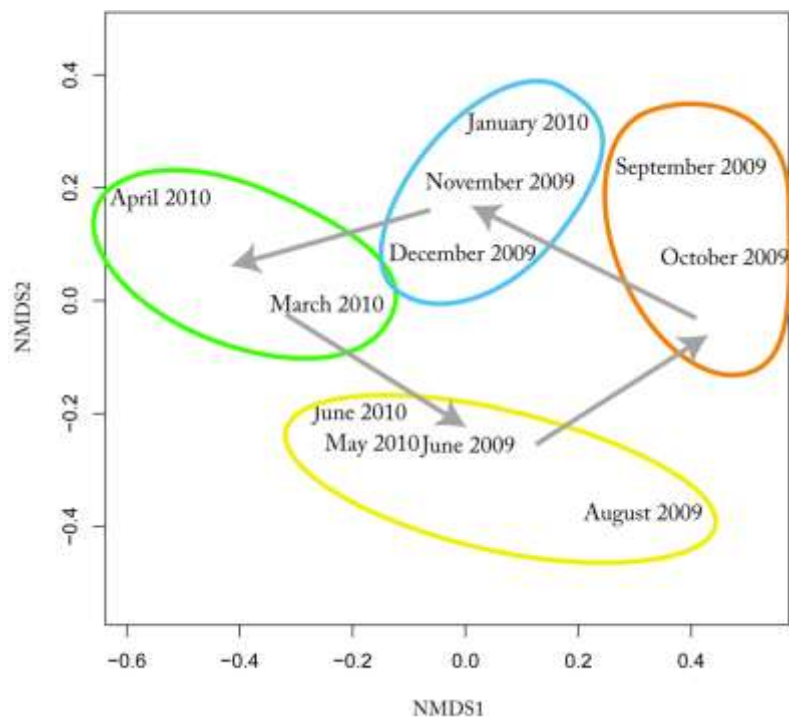


Figure 3.6: Ordination diagram showing seasonal changes in the phytoplankton community during the sampling year, where the circles indicate different seasons: yellow-summer, orange-autumn, blue-winter, and green-spring. Arrows show the seasonal pattern.

Table 3.1: Composition and seasonal cycle of phytoplankton species identified from vertical net hauls, at OF2 Outer Oslofjorden through June 2009-June 2010.

| Date of sampling | 22 June 09 | 05 Aug. 09 | 22 Sep. 09 | 20 Oct. 09 | 17 Nov. 09 | 09 Dec. 09 | 21 Jan. 10 | 11 Mar. 10 | 13 Apr. 10 | 11 May 10 | 22 June 10 |
|---|------------------|------------------|------------------|------------------|------------------|------------------|------------------|------------------|------------------|-----------------|------------------|
| Diatoms-Bacillariophyceae | | | | | | | | | | | |
| <i>Asterionellopsis glacialis</i> (Castr.) Round | | | x | x | | | | | x | | |
| <i>Attheya septentrionalis</i> (Østrup) Craw. | | | | | x | x | x | x | | | x |
| <i>Cerataulina pelagica</i> (Cleve) Hendey | x | x | x | | x | | | | | | x |
| <i>Chaetoceros cf. atlanticus</i> Cleve | | x | x | x | x | x | | | | | |
| <i>C. cf. brevis</i> Schütt | | | x | | | | x | | | | |
| <i>C. contortus</i> Schütt | | | x | | x | | | | | | |
| <i>C. cf. constrictus</i> Gran | | x | x | | | | x | | x | | |
| <i>C. curvisetus</i> Cleve | | | x | x | x | | x | x | | | |
| <i>C. danicus</i> Cleve | | x | x | x | x | x | x | | | | |
| <i>C. debilis</i> Cleve | | | x | x | x | | x | x | | | x |
| <i>C. decipiens</i> Cleve | | | x | x | | | | x | x | X | |

| Table continue | 22 June 09 | 05 Aug. 09 | 22 Sep. 09 | 20 Oct. 09 | 17 Nov. 09 | 09 Dec. 09 | 21 Jan. 10 | 11 Mar. 10 | 13 Apr. 10 | 11 May 10 | 22 June 10 |
|--|------------------|------------------|------------------|------------------|------------------|------------------|------------------|------------------|------------------|-----------------|------------------|
| <i>C. diadema</i> (Ehrenberg) Gran | | | | | | | | | x | X | |
| <i>C. didymus</i> Ehrenberg | | | x | | x | | x | | | | |
| <i>C. lacinosus</i> Schütt | | x | | | x | | x | x | | | |
| <i>C. minimus</i> (Lev.) Mar. Giuf. Mont. & Zing. | x | x | x | | | | | | | | |
| <i>C. similis</i> Cleve | | | | | x | | x | | | | |
| <i>C. simplex</i> Ostenfeld | | | x | | | | | | x | | |
| <i>C. socialis</i> Lauder | | | x | x | x | | | x | x | | |
| <i>C. subtilis</i> Cleve | | | x | | | | x | | | | |
| <i>C. tenuissimus</i> Meunier | x | x | x | | | | x | | | | |
| <i>C. teres</i> Cleve | | | x | x | | | | | | | |
| <i>C. throndsenii</i> (Mar. Montr. Zing.) Marino | x | | | | | | | | | | x |
| <i>C. wighamii</i> Brightwell | x | x | x | | | | x | | | | |
| <i>Chaetoceros</i> sp. | x | x | x | x | x | | x | x | x | X | x |
| <i>Coscinodiscus</i> spp. | | x | x | | x | x | x | x | x | X | x |
| <i>Cylindrotheca closterium</i> ¹ (Ehrenberg) Reimann & J. C. Lewin | x | x | x | x | x | x | x | x | x | X | x |
| <i>Dactyliosolen fragilissimus</i> (Bergon) Hasle | x | x | x | x | x | x | x | x | | X | x |
| <i>Ditylum brightwellii</i> (West) Grun. | | | x | x | x | x | x | x | | | x |
| <i>Eucampia</i> cf. <i>zodiacus</i> Ehrenberg | | | | x | | | | | | | |
| <i>Fragilariopsis</i> sp. | | | | | x | | | | | | |
| <i>Guinardia flaccida</i> (Castr.) Peragallo | x | | x | x | x | x | x | | | X | x |
| <i>Guinardia delicatula</i> (Cleve) Hasle | x | | x | x | x | x | x | x | | | |
| <i>Leptocylindrus danicus</i> Cleve | x | x | x | x | x | x | x | x | | X | x |
| <i>Leptocylindrus minimus</i> Gran | x | | x | | x | | | | | X | x |
| <i>Melosira</i> sp. | | | | | x | | x | x | | | x |
| Naviculoids ² | x | x | x | x | x | | x | x | x | X | x |
| <i>Paralia</i> sp. | | | | | | x | | | | | |
| <i>Pleurosigma normanii</i> Ralfs | | | | x | | | x | x | | | x |
| <i>Proboscia alata</i> (Brightw.) Sund. | x | x | x | x | x | x | x | x | x | X | x |
| <i>Pseudo-nitzschia americana</i> (Hasle) Fryxell | | | | | | x | x | | | | |
| <i>P. calliantha</i> * Lundh., Moestr. & Hasle | x | x | x | x | x | x | x | x | | X | |
| <i>P. cf. cuspidata</i> * (Hasle) Hasle | | | | | x | x | | | | | |

| Table continue | 22 June 09 | 05 Aug. 09 | 22 Sep. 09 | 20 Oct. 09 | 17 Nov. 09 | 09 Dec. 09 | 21 Jan. 10 | 11 Mar. 10 | 13 Apr. 10 | 11 May 10 | 22 June 10 |
|--|------------------|------------------|------------------|------------------|------------------|------------------|------------------|------------------|------------------|-----------------|------------------|
| <i>P. delicatissima</i> * (Cleve) Heiden | x | | | x | x | x | x | x | x | X | x |
| <i>P. fraudulenta</i> * (Cleve) Hasle | x | x | | x | | | | | | X | |
| <i>P. multiseriis</i> * (Hasle) Hasle | | | | x | x | | | | | | |
| <i>P. pseudodelicatissima</i> ** (Hasle) Hasle | x | | | x | | | | | | | |
| <i>P. pungens</i> * (Grunow ex Cleve) Hasle | x | | x | x | x | x | | | | X | |
| <i>P. seriata</i> * (Cleve) Peragallo | x | x | | | | | | x | x | X | |
| <i>Pseudo-nitzschia</i> sp. | x | | | x | | | | | | | |
| <i>Pseudosolenia calcar-avis</i> (Schultze) Sund. | | | | x | x | | x | | | | |
| <i>Rhizosolenia</i> cf. <i>borealis</i> <i>/styliformis</i> Sundsrtöm / Brightwell | x | | | | | | | | | X | |
| <i>R. hebetata</i> f. <i>semispina</i> (Hen.) Gran | x | | | | | | x | x | x | X | |
| <i>R. pungens</i> Cleve-Euler | x | x | x | | x | | x | | | | |
| <i>R. setigera</i> Brightwell | x | | | | | x | | x | | | |
| <i>Rhizosolenia</i> sp. | | | | | x | | | x | x | | |
| <i>Skeletonema</i> cf. <i>marinoi</i> Sargo & Zingone | x | x | x | x | x | x | | | | | x |
| <i>Skeletonema</i> cf. <i>pseudocostatum</i> Medlin | x | | | | x | x | | | | | |
| <i>Skeletonema</i> sp. | | | | | | | x | x | x | X | |
| <i>Striatella unipunctata</i> (Lyngb.) Agardh | | | x | | | | | | | | x |
| <i>Thalassionema nitzschioides</i> (Grun.) Mereschkowsky | x | | x | x | x | x | x | x | x | X | |
| <i>Thalassiosira anguste - lineata</i> (Schm.) Fryxell & Hasle | | | | x | x | | x | x | x | | |
| <i>T. cf. hyalina</i> (Grun.) Gran | | | | | x | x | x | | | | |
| <i>T. cf. rotula</i> Meunier | | | | | x | x | x | | | | |
| <i>T. nordenskiöldii</i> Cleve | | | | | x | x | x | x | x | | |
| <i>Thalassiosira</i> sp. | | | x | x | | x | | x | x | | |
| Dinoflagellates-Dinophyceae | | | | | | | | | | | |
| <i>Actiniscus pentasterias</i> (Ehrenb.) Ehrenberg | x | x | | | | | | | | X | x |
| <i>Akashiwo sanguinea</i> (Hiras.) Hansen & Moestrup | | | x | | x | x | | | x | | |
| <i>Amphidinium</i> cf. <i>longum</i> Lohmann | | | x | | | | | | x | | |
| <i>Amphidinium</i> cf. <i>sphenoides</i> Wulff | | | x | | | | | | | X | |
| <i>Amphidinium</i> * sp. | x | x | | | | | | x | | X | |

| Table continue | 22 June 09 | 05 Aug. 09 | 22 Sep. 09 | 20 Oct. 09 | 17 Nov. 09 | 09 Dec. 09 | 21 Jan. 10 | 11 Mar. 10 | 13 Apr. 10 | 11 May 10 | 22 June 10 |
|--|------------------|------------------|------------------|------------------|------------------|------------------|------------------|------------------|------------------|-----------------|------------------|
| <i>Amylax triacantha</i> (Jorg.) Sournia | | | | | | | | | | X | |
| <i>Azadinium</i> sp. | | | x | | | | | | | X | |
| <i>Ceratium furca</i> ³ (Ehrenberg) Claparède & Lachmann | x | x | x | x | | x | | x | | X | x |
| <i>C. fusus</i> (Ehrenb.) Dujardin | x | | | | x | x | x | x | | X | x |
| <i>C. horridum</i> (Cleve) Gran | x | x | | | x | x | x | x | x | X | x |
| <i>C. lineatum</i> (Ehrenb.) Cleve | x | x | | | x | x | | x | | X | x |
| <i>C. longipes</i> (Bailey) Gran | x | x | | | | x | | x | x | X | x |
| <i>C. macroceros</i> (Ehrenb.) Vanhöf. | x | | | | | | | x | | X | x |
| <i>C. tripos</i> (Müller) Nitzsch | x | x | x | x | x | x | x | x | | X | x |
| <i>Dinophysis acuminata</i> * Clap. & Lachm. | x | | x | | x | | x | x | x | X | x |
| <i>D. acuta</i> * Ehrenberg | | | | | x | x | | | x | | |
| <i>D. norvegica</i> * Clap. & Lachm. | x | x | | | x | x | x | x | x | X | x |
| <i>D. odiosa</i> (Pav.) Tai & Skogsb. | | | | | x | | | | | | |
| <i>D. rotundata</i> * ⁴ Claparède & Lachmann | x | | x | | x | x | | x | x | X | x |
| <i>D. tripos</i> * Gourret | | | | | x | | | | | | |
| <i>Diplopsalis</i> - group ⁵ | x | | | | | | | x | x | | x |
| <i>Gonyaulax digitale</i> (Pouchet) Kof. | x | | x | | | | | | x | | |
| <i>Gymnodinium</i> cf. <i>abbreviatum</i> Kof. & Swezy | | | | | | | | x | x | | |
| <i>Gymnodinium</i> * sp. | x | x | | x | | x | x | | | X | x |
| <i>Gyrodinium</i> cf. <i>spirale</i> (Bergh) Kof. & Swezy | | | x | | | | | | | | |
| <i>Gyrodinium</i> sp. | x | x | x | x | x | x | | x | x | X | x |
| <i>Heterocapsa</i> cf. <i>triquetra</i> (Ehrenb.) Hansen | x | x | x | | x | x | x | | | X | x |
| <i>Karlodinium</i> cf. <i>veneficum</i> * (Ballant.) Larsen | | x | | | | | | | | | |
| <i>Katodinium</i> sp. | | | | | | | | x | | X | |
| <i>Micracanthodinium</i> cf. <i>claytoni</i> (Holmes) Dodge | | | | | | | | | | | x |
| <i>Oxytoxum</i> sp. | | | x | | x | x | | | | | |
| <i>Prorocentrum</i> cf. <i>gracile</i> Schütt | | | x | | | | | | | | |
| <i>P. micans</i> Ehrenberg | x | | x | | x | x | | | | X | x |
| <i>P. minimum</i> * (Pavil.) Schiller | | | x | | | | | | | X | x |
| <i>Protoceratium reticulatum</i> * (Clap. & Lachm.) Butschli | x | | | | | | | | x | X | x |
| <i>Protoperidinium bipes</i> ⁶ (Paulsen) Balech | x | x | x | | x | | x | x | | X | x |

| Table continue | 22 June 09 | 05 Aug. 09 | 22 Sep. 09 | 20 Oct. 09 | 17 Nov. 09 | 09 Dec. 09 | 21 Jan. 10 | 11 Mar. 10 | 13 Apr. 10 | 11 May 10 | 22 June 10 |
|--|------------------|------------------|------------------|------------------|------------------|------------------|------------------|------------------|------------------|-----------------|------------------|
| <i>P. breve</i> Paulsen | | | | | x | | | | | | |
| <i>P. brevipes</i> (Paulsen) Balech | x | | | | | x | | x | x | X | |
| <i>P. conicum</i> (Gran) Balech | x | | | | x | x | | x | | X | x |
| <i>P. depressum</i> (Bailey) Balech | x | | | | | x | | x | x | X | x |
| <i>P. divergens</i> (Ehrenb.) Balech | x | | | | x | | | x | | X | x |
| <i>P. granii</i> (Ostenf.) Balech | x | | | | | | | | | | |
| <i>P. leonis</i> (Pav.) Balech | x | | | | x | | | | | | |
| <i>P. oblongum</i> (Aurivil.) Parke & Dodge | x | | | | | | | | | | |
| <i>P. pallidum</i> (Ostenf.) Balech | | | | | x | x | x | x | x | X | x |
| <i>P. pellucidum</i> Bergh | x | | x | | x | x | | x | | | x |
| <i>P. steinii</i> (Jørgen.) Balech | x | | x | | x | x | x | x | | X | x |
| <i>Protoperidinium</i> sp. | | | x | | x | | | | | | |
| <i>Polykrikos</i> cf. <i>schwartzii</i> Bütschli | | | | | | | | x | | | |
| <i>Scrippsiella</i> - group ⁷ | x | x | x | | x | x | x | | x | X | x |
| Haptophytes - Coccolithophyceae | | | | | | | | | | | |
| <i>Phaeocystis globosa</i> * Scherffel | | | x | | | | | | | | |
| <i>Phaeocystis pouchetii</i> * (Har.) Lagerh. | | | | | | | | x | | X | |
| Euglenophytes - Euglenophyceae | | | | | | | | | | | |
| <i>Eutreptiella</i> cf. <i>braarudii</i> Throndsen | | | | x | | | x | x | | | |
| <i>Eutreptiella</i> sp. | x | | x | | | | | | | | |
| Various | | | | | | | | | | | |
| Monads ⁸ | x | x | x | x | x | x | x | x | x | X | x |
| Choanoflagellates | x | | | | | | | x | | X | x |
| Chrysophytes - Chrysophyceae | | | | | | | | | | | |
| <i>Dinobryon</i> sp. | x | | | | | | | x | x | X | x |
| <i>Meringosphaera</i> sp. | | x | | | | | | | | | x |
| Silicoflagellates - Dictyochophyceae | | | | | | | | | | | |
| <i>Dictyocha fibula</i> Ehrenberg | | x | | | x | x | | | | | |
| <i>Dictyocha speculum</i> Ehrenberg | | x | x | x | x | x | x | x | | X | |
| Ebridians-Thecofilosea | | | | | | | | | | | |
| <i>Ebria tripartita</i> (Schum.) Lemm. | x | x | x | | | | | | | X | x |

| Table continue | 22 June 09 | 05 Aug. 09 | 22 Sep. 09 | 20 Oct. 09 | 17 Nov. 09 | 09 Dec. 09 | 21 Jan. 10 | 11 Mar. 10 | 13 Apr. 10 | 11 May 10 | 22 June 10 |
|--|------------------|------------------|------------------|------------------|------------------|------------------|------------------|------------------|------------------|-----------------|------------------|
| <i>Myrionecta rubra</i> (Lohm.)Jankowski | x | | | | x | | | | | | |
| Ciliates–<i>Ciliophora</i> | x | x | x | x | x | x | x | x | x | X | x |
| Tintinnids–<i>Spirotrichea</i> (<i>Ciliophora</i>) | x | | | | | x | | | | X | |

¹ *Cylindrotheca closterium* (Ehrenberg) Reimann & J. C. Lewin (1964) and *Nitzschia longissima* (Brébisson) Ralfs (1861) are morphologically similar species; they may occur simultaneously and can easily be confused with each other.

² Naviculoids as a general description refer to morphologically similar diatom species (boat-shaped to linear valves with raphe) including genera such as *Navicula* and *Amphora*.

³ *Neoceratium* as a new genus name for the marine species of *Ceratium* was recently suggested by F. Gómez, D. Moreira and D. & P. López – Garcia in 2010 (Gomez et al. 2010).

⁴ *Dinophysis rotundata* Claparède & Lachmann (1859) is currently regarded as a taxonomic synonym of *Phalacroma rotundatum* (Claparède & Lachmann) Kofoid & Michener (1911).

⁵ *Diplopsalis* – group includes several morphologically similar genera of thecate dinoflagellates (spherical to lens-shaped cells) such as *Diplopsalis*, *Diplopsalopsis*, *Oblea*, *Boreadinium*, and *Preperidinium*; in order to distinguish the genera from each other electron microscopy methods must be applied.

⁶ *Minuscula bipes* (Paulsen) Lebour (1925) is a taxonomic synonym of *Protopteridinium bipes* (Paulsen) Balech (1974).

⁷ *Scrippsiella* – group comprises several genera of thecate dinoflagellates with morphological resemblance in the cell structure; includes species from genera *Protopteridinium*, *Scrippsiella* and *Ensiculifera* which can be easily confused with each other.

⁸ Monads in this study refer to the group of small flagellates and non-motile cells that includes species from genera such as e.g. *Cryptomonas*, *Rhodomonas*, *Teleaulax*, and *Pyramimonas*.

* Toxic and potentially toxic species or genera according to UNESCO “Taxonomic Reference List of Harmful Micro Algae” (<http://www.marinespecies.org/HAB/>).

** Recently, *Pseudo-nitzschia pseudodelicatissima* strains isolated from the Thermaikos Gulf, Greece have been reported to produce domoic acid (Moschandreu et al. 2010)

3.3 Abundance of phytoplankton species in the surface layer

During the quantitative examination of samples collected from the surface layer, more than 88 phytoplankton taxa were identified and counted. A total of 36 species and 8 genera within the diatoms; 27 species and 9 genera within the dinoflagellates; 2 dictyochophytes, 1 euglenophyte, 1 chrysophyte, and 1 ebridian were enumerated.

Throughout the cell counting, the members of flagellate algae, such as haptophytes, cryptophytes, and chlorophytes, were counted and gathered into one group called monads (5 – 20 μm). The different *Pseudo-nitzschia* species cannot be distinguished with certainty in light microscopy water mounts; in order to avoid misleading results, cells of *Pseudo-nitzschia* species were counted as one group called *Pseudo-nitzschia* spp. In many samples species identification was difficult due to the small size, discoloration and/or deformation of the cells as a result of fixation. In these cases, unidentified cells were counted and assembled into groups according to their cell size and their approximate taxonomic position (unidentified centric diatom size range 3-20 μm ; unidentified thecate dinoflagellates size range circa 15 μm ; a.o.). Ciliates including tintinnids, and choanoflagellates were counted, but not identified to species level. Results from quantitative examinations (cells per L) are represented in the table 3.2.

3.3.1 Cell counts

The results from cell counting showed that total phytoplankton densities varied greatly during the sampling year; surface phytoplankton cell number peaks were detected in June 2009, September 2009, and January 2010; whereas the lowest phytoplankton density was observed in August and December 2009 (Figure 3.7 A). Seasonal fluctuations in cell abundance of the major algal groups are depicted in Figure 3.7 B.

Diatoms were dominant species most of the time during the sampling period and showed great variations in cell density. The diatom blooms generated high cell concentrations, observable in June-September 2009 and January-March 2010. However, low concentrations of diatom cells were recorded several times, in August and in

December 2009, with 2.1×10^4 cells L^{-1} counted in the samples. In May and June 2010, diatoms were replaced by other phytoplankton groups; dinoflagellates, monads, and small flagellates. Dinoflagellates had minimum abundance in August 2009 (0.6×10^4 cells L^{-1}) and maximum density was observed in the consecutive sample, collected in September 2009 (5.33×10^4 cells L^{-1}).

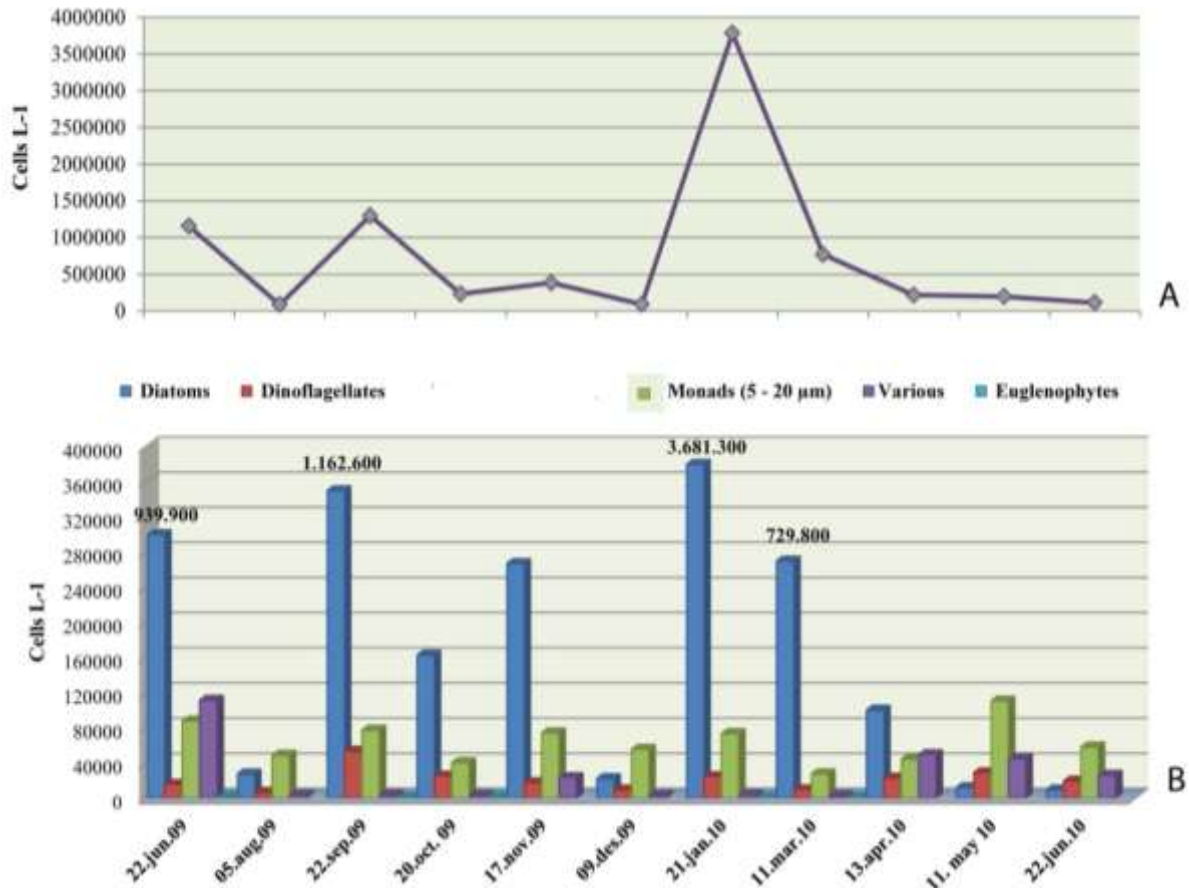


Figure 3.7: Seasonal variation in (A) total phytoplankton density and (B) abundances of the major algal groups in the surface layer during the sampling period.

Generally, the seasonal abundance of the other counted algal groups (such as small monads) in the surface layer was more or less evenly distributed all through the year, except euglenophytes which were observed only in four out of the eleven examined months. The individual contribution of each taxon to the total phytoplankton density, as well as their seasonal changes during June 2009 – June 2010 are shown in Table 3.2.

Already in the first sample collected in June 2009 the diatoms exhibited high cell density, with the phytoplankton assemblage composed of the bloom-forming species

Dactyliosolen fragilissimus and *Skeletonema* spp. (429.200 and 149.200 cells L⁻¹); followed by the *Chaetoceros* community composed of *C. minimus* (36.500 cells L⁻¹), *C. thronsdensii* (57.400 cells L⁻¹), *Chaetoceros* spp. (68.500 cells L⁻¹), and species of the genus *Pseudo-nitzschia* (69.100 cells L⁻¹). *Cylindrotheca closterium* (55.500 cells L⁻¹) and *Leptocylindrus danicus* (35.900 cells L⁻¹) were also important components during the summer diatom peak. *Heterocapsa* cf. *triquetra* and species of the *Scrippsiella*-group dominated among the small sized dinoflagellates with cell densities ranging from 3.600 to 5.600 cells L⁻¹, accordingly. The species of the genera *Ceratium*, *Dinophysis*, and *Protoperidinium* were present, but not abundant. Among the other algal groups, *Dinobryon* sp. (90.400 cells L⁻¹), ciliates (14.300 cells L⁻¹), and unidentified monads (88.000 cells L⁻¹) were most abundant. In samples collected a month later (August 2009), the dynamics between algal groups had changed and the group of unidentified monads became dominant at 48.900 cells L⁻¹, followed by a diatom assemblage consisting of *Pseudo-nitzschia* spp. (15.000 cells L⁻¹), *Skeletonema* spp. (4.600 cells L⁻¹), *Leptocylindrus danicus* (1.700 cells L⁻¹), and a more diverse *Chaetoceros* community represented by *Chaetoceros* cf. *constrictus*, *C. danicus*, *C. lacinosus*, and *C. cf. atlanticus*, with densities of 2.400 cells L⁻¹ on average. In addition to the earlier mentioned taxa, ciliates were the most abundant organisms, followed by *Dictyocha speculum* (1.100 cells L⁻¹) and *D. fibula* (100 cells L⁻¹).

In autumn 2009, a second diatom peak was observed where several individual diatom species generated the high level of dominance. Samples collected in September 2009 revealed that cell concentrations of *Skeletonema* spp. and *Pseudo-nitzschia* spp. reached up to 270.500 and 208.700 cells L⁻¹, respectively. The *Chaetoceros* community was dominated by *C. socialis* (212.000 cells L⁻¹), *C. curvisetus* (44.200 cells L⁻¹), *C. wighamii* (25.200 cells/L⁻¹), and nine other less numerous *Chaetoceros* species (see table 3.2). These genera comprised only 57% of the total diatom population, whereas the remaining 43% was generated by other bloom-forming diatom species (*Leptocylindrus danicus*, *Guinardia* spp., *Asterionellopsis glacialis*, *Dactyliosolen fragilissimus*, *Thalassiosira* spp., and naviculoids). *Skeletonema* spp., *Pseudo-nitzschia* spp., and *Chaetoceros* spp. were still present but less abundant in the samples collected in the following autumn months; whereas the density of *Thalassiosira* species gradually increased and reached 8.300 cells L⁻¹ in November 2009. A diverse dinoflagellate

community was observed in the beginning of autumn (September 2009), where the *Scrippsiella* – group (11.200 cells L⁻¹), *Prorocentrum* spp. (total of 16.600 cells L⁻¹), unidentified naked dinoflagellates (size range 10-24 µm, 8.800 cells L⁻¹), and *Heterocapsa* cf. *triquetra* (8.100 cells L⁻¹) were dominant components, followed by unidentified naked dinoflagellates (size range 25-110 µm) with 1.888 and 1.200 cells L⁻¹, *Oxytoxum* sp. with 2.600 cells L⁻¹, and *Protoperdinium bipes* with 1.500 cells L⁻¹. In the samples collected a month later (October 2009), this community had disappeared and unidentified naked dinoflagellates (size range 10-24 µm) became the dominant taxon with densities of 25.000 cells L⁻¹. By the end of autumn 2009, most dinoflagellates found in the September samples had re-appeared, with an assemblage dominated by unidentified naked dinoflagellates (size range 10-24 µm, 13.000 cells L⁻¹). All through the autumn the small monads were abundant with cell densities ranging from 77.400 cells L⁻¹ in September to 74.400 cells L⁻¹ in November. *Eutreptiella* sp. was present in the beginning and the middle of autumn, with a maximum cell density in October 2009 (1.000 cells L⁻¹); *Dictyocha speculum* reached its highest concentration of 22.200 cells L⁻¹ by the end of autumn (November 2009).

In winter, phytoplankton density dramatically changed from an average of 90.400 cells L⁻¹ in December to 3.783.800 cells L⁻¹ in January, and an increased abundance of several bloom-forming species indicated an early winter diatom bloom. In December, *Pseudo-nitzschia* spp. (11.400 cells L⁻¹) and *Skeletonema* sp. (5.800 cells L⁻¹) contributed most to the diatom community, while the dinoflagellate component was dominated by 10-24 µm size unidentified naked dinoflagellates (5.700 cells L⁻¹), and an assemblage composed of five *Ceratium* species where *C. lineatum* contributed most with 1.100 cells L⁻¹. In January, the diatom community was still dominated by *Pseudo-nitzschia* spp. and *Skeletonema* sp., which reached their maximum cell densities of 1.616.000 cells L⁻¹ and 1.396.900 cells L⁻¹, respectively. Other diatom species which generated high cell concentrations were *Thalassiosira* spp. (325.500 cells L⁻¹), *Leptocylindrus danicus* (96.900 cells L⁻¹), *Chaetoceros* spp. (98.000 cells L⁻¹), with a chaetocerid assemblage of six species (dominated by *C. danicus* with 7.800 cells L⁻¹ and *C. tenuissimus* with 4.200 cells L⁻¹), *Thalassionema nitzschoides* (86.400 cells L⁻¹), *Proboscia alata* (11.900 cells L⁻¹), *Attheya septentrionalis* (9.400 cells L⁻¹), and unidentified centric diatoms (size range 3-20 µm, 6.500 cells L⁻¹), followed by *Rhizosolenia* sp. (3.500 cells L⁻¹),

Cylindrotheca closterium (3.200 cells L⁻¹), *Ditylum brightwellii* (3.000 cells L⁻¹), and *Guinardia delicatula* (2.500 cells L⁻¹). Other phytoplankton groups were less important; the most abundant species were unidentified naked dinoflagellates (size range 10-24 µm, 13.400 cells L⁻¹) and small unidentified thecate dinoflagellates (9.100 cells L⁻¹), followed by *Gymnodinium* sp. (900 cells L⁻¹) and *Protoperidinium pallidum* (400 cells L⁻¹). The group of unidentified monads contributed to the total phytoplankton concentration with 73.500 cells L⁻¹, followed by *Dictyocha speculum* with 2.700 cells L⁻¹, and ciliates with 1.300 cells L⁻¹.

During spring 2010, the phytoplankton community went into a *Chaetoceros*-phase with an average of 196.100 cells L⁻¹, where *C. socialis* with a density of 53.000 cells L⁻¹ was a dominant component in March, whilst *C. simplex* with 50.100 cells L⁻¹ and *C. diadema* with 30.800 cells L⁻¹ were the main chaetocerids in April. In addition to chaetocerids, several diatom taxa reached their maximum concentrations: *Thalassionema nitzschoides* (128.000 cells L⁻¹), *Rhizosolenia* sp. (7.800 cells L⁻¹), *Coscinodiscus* sp. (500 cells L⁻¹), and small unidentified centric diatoms (9.800 cells L⁻¹). However, *Thalassiosira* spp. (178.600 cells L⁻¹), *Pseudo-nitzschia* spp. (141.200 cells L⁻¹), *Leptocylindrus danicus* (30.900 cells L⁻¹), and *Skeletonema* sp. (28.000 cells L⁻¹), were still important taxa in the beginning of spring. Towards summer, *Thalassiosira* spp. and *Leptocylindrus danicus* disappeared, while *Skeletonema* sp. maintained a sizable population throughout the spring and beginning of summer. The dinoflagellate community was less abundant in the beginning of spring; an assemblage composed of *Dinophysis*, *Protoperidinium*, and diverse naked dinoflagellates species was observed in April and May. Several dinoflagellate taxa reached their highest concentrations during the spring, such as *Dinophysis norvegica* (1.600 cells L⁻¹), *D. acuminata* (500 cells L⁻¹), *Gymnodinium* sp. (1.200 cells L⁻¹), *Scropsiella*- group (2.500 cells L⁻¹), *Heterocapsa* cf. *triquetra* (1.200 cells L⁻¹), *Protoperidinium steinii* (1.100 cells L⁻¹), and *Katodinium* sp. (700 cells L⁻¹). Among other phytoplankton groups the unidentified monads were abundant components with densities ranging from 27.800 cells L⁻¹ in March to 110.600 cells L⁻¹ in May. *Eutreptiella* sp. (400 cells L⁻¹) was found for the last time in March, while a population of *Dinobryon* sp. re-appeared and increased during the spring.

Considerably reduced populations of *Chaetoceros* spp. (1.500 cells L⁻¹), *Pseudo-nitzschia* spp. (with minimum of 500 cells L⁻¹), *Proboscia alata* (400 cells L⁻¹), and *Cylindrotheca closterium/Nitzschia longissima* (200 cells L⁻¹) were found in June 2010. Dinoflagellates, however, were still a dominant component of the phytoplankton community which began its transformation into a dinoflagellate-phase already in the end of spring. Among the important dinoflagellates were *Gymnodinium* sp. (2.000 cells L⁻¹), *Scrippsiella*-group (1.500 cells L⁻¹), *Proto-peridinium* spp. (more than 1.000 cells L⁻¹), and unidentified naked dinoflagellates of different size group (see Table 3.2); followed by *Dinophysis norvegica* (1.400 cells L⁻¹), *D. acuminata* (500 cells L⁻¹), *D. rotundata* (100 cells L⁻¹), *Ceratium fusus* (300 cells L⁻¹), and *C. lineatum* (100 cells L⁻¹). In the samples collected in June 2010, a colony of choanoflagellates (8.800 cells L⁻¹) appeared once again, while the dinoflagellate *Prorocentrum reticulatum* (100 cells L⁻¹) and the embridian *Ebria tripartita* (9.900 cells L⁻¹) were counted for the first time during the sampling period. Stable populations of *Dinobryon* sp. (4.600 cells L⁻¹), and monads (58.200 cells L⁻¹) persisted.

3.3.2 Species diversity

The number of species in a phytoplankton community is commonly used as a measure of species diversity (species richness). This measure (here number of identified species) is however to a large extent affected by sample size (total number of counted cells in each sample). During the quantitative examination, different numbers of species were identified and counted in eleven samples.

To be able to compare species diversity in the counted samples of different size, the data was analysed by the rarefaction method. Rarefaction uses the data from the smallest samples to estimate species diversity in the other samples by assuming that they are equally small. For example, if N organisms were found in the smallest sample, rarefaction uses hypothetical subsamples of N organisms from the largest sample, and calculates the average number of species; this average can be compared to the number of species actually found in the smallest sample. The smallest number of cells was counted in the samples from December 2009 (851 cells per 10 mL) and June 2010 (1,032 cells per 10 mL). An approximate cell count of 1000 cells was used to standardize all samples by the rarefaction method to make species diversity comparable. Figure 3.8

shows the results from the rarefaction analysis, on the plot the original and rarefied numbers of species are a function of the sampling effort. As the rarefaction plot shows, the species diversity has a slight fluctuation during the sampling year but it is not dramatically different before and after rarefaction (Figure 3.8, A and B). According to the raw data, the highest species diversity was found in the sample from September 2009, when more than 50 species were identified. The plot with estimated number of species, however, shows that the diversity in the September-sample is not that different from the species diversity found in samples collected in August 2009.

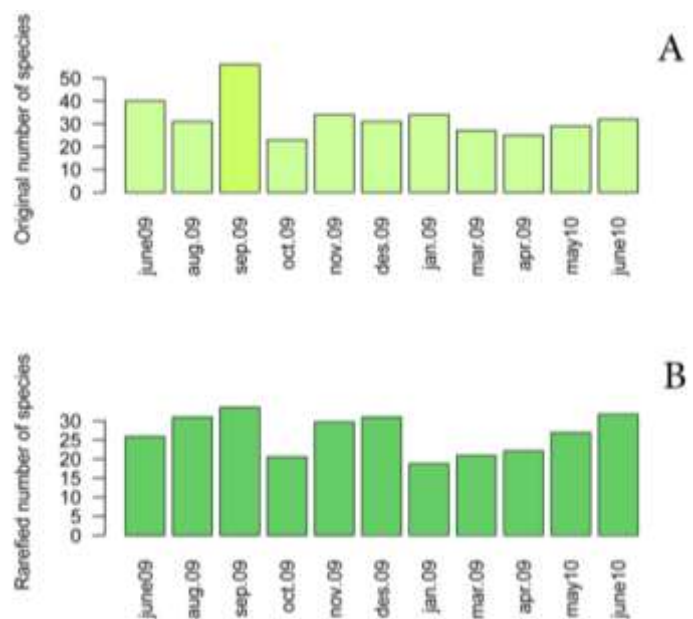


Figure 3.8: Rarefaction plot of original number of species (A) identified during the quantification analysis of the sampling period (June 2009-June 2010) and estimated number of species (B) in the same samples

Table 3.2: Phytoplankton densities (cells L⁻¹) and their seasonal contribution during the sampling year (June 2009-June 2010).

| Date of sampling | 22 June 09 | 05 Aug. 09 | 22 Sep. 09 | 20 Oct. 09 | 17 Nov. 09 | 09 Dec. 09 | 21 Jan. 10 | 11 Mar. 10 | 13 Apr. 10 | 11 May 10 | 22 June 10 |
|-----------------------------------|------------|------------|------------|------------|------------|------------|------------|------------|------------|-----------|------------|
| Diatoms-Bacillariophyceae | | | | | | | | | | | |
| <i>Asterionellopsis glacialis</i> | | | 4400 | | | | | | 400 | 800 | 800 |
| <i>Attheya septentrionalis</i> | | | | | 400 | 1000 | 9400 | 3500 | | | |
| <i>Cerataulina pelagica</i> | 1000 | 1000 | 500 | | | | | | | | |
| <i>Chaetoceros contortus</i> | | | 600 | | | | | | | | |
| <i>C. cf. constrictus</i> | | 1100 | | | | | 1300 | | | | |
| <i>C. curvisetus</i> | | | 44200 | 1500 | 3700 | | | | | | |
| <i>C. danicus</i> | | 200 | 400 | 200 | 5100 | 100 | 7800 | | | | |
| <i>C. debilis</i> | | | | 500 | 4200 | | | | | | |
| <i>C. decipiens</i> | | | 8000 | 800 | | | | | | 1900 | |
| <i>C. diadema</i> | | | | | | | | | 30800 | | |
| <i>C. didymus</i> | | | | | | | 700 | | | | |
| <i>C. laciniosus</i> | | 500 | | | 1600 | | | 8300 | | | |
| <i>C. minimus</i> | 36500 | | 17600 | | | | | | | | |
| <i>C. cf. atlanticus</i> | | 200 | 8000 | | 5100 | 100 | | | | | |

| Table continue | 22 June 09 | 05 Aug. 09 | 22 Sep. 09 | 20 Oct. 09 | 17 Nov. 09 | 09 Dec. 09 | 21 Jan. 10 | 11 Mar. 10 | 13 Apr. 10 | 11 May 10 | 22 June 10 |
|--|------------------|------------------|------------------|------------------|------------------|------------------|------------------|------------------|------------------|-----------------|------------------|
| <i>C. similis</i> | | | | | 700 | | 1500 | | | | |
| <i>C. simplex</i> | | | 600 | | | | | | 50100 | | |
| <i>C. socialis</i> | | | 212000 | | 700 | | | 53000 | | | |
| <i>C. subtilis</i> | | | 1000 | | | | 500 | | | | |
| <i>C. tenuissimus</i> | 7000 | 100 | 12400 | | | | 4200 | | | | |
| <i>C. teres</i> | | | 15600 | | | | | | | | |
| <i>C. throndsenii</i> | 57400 | | | | | | | | | | |
| <i>C. wighamii</i> | 3800 | | 25200 | | | | | | | | |
| <i>Chaetoceros</i> spp. | 68500 | 300 | 138000 | 5800 | 5900 | 500 | 98000 | 134800 | 9000 | 1500 | 1500 |
| <i>Coscinodiscus</i> spp. | | 100 | 100 | | 200 | 300 | 200 | 500 | | | |
| <i>Cylindrotheca closterium</i> | 55500 | 200 | 116500 | 3000 | 400 | 100 | 3200 | 300 | 200 | 700 | 200 |
| <i>Dactyliosolen fragilissimus</i> | 429200 | 800 | 3600 | 2100 | 1200 | 200 | 1000 | | | | |
| <i>Ditylum bringhtwellii</i> | | | 100 | 500 | 300 | 100 | 3000 | | | | |
| <i>Guinardia flaccida</i> | | | 100 | | | | | | | 500 | 200 |
| <i>Guinardia delicatula</i> | 1000 | | 3600 | 1300 | | 100 | 2500 | 300 | | | |
| <i>Leptocylindrus danicus</i> | 35900 | 1700 | 61600 | 900 | 5300 | 500 | 96900 | 30900 | | | |
| <i>Leptocylindrus minimus</i> | 10500 | | 5400 | | 4000 | | | | | | |
| Naviculoids | | 200 | 1000 | 300 | 1700 | | 2800 | 3300 | 2500 | 3600 | 4800 |
| <i>Pleurosigma normanii</i> | | | | 200 | | | | | | | 100 |
| <i>Proboscia alata</i> | 4700 | 600 | 300 | | 2300 | 1200 | 11900 | 1500 | 600 | 300 | 400 |
| <i>Pseudo-nitzschia</i> spp.* | 69100 | 15000 | 208700 | 91500 | 150100 | 11400 | 1616000 | 141200 | 1400 | 800 | 500 |
| <i>Pseudosolenia calcar-avis</i> | | | | | | | 100 | | | | |
| <i>Rhizosolenia</i> cf. <i>borealis</i> / <i>styliformis</i> | 100 | | | | | | | | | 100 | |
| <i>R. hebetata</i> f. <i>sempina</i> | 300 | | | | | | 1500 | | | | |
| <i>R. pungens</i> | | 400 | 300 | 200 | | | | | | | |
| <i>Rhizosolenia</i> sp. | 300 | | 400 | | 1700 | | 3500 | 7800 | 100 | | |
| <i>Skeletonema</i> spp. | 149200 | 4600 | 270500 | 47200 | 64300 | 5800 | 1396900 | 28000 | 1400 | 1600 | 1000 |
| <i>Thalassionema nitzschoides</i> | 8900 | | 300 | | | | 86400 | 128000 | 3400 | 400 | |
| <i>Thalassiosira</i> spp. | | | 1600 | 1800 | 8300 | | 325500 | 178600 | | | |
| Unidentified centr. diatoms (3 - 20 µm) | 1000 | 600 | | 5000 | | 1000 | 6500 | 9800 | 300 | | |
| Dinoflagellates-Dinophyta | | | | | | | | | | | |
| <i>Actiniscus pentasterias</i> | | | | | | | | | | | 100 |
| <i>Akashiwo sanguinea</i> | | | 100 | | | 200 | | | 100 | | |
| <i>Amphidinium</i> cf. <i>longum</i> | | | 300 | | | | | | | | |
| <i>Amphidinium</i> sp.* | | 100 | | | | | | | | | |
| <i>Ceratium furca</i> | | 100 | | 100 | | | | | | | |
| <i>C. fusus</i> | | | | | 300 | 100 | | 100 | | | 300 |
| <i>C. horridum</i> | | 300 | | | | 100 | | | | 200 | |
| <i>C. lineatum</i> | 100 | 600 | | | 1000 | 1100 | | | | | 100 |
| <i>C. longipes</i> | 200 | 100 | | | | 200 | | | | | |
| <i>C. tripos</i> | 200 | 200 | 100 | | 700 | 400 | | | | | |

| Table continue | 22 June 09 | 05 Aug. 09 | 22 Sep. 09 | 20 Oct. 09 | 17 Nov. 09 | 09 Dec. 09 | 21 Jan. 10 | 11 Mar. 10 | 13 Apr. 10 | 11 May 10 | 22 June 10 |
|---|------------------|------------------|------------------|------------------|------------------|------------------|------------------|------------------|------------------|-----------------|------------------|
| <i>Dinophysis acuminata*</i> | 200 | | 300 | | | | | | 200 | 1000 | 500 |
| <i>D. acuta *</i> | | | | | | | | | | 200 | |
| <i>D. norvegica *</i> | 100 | | | | 100 | 100 | | | 1600 | 1200 | 1400 |
| <i>D. rotundata *</i> | | | 100 | | | | | | | | 100 |
| <i>Diplopsalis</i> – group | | | | | | | | | 200 | | |
| <i>Gonyaulax digitale</i> | | | 100 | | | | | | | | |
| <i>Gymnodinium</i> sp. | 1900 | | | | | 100 | 900 | | | 600 | 2000 |
| <i>Gyrodinium</i> cf. <i>spirale</i> | | | 100 | | | | | | | | |
| <i>Gyrodinium</i> sp. | | | 100 | 100 | 400 | | | 700 | 200 | 1200 | 200 |
| <i>Heterocapsa</i> cf. <i>triquetra</i> | 3600 | 100 | 8100 | | | 300 | | | | 1200 | |
| <i>Katodinium</i> sp. | | | | | | | | | | 700 | |
| <i>Micracanthodinium</i> cf. <i>claytoni</i> | 900 | | | | | | | | | | 100 |
| <i>Oxytoxum</i> sp. | | | 2600 | | 700 | 100 | | | | | 300 |
| <i>Prorocentrum</i> cf. <i>glacile</i> | | | 2400 | | | | | | | | |
| <i>P. micans</i> | | | 5900 | | | | | | | | |
| <i>Prorocentrum</i> spp. | | | 8300 | | | | | | | | |
| <i>Protoceratium reticulatum *</i> | | | | | | | | | | | 100 |
| <i>Protoperidinium bipes</i> | 100 | 100 | 1500 | | 300 | | 300 | 300 | | 100 | 300 |
| <i>P. brevipes</i> | 600 | | | | | | | 200 | | | |
| <i>P. conicum</i> | 100 | | | | | | | | | | |
| <i>P. depressum</i> | | | | | | | | | 100 | | |
| <i>P. pallidum</i> | | | | | | 200 | 400 | 700 | 600 | 100 | |
| <i>P. pellucidum</i> | 200 | | 100 | | | | | | | | |
| <i>P. steinii</i> | 400 | | 200 | | | | | | | 1100 | 100 |
| <i>Protoperidinium</i> spp. | | | | | 400 | | | | | | 1000 |
| <i>Scrippsiella</i> – group | 5600 | 200 | 11200 | | 700 | 700 | 100 | | 2500 | 900 | 1500 |
| Unidentified thekate dinoflagellates (ca 15 µm) | | | | | | | 9100 | | | | |
| Unidentified naked dinoflagellates (ca 10-24 µm) | 1500 | 4700 | 8800 | 25000 | 13100 | 5700 | 13900 | 4800 | 13400 | 16300 | 9800 |
| Unidentified naked dinoflagellates (ca 25-40 µm) | | | 1888 | | | | | 2800 | 4000 | 4300 | 1600 |
| Unidentified naked dinoflagellates (ca 50-110 µm) | | | 1200 | | | | | | | | |
| Monads (5 - 20 µm) | 88000 | 48900 | 77400 | 40600 | 74400 | 55600 | 73500 | 27800 | 44600 | 110600 | 58200 |
| Euglenophytes - Euglenophyceae | | | | | | | | | | | |
| <i>Eutreptiella</i> spp. | 1100 | | 500 | 1000 | | | 300 | 400 | | | |
| Various | | | | | | | | | | | |
| Choanoflagellates | 6700 | | | | | | | | | | 8800 |

| Table continue | 22 June 09 | 05 Aug. 09 | 22 Sep. 09 | 20 Oct. 09 | 17 Nov. 09 | 09 Dec. 09 | 21 Jan. 10 | 11 Mar. 10 | 13 Apr. 10 | 11 May 10 | 22 June 10 |
|---|------------------|------------------|------------------|------------------|------------------|------------------|------------------|------------------|------------------|-----------------|------------------|
| Chrysophytes - Chrysophyceae | | | | | | | | | | | |
| <i>Dinobryon</i> sp. | 90400 | | | | | | | 1900 | 28600 | 38500 | 4600 |
| Silicoflagellates - Dictyochophyceae | | | | | | | | | | | |
| <i>Dictyocha fibula</i> | | 100 | | | | 200 | | | | | |
| <i>Dictyocha speculum</i> | | 1100 | 100 | | 22200 | 1400 | 2700 | | | | |
| Ebridians-Thecofilosea | | | | | | | | | | | |
| <i>Ebria tripartita</i> | | | | | | | | | | | 9900 |
| Ciliates-Ciliophora | 14300 | 2300 | 3500 | 3500 | 1300 | 1500 | 1300 | 600 | 21100 | 6700 | 2800 |
| Tintinnids-Spirotrichea (Ciliophora) | 100 | | 100 | | | | | | | 100 | 100 |

* Toxic and potentially toxic species or genera according to UNESCO “Taxonomic Reference List of Harmful Micro Algae” (<http://www.marinespecies.org/HAB/>).

3.4 *Pseudo-nitzschia* species

3.4.1 Species composition and seasonal occurrence

To determine relationships between the *Pseudo-nitzschia* species and different seasons, the occurrence and composition of the *Pseudo-nitzschia* species were compared by using a non-metric multidimensional scaling (NMDS) method with a Bray-Curtis index of dissimilarity (Figures 3.9 and 3.10).

The first NMDS ordination diagram (Figure 3.9) shows similarity patterns of the eleven samples, where the relative distance between the dates indicates the amount of similarity or difference. The spreading pattern of the dates showed a certain degree of dissimilarity according to their distributions along the ordination axes and the dates cannot be clearly separated in the ordination diagram. However, the sampling months can be divided into two seasonal groups according to their clustering, which also outlines the seasonal cycle within the *Pseudo-nitzschia* assemblages. The second NMDS ordination diagram (Figure 3.10) illustrates similarity patterns in species composition of the genus *Pseudo-nitzschia*. It indicates that the nine species identified from vertical net

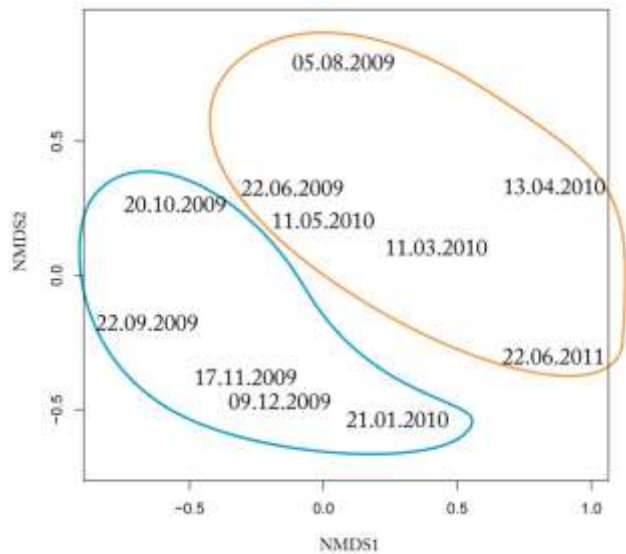


Figure 3.9: Ordination diagram showing seasonal changes in the occurrence of the *Pseudo-nitzschia* assemblage within the sampling year (June 2009-June 2010); the circles indicate different seasons: orange-summer and spring, blue-autumn and winter.

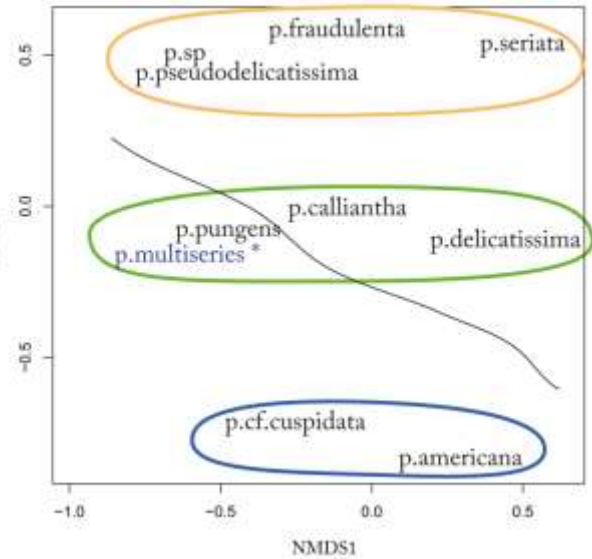


Figure 3.10: Ordination diagram showing seasonal changes in the species composition of the genus *Pseudo-nitzschia* during the sampling year (June 2009-June 2010); explanation is in the text.

haul samples in association with the different seasons could be separated into three clearly distinct groups: summer-spring (species contoured with orange circle: *Pseudo-nitzschia fraudulenta*, *P. pseudodelicatissima*, *P. sp.*, and *P. seriata*), “all year round” (species contoured with green circle: *P. calliantha*, *P. delicatissima*, and *P. pungens*) and autumn-winter (species contoured with blue circle: *P. americana* and *P. cf. cuspidata*) (Figure 3.10). Occurrence of the *P. multiserries* in the “all year round” group needs to be interpreted; this species was observed only in October and November 2009.

3.4.2 Morphology

A detailed morphological examination of the *Pseudo-nitzschia* species was performed with scanning (SEM) and transmission (TEM) electron microscopy; five grids and one stub from each month were analysed. At least ten species of *Pseudo-nitzschia* were found, nine of them were identified to the species level: *Pseudo-nitzschia delicatissima*, *P. pseudodelicatissima*, *P. calliantha*, *P. cf. cuspidata*, *P. pungens*, *P. multiserries*, *P. fraudulenta*, *P. seriata*, and *P. americana*. One unidentified *Pseudo-nitzschia* species was

observed (*Pseudo-nitzschia* sp.). It resembled *P. pseudodelicatissima* in all morphometric characteristics but differed in poroid structure.

The following descriptions of the *Pseudo-nitzschia* species include the specific morphological features of the cells, such as colonies and valve shapes; measurements of apical and transapical axis; density and structure of the valve striae, fibulae, and poroids; number and structure of girdle bands; as well as ultrastructure of the valve poroid hymen.

The identified *Pseudo-nitzschia* species were sorted into three groups based on morphological similarity of the cell features. The *delicatissima*-group (Table 3.3) comprises thin, narrow species with a transapical valve axis ca. 3 µm long: *P. delicatissima*, *P. pseudodelicatissima*, *P. calliantha*, *P. cf. cuspidata*, and *Pseudo-nitzschia* sp. The *seriata*-group (Table 3.4) includes larger and wider species with a transapical valve axis more than 3 µm. It consisted of *P. pungens*, *P. multiseriata*, *P. fraudulenta* and *P. seriata*. The *americana*-group encompasses species with short and wide cell valves, and was represented by *Pseudo-nitzschia americana*, which was included in the *seriata*-group in this study (see Table 3.4).

A summary of the measurements and morphometric characteristics of the *Pseudo-nitzschia* species is present in the Tables 3.3 and 3.4; a full overview of measurements for each *Pseudo-nitzschia* spp. can be found in Appendix 2 (Morphometric measurements of *Pseudo-nitzschia* species collected in Outer Oslofjorden).

The *delicatissima*-group

***Pseudo-nitzschia delicatissima* (Cleve) Heiden in Heiden & Kolbe, 1928**

Plate 1

Basionym: *Nitzschia delicatissima* Cleve, 1897

Synonym: *Nitzschia actydrophila* Hasle, 1965

Occurrence: *Pseudo-nitzschia delicatissima* was one of the two most frequently observed *Pseudo-nitzschia* species and was present on 9 of the 11 sampling dates. It was not observed in August and September 2009, but was the only species of the genus present in the water sample in June 2010.

Description: *Pseudo-nitzschia delicatissima* occurred in 2 – 6 cell long stepped colonies. The overlap of cells was short, approximately 1/9 – 1/10 of cell length (Plate 1, pic. A and B). In girdle view valve shape was narrow and linear with slightly sigmoid, cut ends (Plate 1, pic. C and D). In valve view, cells were somewhat wider in the middle and gradually tapered towards rounded cell ends; the two ends of the valves had a similar structure (Plate 1, pic. D and F) in girdle and valve view. Transapical axis of valves varied between 1.2 and 2 μm , apical axis between 51.2 and 69.3 μm . A central nodule divided the eccentric raphe in the middle and the central interspace occupied 4 – 6 striae (Plate 1, pic. E).

The number of striae varied from 36 – 42 in 10 μm , the number of fibulae from 21 – 25 in 10 μm . Both striae and fibulae were regularly spaced. The valve striae were biseriate and had five to 11 poroids in 1 μm . Poroids were located close to the interstriae and varied in size and shape (Plate 1, pic. H). Poroid hymens had a hexagonal perforation pattern. The distal and proximal mantles were one poroid high and divided into several sectors (not shown). The girdle consisted of three bands. The first girdle band (valvocopula) had striae and one row of split perforated poroids, the second band had a silicified ridge dividing the band into two parts and irregular poroids; a third unperforated band was also observed (Plate 1, pic. G).

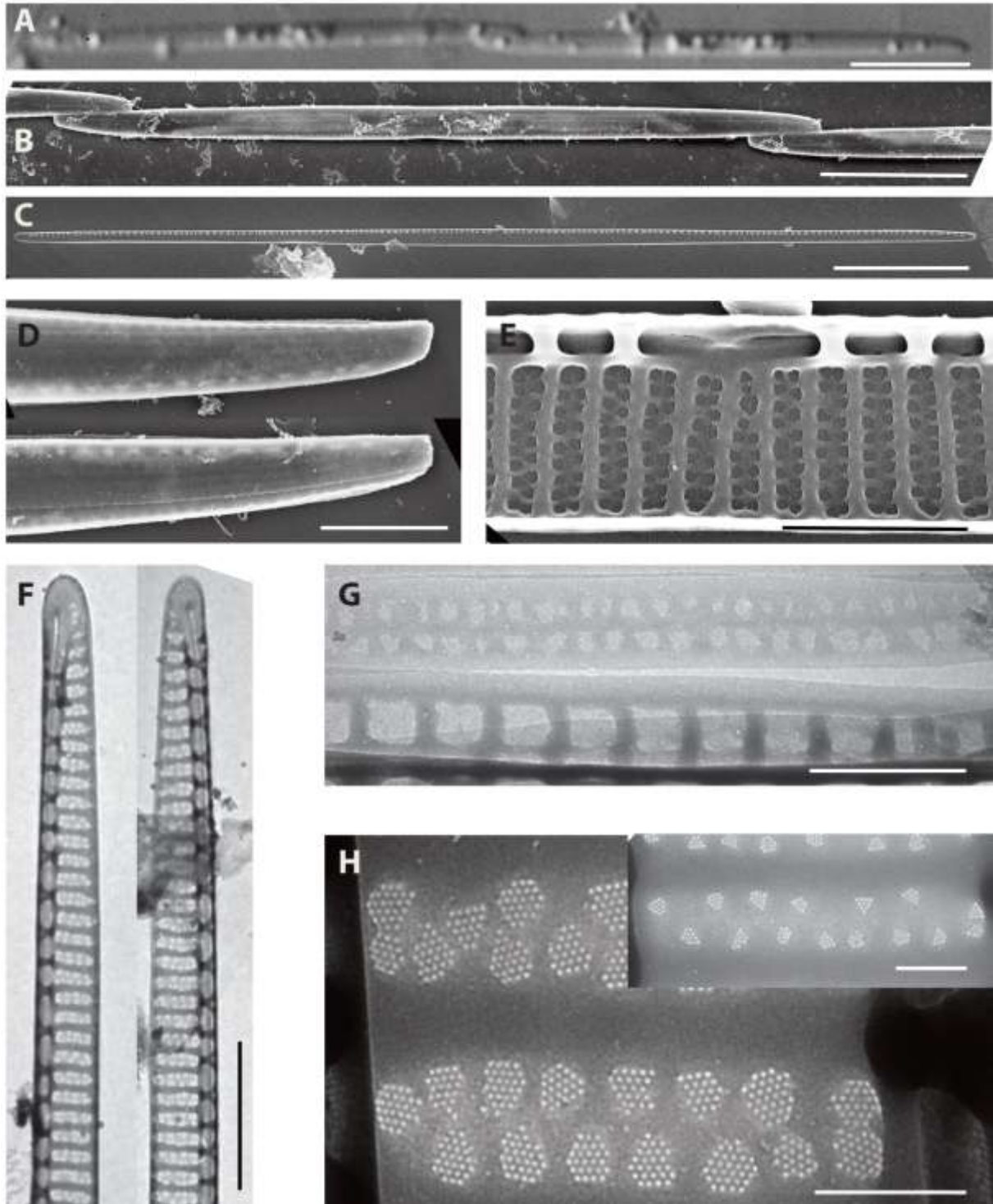


Plate 1: *Pseudo-nitzschia delicatissima*. Light (A), SEM (B, C, D, E) and TEM (F, G, H) micrographs. (A, B and C) Scale bars = 10 μm . (D and F) Scale bars = 2 μm . (E) Scale bar = 1 μm . (G) Scale bar = 0.5 μm . (H) Scale bar = 0.2 μm .

(A) Part of a chain in girdle view, lugol-preserved sample, DIC. (B) Colony with cell overlap, girdle view. (C) Whole valve, internal view. (D) Girdle view of “cut-off” valve ends. (E) Internal view of middle part of valve, showing larger central interspace, biseriate striae and central nodule. (F) The two ends of one valve from valve view; note rounded shape and no difference in structure. (G) Fragment of the first two girdle bands. (H) Poroids in two rows with hexagonal perforation pattern; note the different poroid shape and size.

The *delicatissima*-group

***Pseudo-nitzschia pseudodelicatissima* (Hasle) Hasle *emend.* Lundholm, Hasle et Moestrup, 2003**

Plate 2

Basionym: *Nitzschia pseudodelicatissima* Hasle, 1976

Synonym: *Nitzschia delicatula* Hasle, 1965

Occurrence: *Pseudo-nitzschia pseudodelicatissima* was found only in the samples taken in June and October 2009.

Description: In light microscope *Pseudo-nitzschia pseudodelicatissima* can be easily confused with morphologically similar *P. delicatissima*. Observed cells of *P. pseudodelicatissima* had narrow and linear shape both in girdle and valve views, with short tapering parts towards valve ends (Plate 2, pic. A). The ends of valves were similar in shape and structure (Plate 2, pic. B). Apical axis ranged from 58.7 to 68.4 μm and transapical axis from 0.7 to 1.5 μm . A larger central interspace occupied five striae and the eccentric raphe was divided in the middle by a central nodule (Plate 2, pic. C).

Fibulae and striae were relatively regularly spaced. The number of fibulae and striae ranged from 22 to 25 in 10 μm and from 41 to 43 in 10 μm , respectively. The observed valve striae were uniseriate, with one row of oval to square poroids and a density of 4 – 5 poroids in 1 μm . The poroid hymen was divided into several perforated parts, usually into two larger sectors separated from each other by an unperforated strip of silica (Plate 2, pic. E). The distal and proximal mantels were similar to the valves and about one poroid high. Both valves and bands had a hexagonal pattern of perforations. The three girdle bands were ornamented and had an unperforated margin (Plate 2, pic. D). First girdle band (valvocopula) was striated and contained one row of large elongated poroids usually split into 2 – 3 perforated sectors, while the poroids of the other two girdle bands were smaller and rarely perforated (Plate 2, pic. D).

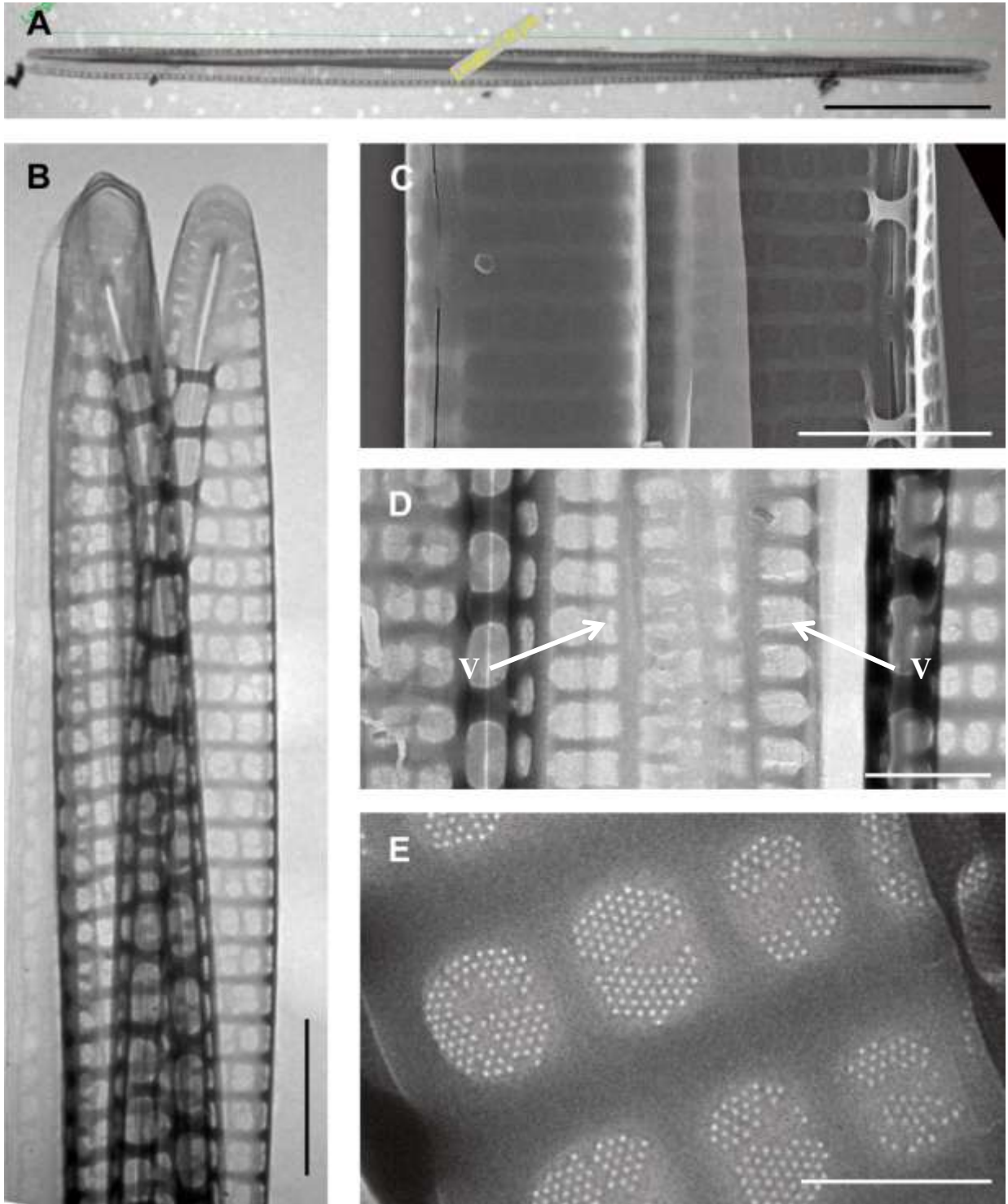


Plate 2: *Pseudo-nitzschia pseudodelicatissima*. TEM (A, B, D and E) and SEM (C) micrographs. (A) Scale bar = 10 μm . (B and C) Scale bars = 1 μm . (D) Scale bar = 0.5 μm . (E) Scale bar = 0.2 μm .

(A) Valves from the same cell. (B) Valve ends with cingular band (left), no difference in shape and structure of valve ends. (C) Middle part of valve with large central interspace and central nodule, internal and external views. (D) Girdle bands, valvocopulas are shown with arrows. (E) Striae with one row of poroids; note hexagonal pattern of perforations.

***Pseudo-nitzschia calliantha* Lundholm, Moestrup et Hasle, 2003**

Plate 3

Occurrence: The second most frequently observed species was *Pseudo-nitzschia calliantha*. Like *P. delicatissima*, *P. calliantha* was detected in 9 out of the 11 examined samples. It was found every month, except in April and June 2010.

Description: *Pseudo-nitzschia calliantha* occurred in stepped colonies. In the colonies the overlap of cells was short, approximately $1/7 - 1/9$ of the cell length (Plate 3, pic. A). In girdle view, cells were linear with a short tapered part towards narrow pointed ends. In valve view, cells had linear to lanceolate shape with abrupt tapering towards slightly pointed ends (Plate 3, pic. B and C). Valve ends were similar in structure and shape (Plate 3, pic. D). The size of observed cells varied: apical axis of valves ranged from 66.6 to 113.3 μm and transapical axis from 1.6 to 2.5 μm . A central nodule divided the eccentric raphe and the central interspace occupied 3 – 4 striae.

Fibulae and striae were more or less regularly spaced. The number of striae and fibulae in 10 μm was 30 – 40 and 16 – 24, respectively. The uniseriate valve striae had 4 – 5 round poroids in 1 μm . The valve poroids in observed cells was divided into 4 - 10 sectors. The central part of the poroids, which was either perforated or not, was encircled by 4 – 9 perforated sectors and together they resembled a flower (Plate 3, pic. F). The distal and proximal mantels were similar to the valves and one poroid high. The girdle contained three bands, each with perforated poroids and bordered by an unperforated margin. The valvocopula were 2 – 3 poroids wide and 6 – 8 poroids high (Plate 3, pic. E). Both valves and girdle bands had a hexagonal perforation pattern.

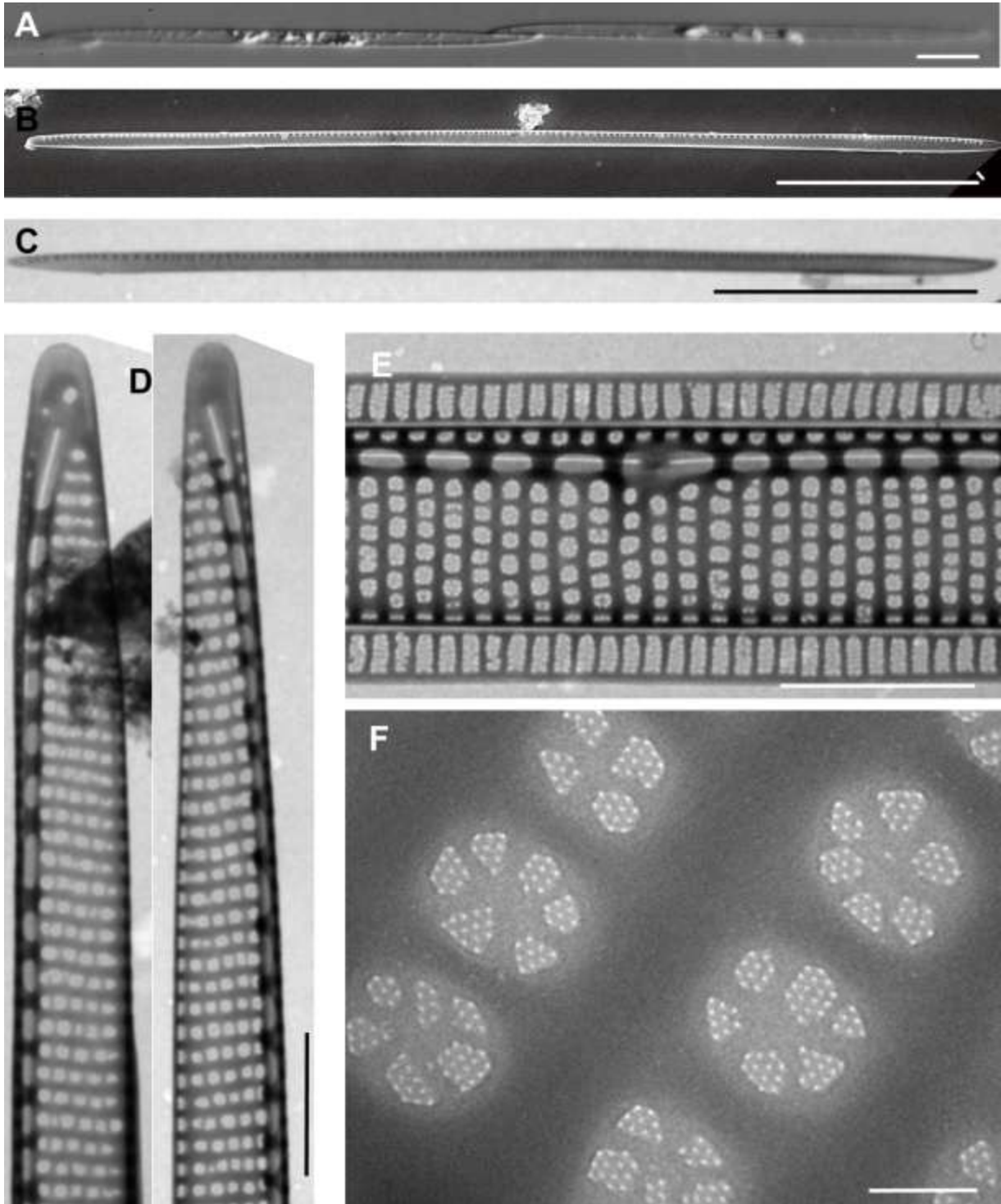


Plate 3: *Pseudo-nitzschia calliantha*. Light (A), SEM (B) and TEM (C, D, E and F) micrographs. (A) Scale bar = 10 μm . (B and C) Scale bars = 20 μm . (D) Scale bars = 5 μm . (E) Scale bar = 2 μm . (F) Scale bar = 0.1 μm .

(A) Girdle view of two cells in chain with overlap, lugol-preserved samples, DIC. (B and C) Whole valves. (D) The two ends of one valve showing similar structure. (E) Central part of valve showing central interspace and central nodule, proximal mantle structure, uniseriate striae and the first girdle band (valvocopula). (F) The poroid hymens is divided into 4-7 sectors resembling a flower pattern; note the hexagonal pattern of perforation.

***Pseudo-nitzschia cf. cuspidata* (Hasle) Hasle emend. Lundholm,
Moestrup & Hasle, 2003**

Plate 4

Basionym: *Nitzschia cuspidata* Hasle, 1965

Occurrence: Cells of the species *Pseudo-nitzschia cf. cuspidata* were observed in the samples taken in November and December 2009.

Description: All cells of *Pseudo-nitzschia cf. cuspidata* were observed in valve view and had lanceolate shape with a gradual tapering from the middle part towards pointed ends (Plate 4, pic. A and B). The valve ends had similar structure and shape as shown on the Plate 4, pic. C.

Transapical axis of valves ranged from 2.3 to 2.9 μm and apical axis from 66.7 to 71.3 μm . A central nodule divided the eccentric raphe and the central interspace occupied 4 – 5 striae. Fibulae and striae were more or less regularly spaced. The number of striae and fibulae in 10 μm was 30 – 33 and 14 – 16, respectively. Valves had uniseriate striae with round, square to oval poroids; 4 – 6 poroids in 1 μm . The poroid hymen had a hexagonal perforation pattern and was usually divided into two sectors separated by an unperforated strip, but poroids with 3 – 4 perforated sectors of different size were also observed (Plate 4, pic. E). The proximal and distal mantles were 3 – 4 poroids high; mantle poroids split in two or several perforated parts were also found. Girdle bands were not observed due to the small number of valves in the samples.

Notes: Since the proximal and distal mantles of observed cells diverge from description given by Lundholm et al. (2003): “the proximal and distal mantles are similar to the valve and one (seldom two) poroids high” in contrast to the multiple poroids observed in this study, it can only be identified as *P. cf. cuspidata*.

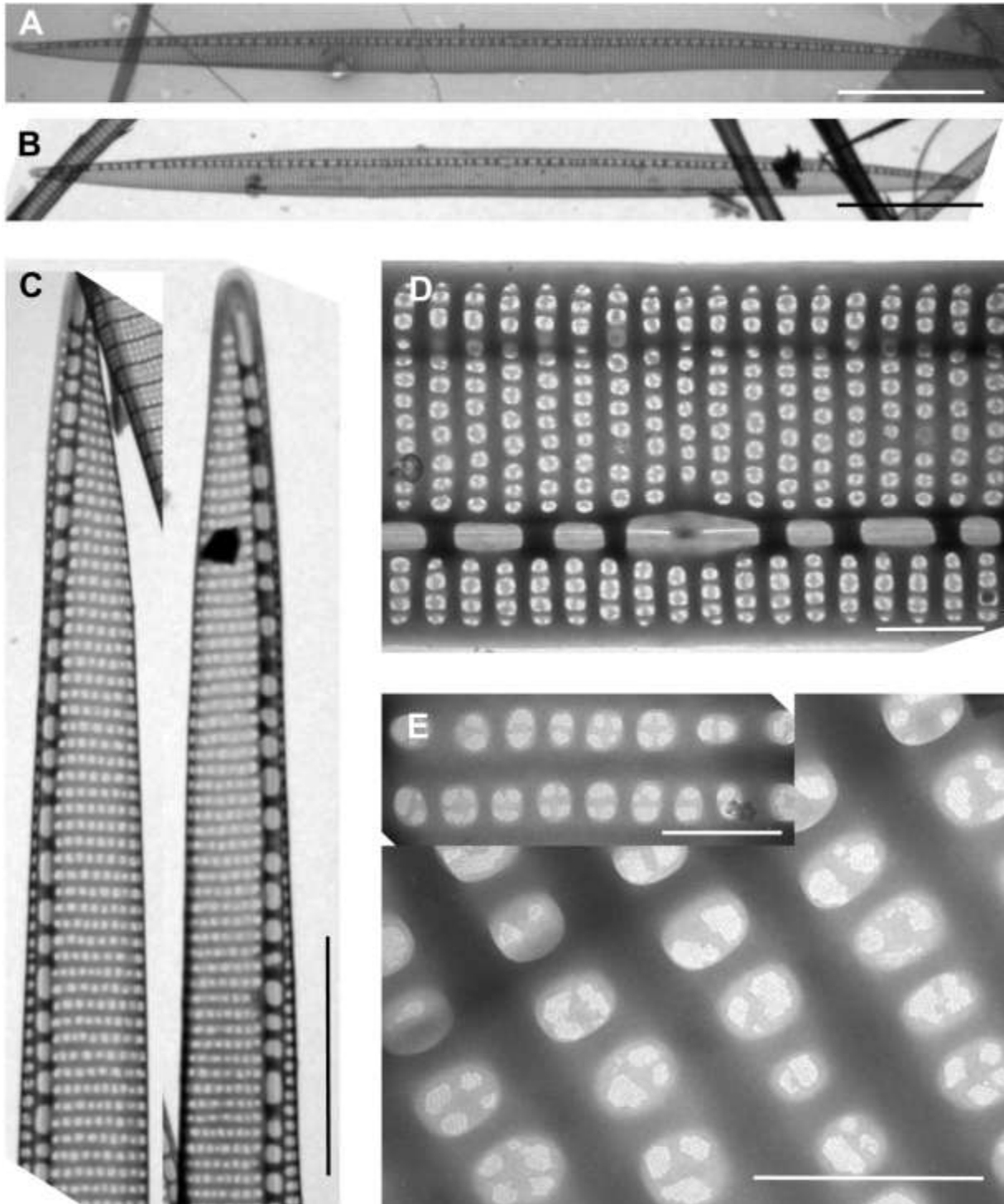


Plate 4: *Pseudo-nitzschia* cf. *cuspidata*. TEM micrographs. (A and B) Scale bars = 10 μm . (C) Scale bar = 5 μm . (D) Scale bar = 1 μm . (E) Scale bar = 0.5 μm .

(A and B) Whole valves from two different cells; note increased tapering towards pointed ends. (C) The two ends of one valve. (D) Middle part of valve showing distal (upper) and proximal (bottom) mantles, uniseriate striae, central interspace and central nodule. (E) Part of the valve with perforated poroids; note variation in poroid structure, usually hymen of poroids divided into two perforated sectors.

The *delicatissima*-group

Pseudo-nitzschia sp.

Plate 5

Occurrence: An unidentified species of the genus *Pseudo-nitzschia* was observed in the samples taken in June and October 2009. During TEM examination a few cells and several fragments were found.

Description: Based on the general valve features and morphometric measurements this species can be placed in the *delicatissima* – group.

In valve view the cells were long, narrow to linear, with gradual tapering parts towards the valve ends (Plate 5, pic. A). The valves of some cells had a slight inflation in the middle part, resembling the valve of *P. inflatula*. The valve ends of observed cells and fragments were pointed and a bit rounded with similar structure (Plate 5, pic. B). Transapical axis ranged from 1.0 to 1.6 μm and apical axis from 65.5 to 72 μm .

The eccentric raphe was divided in the middle by a central nodule; a larger central interspace occupied 4 – 5 striae (plate 5, pic. C). Both fibulae and striae were regularly spaced. However, in several cells striae irregularity in the middle part of the valve was observed. There were 22 – 26 fibulae in 10 μm and 40 – 43 striae in 10 μm . Measurements correspond to general valve features of *P. delicatissima* and *P. pseudodelicatissima* species.

The valve striae of the cells, as well as the observed fragments, were uniseriate; with one row of oval to slightly squared poroids. Hymenate poroids had a density of four to five in 1 μm . The poroid hymen was divided into several irregularly perforated parts (3- 8) separated from each other by unperforated silica strips (Plate 5, pic. C and E). The poroid structure does not fit any known descriptions. The valve mantles were not studied due to the small number of valves observed.

Three girdle bands comprised one row of elongated poroids; the hymen was perforated and divided in several sectors. All girdle bands were bordered by an unperforated margin (Plate 5, pic. D). Both valve and band poroids had a hexagonal pattern of perforation.

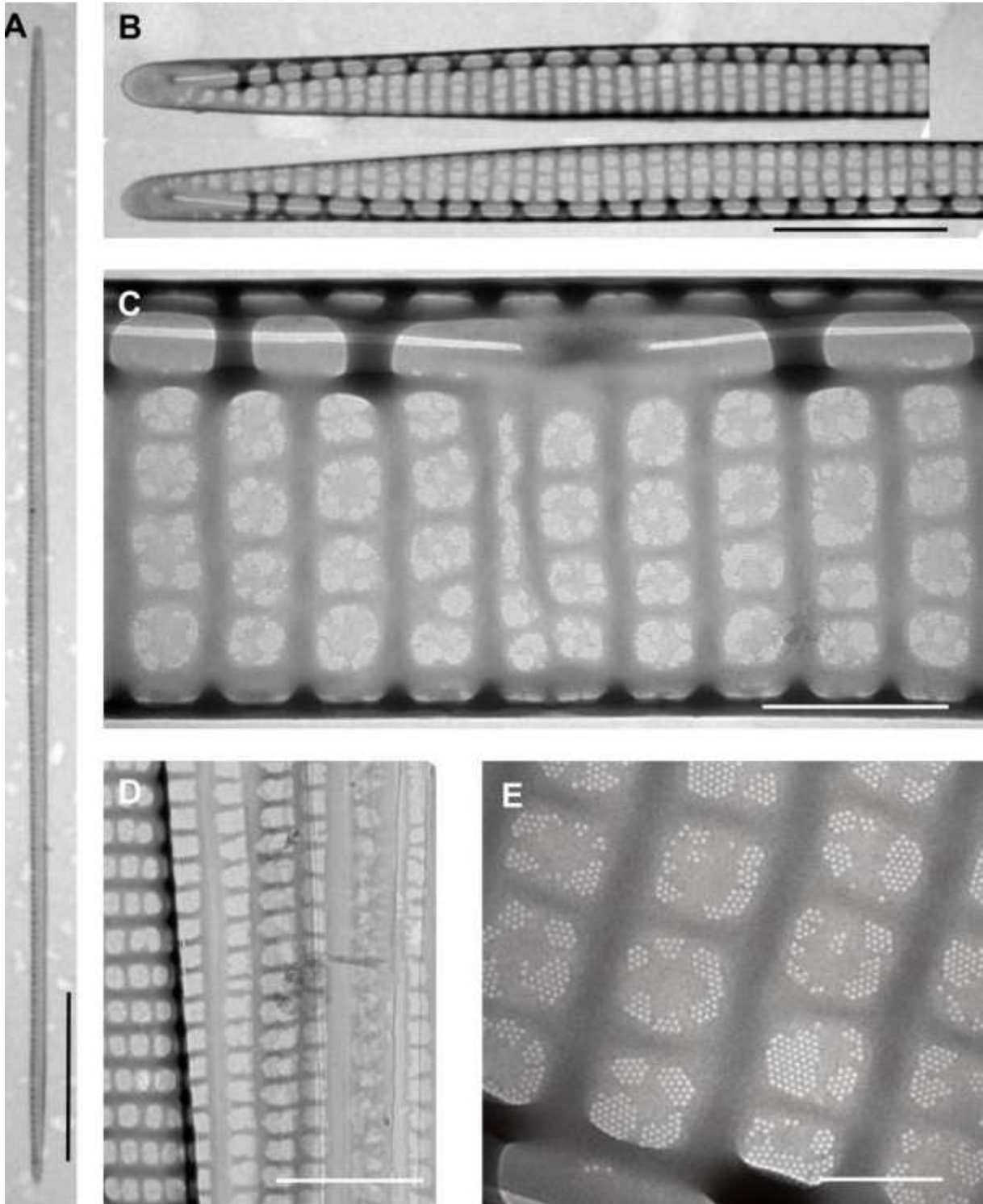


Plate 5: *Pseudo-nitzschia* sp.. TEM micrographs. (A), Scale bar = 10 μm. (B), Scale bar = 2 μm. (C), Scale bar = 0.5 μm. (D), Scale bar = 1 μm. (E), Scale bar = 0.2 μm.

(A) Whole valve; note slight swelling in the middle of cell. (B) The two ends of one valve showing similar structure and tapering toward rounded ends. (C) Middle part of valve with larger central interspace, central nodule and uniseriate striae; note irregularity in the striae pattern. (D) Fragment of the girdle bands. (E) Poroids with different hymen structure; note hexagonal perforation of the hymen.

The *seriata*-group

Pseudo-nitzschia pungens (Grunow ex P.T. Cleve, 1897) Hasle, 1993

Plate 6

Basionym: *Nitzschia pungens* Grunow ex Cleve, 1897

Occurrence: *Pseudo-nitzschia pungens* was a common species and found on 6 out of the 11 examined sampling dates. *P. pungens* first occurred in the sample taken in June 2009; in the next summer sample, from August 2009, *P. pungens* was not found. All through autumn and beginning of winter 2009 *P. pungens* was frequently observed. It was not recorded in the samples from January, March and April 2010. *P. pungens* appeared again in May 2010, but was not found in the last sample collected in June 2010.

Description: Cells of observed *Pseudo-nitzschia pungens* were coarsely silicified, both fibulae and interstriae were visible in the light microscope. Cells were arranged in stepped colonies and the cell overlap in the chains was approximately one - third of cell length (Plate 6, pic. A). In girdle view, cells had linear to lanceolate shape with sharply pointed ends (Plate 6, pic. C). In valve view, cells were lanceolate and symmetrical with short tapering parts towards the cell ends (Plate 6, pic. B). Valve ends had similar shape, but differed in the structure: usually one end had less poroids per stria than the other (Plate 6, pic. D).

The transapical axis of observed cells ranged from 2.5 to 4.6 μm and the apical axis from 82.1 to 120.0 μm . A central nodule was missing. Both fibulae and striae were regularly spaced and equal in number, 11 – 13 in 10 μm . The valve striae of the observed cells were biseriate with two rows of large poroids separated by a non-perforated part (Plate 6, pic. E); regularly as well as irregularly spaced poroids were observed. Hymenate poroids had a hexagonal perforation pattern (Plate 6, pic. F). The number of poroids in 1 μm varied from two to four. Valve mantles and girdle bands were not observed.

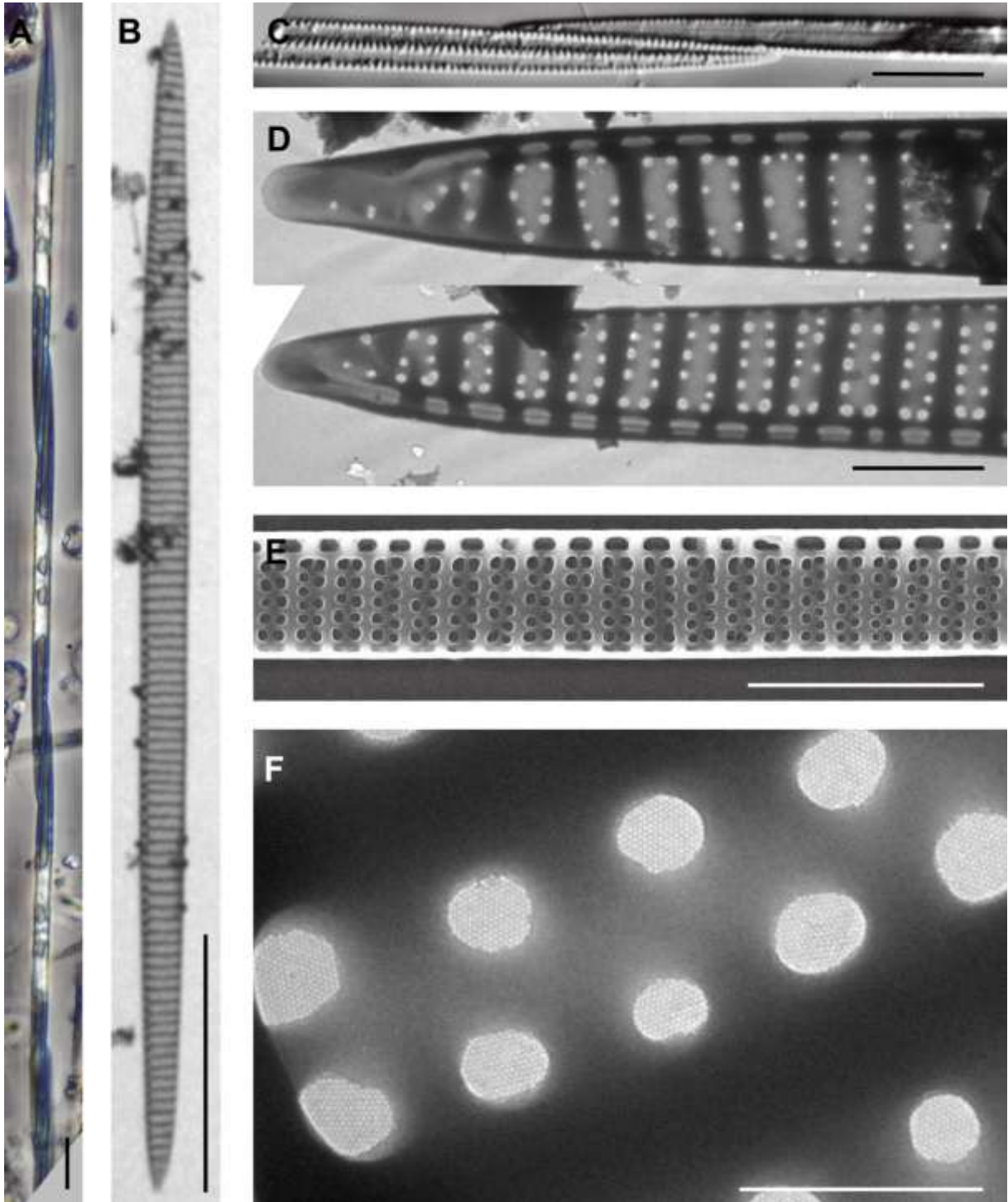


Plate 6: *Pseudo-nitzschia pungens*. Light (A and C), SEM (E) and TEM (B, D and F) micrographs. (A to C) Scale bars = 10 μm . (D) Scale bar = 2 μm . (E) Scale bar = 5 μm . (F) Scale bar = 0.5 μm .

(A) Part of a chain in girdle view, formaldehyde-preserved sample, phase contrast. (B) Whole valve. (C) Girdle view of cell overlaps, formaldehyde-preserved sample, DIC; note pointed ends. (D) The two ends of one valve showing similar structure. (E) Internal view of middle part of valve showing biseriate striae structure. (F) Poroids with regular hexagonal perforations.

The *seriata*-group

Pseudo-nitzschia multiseriata (Hasle) Hasle, 1995

Plate 7

Basionym: *Nitzschia pungens* f. *multiseriata* Hasle, 1974

Synonym: *Pseudo-nitzschia pungens* f. *multiseriata* (Hasle) Hasle, 1993

Occurrence: *Pseudo-nitzschia multiseriata* was seldom observed during the sampling period. This species was found only twice in the autumn samples from October and November 2009.

Description: In the light microscope *Pseudo-nitzschia multiseriata* can be easily confused with *P. pungens*, especially in the girdle view. In valve view, cells had a lanceolate valve outline with short tapering parts towards sharply pointed ends (Plate 7, pic. A). The valve ends were similar in both shape and structure. Several of the observed cells had slightly different interstriae branching of the valve ends, as shown on Plate 7, pic. B.

The length of the transapical axis ranged for 4.9 to 5.8 μm and that of the apical axis from 85.7 to 104.0 μm . A central nodule as well as a larger central interspace was not present. Striae and fibulae were regularly spaced and were present in equal number, 11 – 12 in 10 μm (Plate 7, pic. C). The valve striae had three to five rows of hymenate poroids. Two of these rows were placed close to the interstriae and in between them there were up to three rows in an irregular pattern (Plate 7, pic. D). The number of poroids in 1 μm within each row was 6, however 3 – 5 poroids per 1 μm were also observed. Hymen of poroids had a hexagonal perforation pattern.

The descriptions of valve mantles and girdle bands are not presented in this work due to the small number of observed cells.

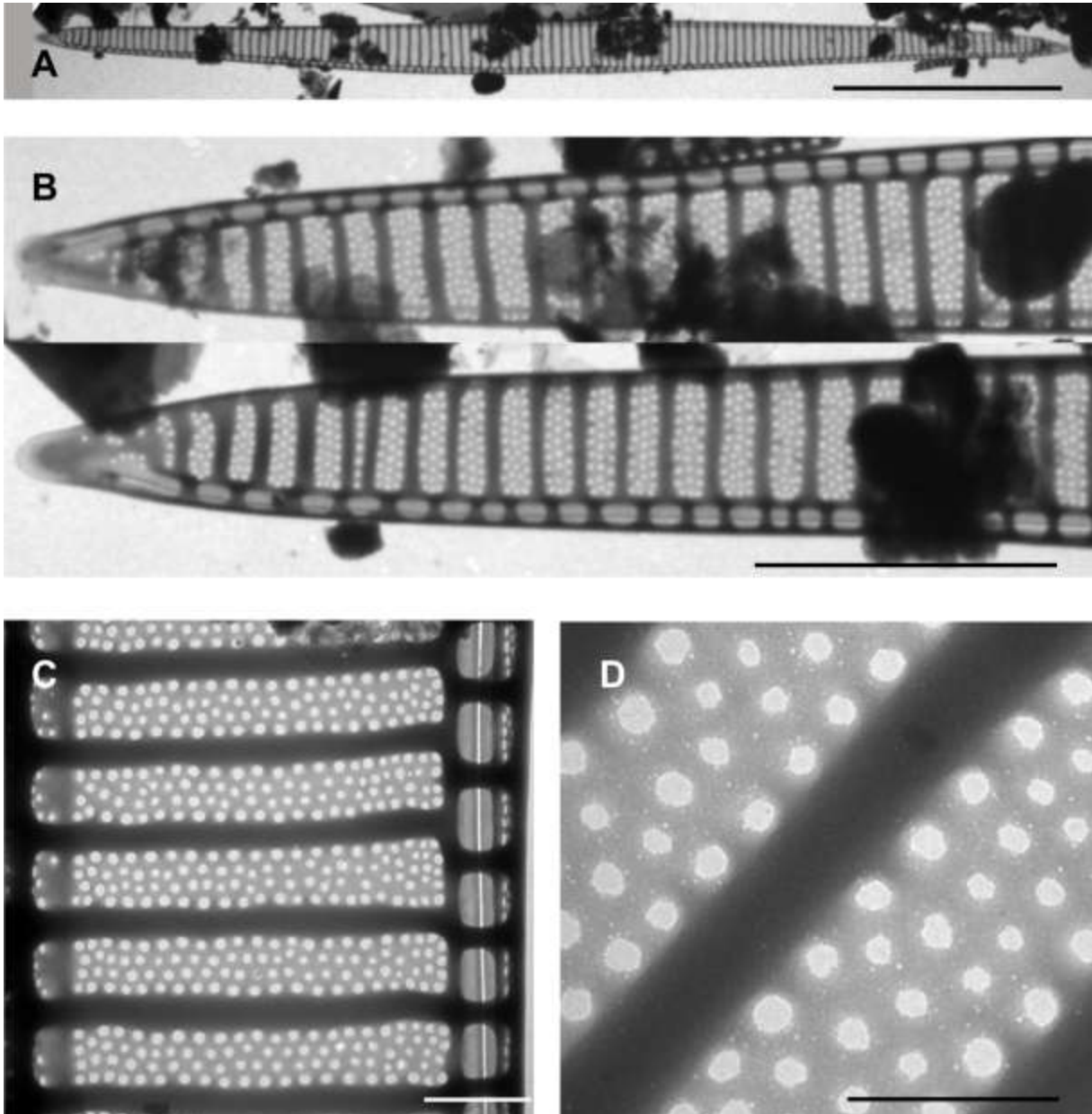


Plate 7: *Pseudo-nitzschia multiseries*. TEM micrographs. (A) Scale bar = 20 μm . (B) Scale bar = 5 μm . (C) Scale bar = 1 μm . (D, Scale bar = 0.5 μm .

(A) Whole valve. (B) The two ends of one valve; note pointed ends and similar structure. (C) Middle part of the valve showing multiseriate striae, interstriae and fibulae. (D) Poroids; note four rows and perforated poroid hymen.

The *seriata*-group

Pseudo-nitzschia fraudulenta (Cleve) Hasle, 1993

Plate 8

Basionym: *Nitzschia fraudulenta* Cleve, 1897

Synonym: *Pseudo-nitzschia seriata* var. *fraudulenta* (Cleve) H. Peragallo in H. & M. Peragallo, 1900

Occurrence: *Pseudo-nitzschia fraudulenta* had sporadic occurrence during the sampling year. This species was observed three times in 2009 (in the samples from June, August, and October) and once in 2010 (sample from May).

Description: In girdle view, the valves of *Pseudo-nitzschia fraudulenta* were linear to lanceolate with pointed ends, in light microscopy they could be easily confused with the morphologically similar *P. seriata*.

In valve view, cells were symmetrical and lanceolate, gradually tapering towards pointed ends (Plate 8, pic. A). The valve ends were slightly rounded; one of the ends had one or two skew rows of poroids (Plate 8, pic. B).

The length of the transapical axis of observed cells varied between 4.2 and 6.1 μm , that of the apical axis from 63.9 to 93.3 μm . A central nodule divided the eccentric raphe and the central interspace corresponded to 3 – 4 striae (Plate 8, pic. C). Fibulae and striae were regularly spaced and similar in number, ranging from 18 to 25 in 10 μm . The valve striae had two to three rows of closely placed poroids, 5 – 6 in 1 μm . The poroids of the examined cells consisted of a central unperforated part surrounded by three to seven hymenate sectors; the unperforated part was star shaped (Plate 8, pic. D). The hymenate parts of the valve poroids had a hexagonal perforation pattern. Proximal and distal valve mantles were one or two poroids high.

Fragments of girdle bands were found in the samples, but there was not enough material for a detailed description.

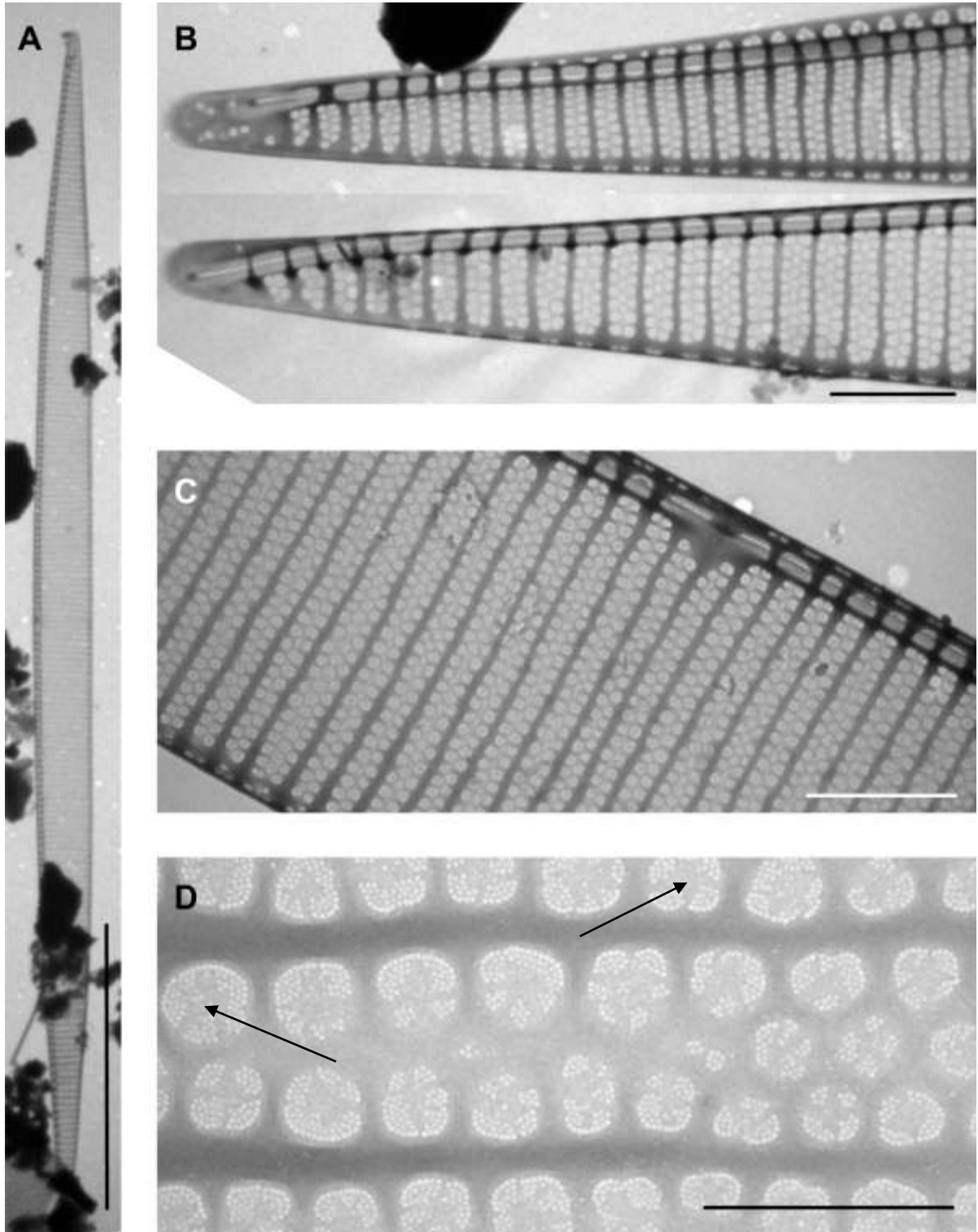


Plate 8: *Pseudo-nitzschia fraudulentus*. TEM micrographs. (A) Scale bar = 20 μm . (B and C) Scale bar = 2 μm . (D) Scale bar = 0.5 μm .

(A) Whole valve. (B) The ends of one valve; note difference in the end structure. (C) Middle part of valve face with larger central interspace and central nodule; note bi- and triseriate striae. (D) Poroids; note the poroid hymen, perforated in several sectors (3-7), and the star-shaped pattern of the middle, unperforated part (indicated by arrows).

The *seriata*-group

***Pseudo-nitzschia seriata* (P.T. Cleve, 1883) H. Peragallo in H. & M. Peragallo, 1900**

Plate 9

Basionym: *Nitzschia seriata* Cleve, 1883

Synonym: *Pseudo-nitzschia seriata* f. *seriata* Hasle (Hasle), 1965

Occurrence: *Pseudo-nitzschia seriata* was found in samples from 5 out of the 11 examined months. It was present in the first summer samples collected in June and August 2009. During the winter period *P. seriata* was not observed, but *P. seriata* was present regularly throughout the whole spring sampling period, from March through May 2010.

Description: The cells formed colonies with an overlap between cells of approximately 1/3 – 1/4 of total cell length (Plate 9, pic. B). In girdle view, the cell shape was linear to lanceolate with a short tapering part towards pointed ends. In valve view, cells of *P. seriata* had a characteristic asymmetry in the perception of apical plan. The valve outline resembled a “cigar”-shape with one valve margin curved and the other straight (Plate 9, pic. A and C). In valve view, the cell got narrower towards slightly elongated and rounded ends. The valve ends had similar shape but had different apice structure: the terminal interstriae of one end were more branched than the other (Plate 9, pic. D). Transapical and apical axis ranged between 4.8 – 7.5 and 89.3 – 106.6 μm , respectively. Neither a larger central interspace nor a central nodule was present. Fibulae and striae were aligned with each other, regularly spaced and distributed in equal numbers, 15 – 18 in 10 μm . Most of the observed cells had four rows of poroids per valve striae, where the rows closer to the interstriae had larger poroids and the two rows in the middle had smaller poroids (Plate 9, pic. E). The number of poroids varied between 3 – 5 in 1 μm . Proximal and distal mantles were not observed. The girdle contained three bands with striae, hymenate poroids, and attached unperforated parts. Both valve and band poroids had a hexagonal perforation pattern.

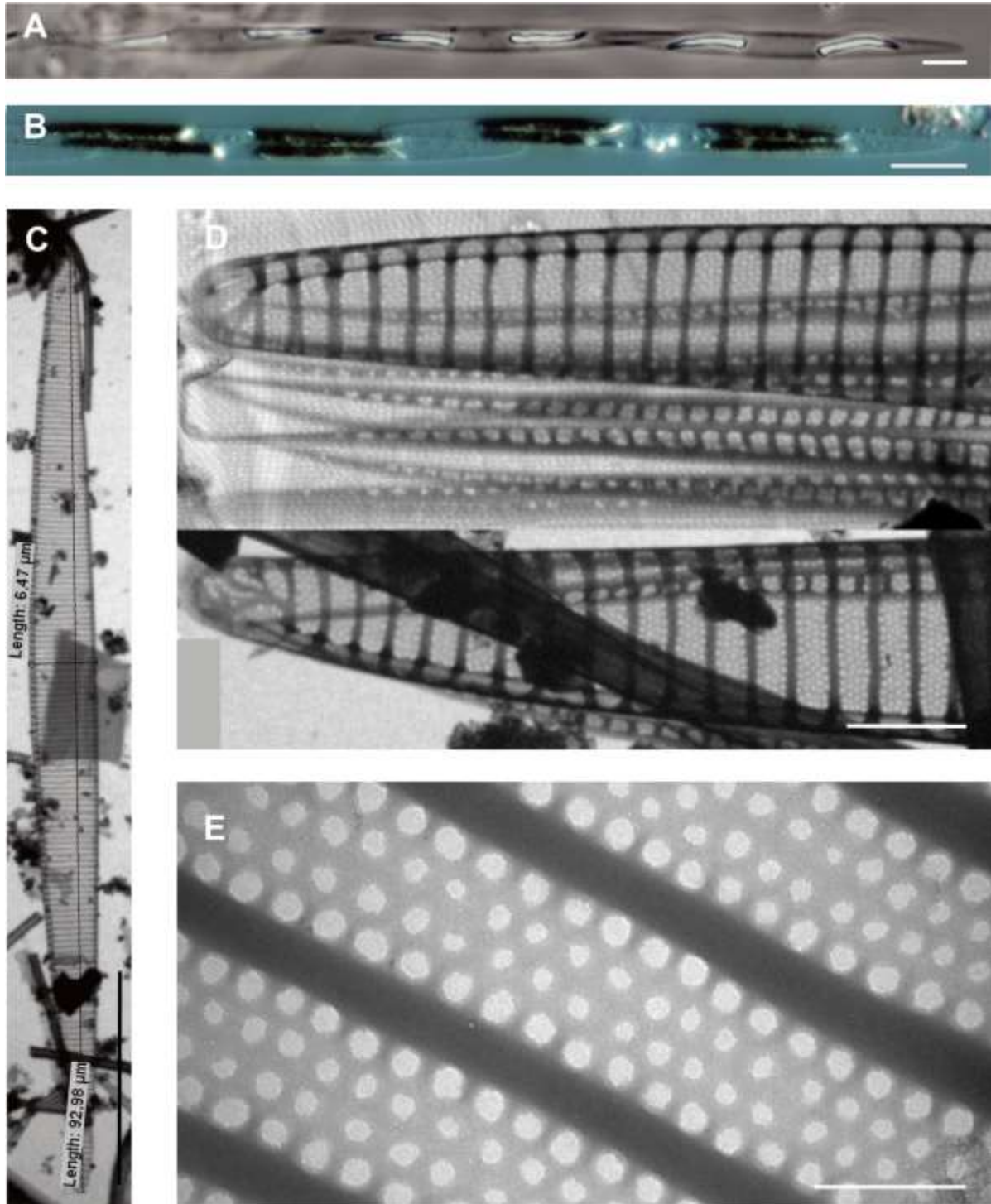


Plate 9: *Pseudo-nitzschia seriata*. Light (A and B), TEM (C, D and E) micrographs. (A and B) Scale bars = 10 μm . (C) Scale bar = 20 μm . (D) Scale bar = 2 μm . (E) Scale bar = 0.5 μm .

(A) Chain in valve view with chloroplasts, formaldehyde-preserved sample, phase contrast. (B) Chain in girdle view with cell overlaps, lugol-preserved sample, DIC. (C) Whole valve; note the curved and straight valve margins. (D) The ends of one valve; note rounded valve ends and difference in structure. (E) Striae, interstriae, and poroids; note the difference in the size (two rows of larger and two rows of smaller poroids is characteristic for this species).

***Pseudo-nitzschia americana* (Hasle) G.A. Fryxell in Hasle, 1993**

Plate 10

Basionym: *Nitzschia americana* Hasle, 1964

Occurrence: *Pseudo-nitzschia americana* was observed twice, in December 2009 and January 2010. *Pseudo-nitzschia americana* was rare in these two samples and only one whole cell and several fragments were found.

Description: The valves of *Pseudo-nitzschia americana* were lightly silicified and were linear to slightly lanceolate, with rounded ends (Plate 10, pic. A). The two ends of each valve had similar structure; in the apices striae diverged and became almost parallel to the apical axis of the valve (Plate 10, pic. A and B).

The transapical axis was 3.3 – 3.4 μm and the apical axis ranged from 21.8 to 27.0 μm . A large central interspace and central nodule were not present. The fibulae were relatively regularly spaced, 19 – 20 in 10 μm . In some cells, valve striae were wider, closer to the valve margins, and irregularly spaced. The number of striae varied between 25 and 28 in 10 μm .

The valve striae were biseriate and had 5 – 6 poroids in 1 μm . Small perforated valve poroids were located close to the interstriae and separated from each other by wide unperforated stripes (Plate 10, pic. C). The first of the three girdle bands (valvecopula) was two poroids wide and three poroids high. Poroid hymens had a hexagonal perforation pattern.

The valve mantles were observed, but unfortunately the images were not good enough to achieve a detailed description.

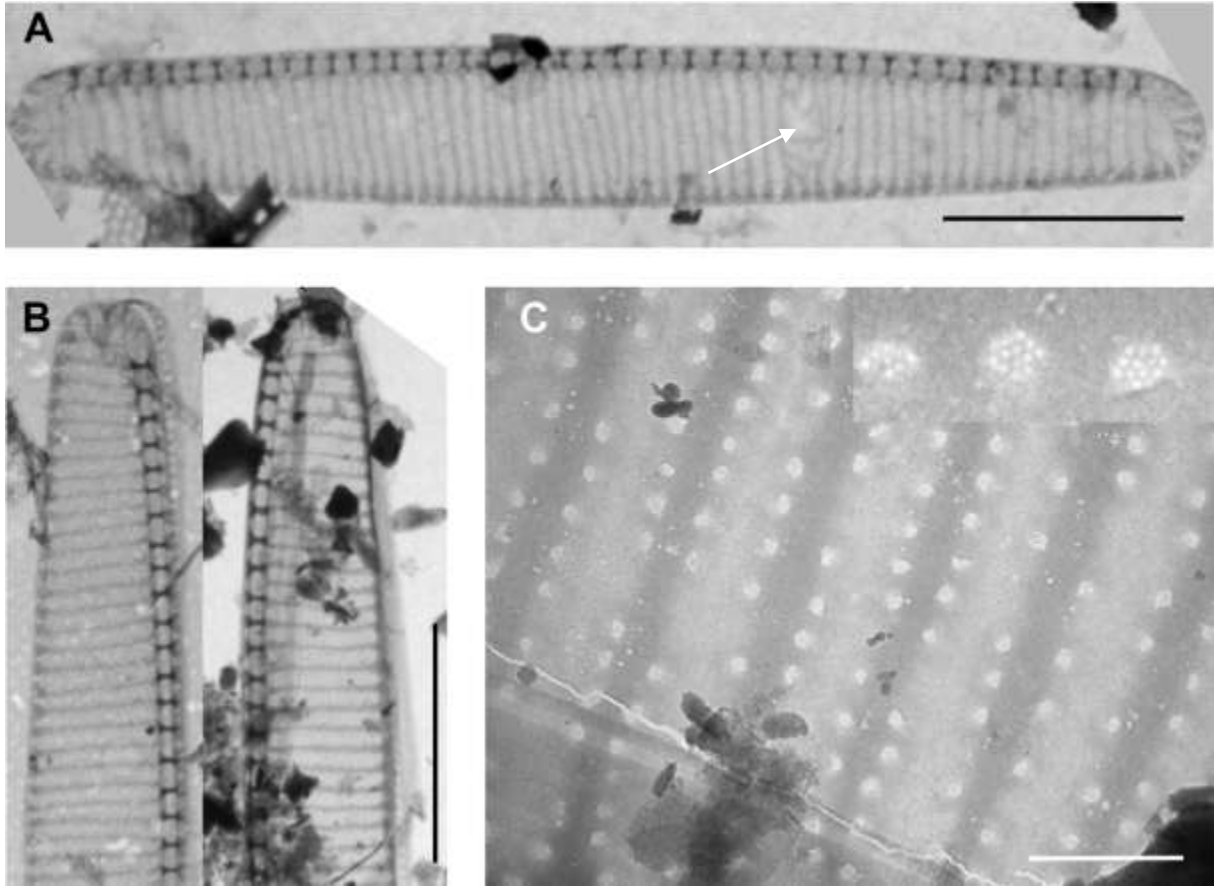


Plate 10: *Pseudo-nitzschia americana*. TEM micrographs. (A and B) Scale bars = 5 μm . (C) Scale bar = 0.5 μm .
(A) Whole valve; note the irregular striae pattern (arrow). (B) Tips of a valve; note the rounded shape and different striae pattern at the cell ends. (C) Biseriate striae and perforated poroids; the perforation has a hexagonal pattern.

Table 3.3: Summary of morphometric characters for *Pseudo-nitzschia delicatissima* group, based on own measurements.


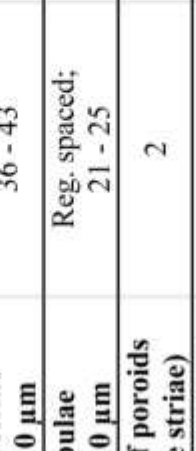
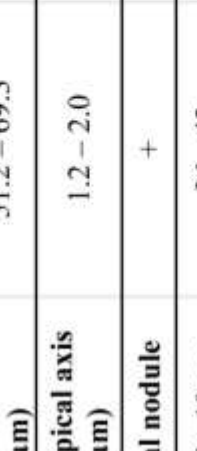
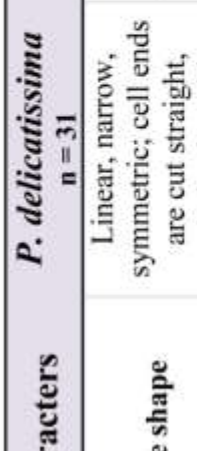

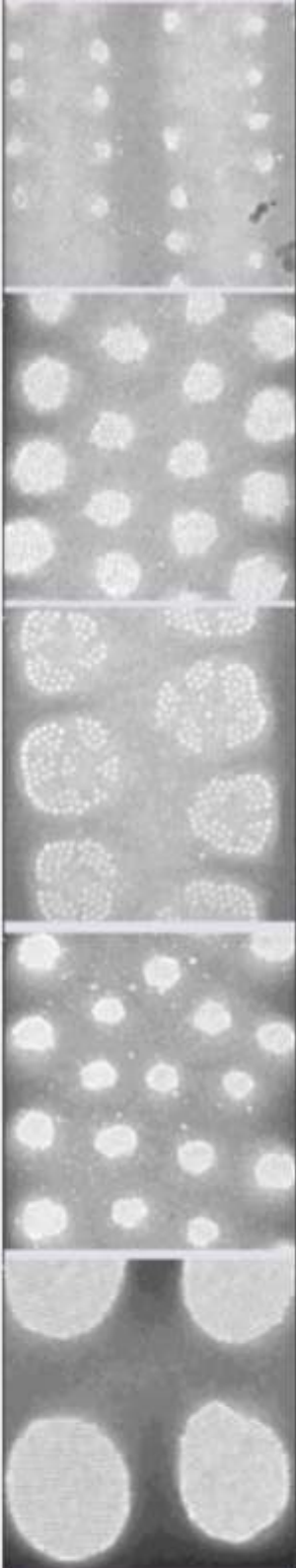
| Characters | <i>P. delicatissima</i> n = 31 | <i>P. pseudodelicatissima</i> n = 7 | <i>P. calliantha</i> n = 28 | <i>P. cf. cuspidata</i> n = 6 | <i>Pseudo-nitzschia</i> sp. n = 6 |
|--------------------------------------|---|---|---|---|---|
| Valve shape | Linear, narrow, symmetric; cell ends are cut straight, slight sigmoid | Linear, narrow, lanceolate, symmetric; tapered towards slightly pointed ends | Linear, lanceolate, symmetric; tapered towards pointed ends | Linear, lanceolate, symmetric; tapered from the middle towards pointed ends | Linear, narrow, symmetric; tapered towards slightly pointed ends |
| Apical axis (µm) | 51.2 – 69.3 | 58.7 – 68.4 | 66.6 – 113.3 | 66.7 – 71.3 | 65.5 – 72.0 |
| Transapical axis (µm) | 1.2 – 2.0 | 0.7 – 1.5 | 1.6 – 2.5 | 2.3 – 2.9 | 1.0 – 1.6 |
| Central nodule | + | + | + | + | + |
| Striae in 10 µm | 36 - 42 | 40 - 43 | 30 - 40 | 30 - 33 | 40 - 43 |
| Interstriae in 10 µm | 36 - 43 | 41 - 43 | 31 - 40 | 31 - 34 | 40 - 43 |
| Fibulae in 10 µm | Reg. spaced; 21 - 25 | Reg. spaced; 22 - 25 | Reg. spaced; 16 - 24 | Reg. spaced; 14 - 16 | Reg. spaced; 22 - 26 |
| Row of poroids (valve striae) | 2 | 1 | 1 | 1 | 1 |
| Poroids in 1µm (valve striae) | 5 - 11 | 4 - 5 | 4 - 5 | 4 | 4 - 5 |
| Poroid type (hymenate velum) |  |  |  |  |  |

Table 3.4: Summary of morphometric characters for *Pseudo-nitzschia seriata* group, based on own measurements.

| Characters | <i>P. pungens</i> n = 26 | <i>P. multiseries</i> n = 6 | <i>P. fraudulenta</i> n = 15 | <i>P. seriata</i> n = 17 | <i>P. americana</i> n = 3 |
|--------------------------------|--|--|--|---|--|
| Valve shape | Linear, lanceolate, symmetric; sharply pointed ends | Spindle, linear, lanceolate, symmetric; sharply pointed ends | Spindle shaped, symmetric; slightly rounded ends | Linear, lanceolate, asymmetric (longit.axis); slightly rounded ends | Linear, lanceolate; broadly rounded ends |
| Apical axis (µm) | 82.1 – 120.0 | 85.7 – 104.0 | 63.9 – 93.3 | 89.3 – 106.6 | 21.8 – 27.0 |
| Transapical axis (µm) | 2.5 – 4.6 | 4.9 – 5.8 | 4.2 – 6.1 | 4.8 – 7.5 | 3.3 – 3.4 |
| Central nodule | - | - | + | - | - |
| Striae in 10 µm | 10 – 13 | 11 – 12 | 18 – 24 | 15 – 18 | 25 – 28 |
| Interstriae in 10 µm | 11 – 13 | 11 – 12 | 19 – 25 | 15 – 18 | 25 – 28 |
| Fibulae in 10 µm | Reg. spaced; 11 – 13 | Reg. spaced; 11 – 12 | Reg. spaced; 19 – 24 | Reg. spaced; 15 – 17 | 19 – 20 |
| Row of poroids (valve striae) | 2 | 4 (3 – 5) | 2 (3) | 4 (3 – 5) | 2 |
| Poroids in 1 µm (valve striae) | 3 (2 – 4) | 6 (3 – 5) | 5 – 6 | 3 – 5 | 5 – 6 |
| Poroid type (hymenate velum) |  | | | | |

4 Discussion

4.1 Evaluation of methods and materials

In order to interpret the results obtained during this study, it will be useful first to make some comments on the methodological aspects of phytoplankton studies and emphasize certain limitations.

The sampling methods are based on the assumption that phytoplankton cells have a random distribution in the water; in fact that is not the case. Spatial heterogeneity or “patchiness” in phytoplankton distribution is a well-known phenomenon (Hardy and Gunther 1935). Horizontal and vertical patchiness may occur on a scale of micrometres up to hundreds of kilometres, as a result of biological (grazing and vertical migration) and physical (wind, currents, turbulence, and mixing) processes.

An advantage of using vertical net tows is that large volumes of water can be filtered to concentrate the phytoplankton. However, they catch only algae that are larger than the mesh size. During this study the mesh size of the net was 20 μm . Most of the microalgae in the size range of picoplankton (less than 2 μm) and nanoplankton (2 μm to 20 μm) were therefore lost; as a result the recorded phytoplankton community is not completely representative. Additional information on total phytoplankton diversity and abundance may be obtained by analysing samples from discrete depths; therefore, in the present study water samples were taken from 1 meter depth, representing the surface layer.

An advantage of the sedimentation method (Utermöhl sedimentation technique) is that microalgal cells can be identified, as well as measured and counted. However, this is a time consuming method (it may take 3-10 hours or more depending on cell density in the sample) and requires training and knowledge of phytoplankton taxonomy. In addition, an unknown portion of the algal species can be destroyed and lost during fixation or not recognizable for other reasons. In this study this was the case for many

small flagellates, naked and thecate dinoflagellates. In order to obtain statistically robust results from the quantitative analysis it is necessary to count a certain number of units (cells, colonies) in the same volume from each sample. To achieve an acceptable precision (95% confidence interval) for the entire sample a total of at least 500 counted units is recommended (Karlson et al. 2010). Disadvantages of the sedimentation method are that living material cannot be used, preserved cells can be distorted beyond recognition, and rare species can go undetected due to the small volume examined. In addition, the counting error (precision) of the less abundant taxa is much higher, which can easily lead to imprecise or even false estimations of the phytoplankton density.

Both qualitative and quantitative methods that are based on light microscopy, suffer from limited magnification and resolution. Electron microscopy significantly improves the identification process, but it is difficult to obtain representative samples that can be used for quantification. The preparation procedure includes many steps, during which many cells can be lost and destroyed. In addition, this is an expensive and time consuming method.

The two most common methods of measuring chlorophyll *a* concentration: fluorescence *in vivo* and chlorophyll *a* concentration *in vitro* were used in this study. Results from the measurements of fluorescence (a proxy for chlorophyll *a* concentration) can be criticized as not necessarily depicting the actual conditions in the water column. *In vivo* fluorescence is re-radiation of light absorbed by algal pigments in intact cells. Since in living cells only a small portion (about 1%) of the absorbed light is re-emitted as fluorescence (Kirk 1994), it can limit the sensitivity of *in vivo* fluorescence measurements (especially when phytoplankton activity is high in the upper part of the euphotic zone during bloom events). As a result, the fluorescence measurements obtained with a fluorometer may show lower values than the *in vitro* chlorophyll *a* measurements, this is termed “Kautsky effect” (Kautsky et al. 1960). In the present study, the results obtained from chlorophyll *a* measurements showed noticeable differences in temporal and spatial profiles. Unrealistically high values of chlorophyll *a* *in vitro* (up to 18 mg L⁻¹) observed in August and September 2009, can be a simple outcome of incorrect measurements.

One of the advantages of the sampling methods used in the present study is that phytoplankton was collected at the same time and place, and complemented by hydrographical measurements such as temperature, salinity, density, and irradiance. A comparison between the phytoplankton composition and hydrographical conditions within the same water body is therefore possible. The hydrographical characteristics of the water masses may give an indication of the general mechanisms determining phytoplankton occurrence, distribution, and bloom formation.

4.2 Phytoplankton seasonal cycle

The results of this study demonstrate that the outer part of Oslofjorden is a heterogenic and dynamic area with regards to hydrographical conditions. During the examined period (June 2009-June 2010), the hydrographical data showed seasonal diversity in the physical and chemical properties of the water masses, and followed previously reported temporal trends (Braarud et al. 1953; DNV 2006; Walday et al. 2010). Considerable fluctuations in the environmental conditions were observed in the upper 10 (or 20) meters, while the situation in underlying water layers (20-40 meters) was more or less stable (Figures 3.1, A and B; 3.2, A and B; 3.4, A and B).

The hydrographical conditions of the water column together with other factors have direct and indirect influence on activity and structure of the phytoplankton community in Outer Oslofjorden (Braarud et al. 1953; Svansson 1975). Also in the present study, the seasonal phytoplankton cycle was shaped by abiotic factors such as light, temperature, and stability of the water column. During the sampling year, phytoplankton composition and abundance showed great seasonal variability. The phytoplankton seasonal cycle observed in the outer part of Oslofjorden conformed to the general pattern reported from previous years (Braarud et al. 1953; DNV 2006; Walday et al. 2010; Naustvoll et al. 2011), with seasonal peaks of phytoplankton in June 2009, September 2009, and January 2010.

One of the factors that may result in shorter or longer periods of increased phytoplankton abundance (blooms) is the supply of nutrients from local run-off during

the summer period (DNV 2006). In summer 2008 and 2009, large phytoplankton blooms were recorded in the outer part of Oslofjorden (Walday et al. 2010; Naustvoll et al. 2011). Similar observations were made in the present study. In June-August 2009, a well-developed pycnocline and low salinities (10-14 psu) in the upper 3 meters were a result of the fresh water input from local run-off /rainfall and high temperatures (17-19 °C). The elevated chlorophyll concentrations (7-18 mg L⁻¹) in the upper eight meters were associated with high cell densities of diatoms (more than 1 x 10⁶ cells L⁻¹) in June 2009. The summer bloom was dominated by typically brackish water species *Cerataulina pelagica*, *Chaetoceros tenuissimus*, *C. wighamii*, and *Dinobryon* sp.; in addition to the coastal species *Leptocylindrus* spp., *Skeletonema* spp., and *Dactyliosolen fragilissimus*. These diatom species are common summer phytoplankton species, opportunists which quickly respond to brackish water rich in silicate and nitrate by developing a high biomass (Anon. 1997). According to Walday et al. (2010), the genus *Ceratium* and *Alexandrium pseudogonyaulax* had also been detected in moderate concentrations at the end of summer 2009, but they were not observed in the present study. In general, dinoflagellate taxa were represented but less abundant during the summer of 2009. High concentrations of chlorophyll *a* were measured in August 2009 (from 13 to 18 mg L⁻¹ in the upper four meters). These values are high for the sampling area and are above the average summer concentrations (7 mg L⁻¹) measured in previous years in the outer part of Oslofjorden (DNV 2006).

Chlorophyll *a* in September 2009 reached concentrations of 4-13 mg L⁻¹ in the upper 20 meters. These high concentrations corresponded to a high cell density (more than 1.2 x 10⁶ cells L⁻¹). Autumn blooms are a common event in Outer Oslofjorden (DNV 2006) and the bloom was associated in this case with still good light conditions, increased salinity, and a slight decline in temperature. During the 2009 autumn bloom the phytoplankton assemblage was dominated by a diverse *Chaetoceros*-community, *Skeletonema* spp., and *Pseudo-nitzschia* spp. (see Table 3.1), all these species had also been regularly found during this time of the year from 2007 to 2009 (Walday et al. 2010). The genus *Prorocentrum* contributed most to the dinoflagellate community detected in September 2009, especially *P. gracile* and *P. micans*. *Prorocentrum gracile* is a common species in more southern ocean areas of the North Atlantic, and the first observation of this species in Outer Oslofjorden was made in 2008 (Walday et al. 2010). The occurrence of *P. gracile*

in 2009 may indicate that this species has been established in the area (Walday et al. 2010). Earlier observations gave reason to believe that dinoflagellate abundance has decreased during the autumn blooms in Outer Oslofjorden for the past several years (DNV 2006). This is consistent with the findings of this study: during the autumn bloom in 2009 the different dinoflagellate taxa were encountered, but not abundant.

In October 2009, most probably strong wind and turbulent vertical mixing broke up the pycnocline. This led to saline (31-34 psu), relatively warm waters (11-14 °C) with low concentrations of chlorophyll *a* in the surface layer. In November 2009, a weak pycnocline had been re-established with low salinity (19-22 psu) and low chlorophyll concentrations in the upper ten meters. The phytoplankton community was diverse and dominated by diatoms. However, *Dinophysis tripos* (which is associated with diarrhetic shellfish poisoning events) and *D. odiosa* was observed in addition to the dinoflagellate community observed in late autumn 2009. Both *D. tripos* and *D. odiosa*, are planktonic species widely distributed in tropical and temperate areas with sporadic occurrences in colder waters (coasts of Norway and Greenland); they probably reached Outer Oslofjorden with Atlantic water masses (Thronsen et al. 2007; Walday et al. 2010).

Compared to the previous years, the winter of 2009/2010 was characterized by higher chlorophyll *a* concentrations, especially in the Skagerrak area where the spring bloom started considerably earlier than usual (Naustvoll et al. 2011). Also in the outer part of Oslofjorden the spring bloom was formed a month earlier than normal (January 2010). Increased phytoplankton productivity during January 2010 may be related to the more or less stratified water column and probably the remaining high nutrient concentrations from earlier vertical mixing. Although the cell densities in January (3.6×10^6 cells L⁻¹) were the highest observed during the sampling year, chlorophyll concentrations reached only 5 mg L⁻¹ in the upper ten meters. The phytoplankton was dominated by an assemblage of coastal/fjord diatom species: *Chaetoceros* spp., *Leptocylindrus* spp., *Pseudo-nitzschia* spp., *Thalassiosira* spp., *Skeletonema* spp., and *Thalassionema nitzschoides*. Due to weather conditions the cruise in February 2010 was not possible, but observations reported by Naustvoll et al. (2011) showed a gradual decrease of phytoplankton production which already started in the beginning of February 2010.

In the beginning of spring 2010, vertical mixing created homogeneous water conditions with a high salinity (32-34 psu) and a temperature of 5 °C. In March 2009, the *Thalassiosira*-community attained a maximum density and together with previously abundant diatom genera contributed most to the phytoplankton community. The phytoplankton abundance gradually decreased and reached its minimum by April 2010.

The improved light conditions and a stratified water column were observed during the rest of the sampling period (April-June 2010), with different salinities as well as low chlorophyll *a* concentrations associated with the phytoplankton community dominated by dinoflagellates. These observations agree well with the general cycle and results from routine monitoring 2009-2010 (Naustvoll et al. 2011), where the dominant species were members of the genera *Dinophysis*, *Ceratium*, and *Protoperidinium*. The presence of monads, ciliates and other flagellates was constant during the sampling year, although a certain periodicity in abundance was observed. In addition to potentially toxic diatoms of the genus *Pseudo-nitzschia*, several potentially toxic dinoflagellates (e.g. *Dinophysis acuta*, *D. norvegica*, *D. rotundata*, *Protoceratium reticulatum*) were observed sporadically in low concentrations (see table 3.1 and 3.2).

4.3 Genus *Pseudo-nitzschia*

4.3.1 Identification and morphology

Pseudo-nitzschia is easily recognised under the light microscope (LM) both in live and preserved samples; however, the identification to the species level can be difficult.

LM observations of live or preserved *Pseudo-nitzschia* in water mounts and counting chambers provide useful information on morphological characters like valve outline in girdle and valve views, overlap of cell ends in the chains, and degree of silicification. For a few species, such as *P. pungens*, this may be sufficient for species identification. Additional valve structures such as central interspace, striae, and fibulae are visible in acid cleaned specimens. However, the identification of morphologically similar species may be difficult in LM (e.g. distinguishing between *P. pungens* and *P. multiseriata*, or *P. pseudodelicatissima* and *P. delicatissima*) and requires the high resolution provided by

electron microscopy (EM). Still, scanning electron microscopy (SEM) can be insufficient and transmission electron microscopy (TEM) is needed to reveal fine structures such as details of the poroid hymen, which are necessary to distinguish between *P. calliantha* and *P. cuspidata*.

The attempt to link different *Pseudo-nitzschia* species by using their morphological features was first made in 1955 by Proschkina-Lavrenko (Proschkina-Lavrenko 1955), who separated members of the genus into two groups according to the valve width: large species with a transapical axis equal or $> 3 \mu\text{m}$ were placed into the *seriata*-group, while smaller species with a transapical axis $< 3 \mu\text{m}$ were placed into the *delicatissima*-group. This traditional arrangement is still useful for the rapid identification of *Pseudo-nitzschia* species under LM, but not sufficient due to broad variation of the valve width within the groups (in this study *P. pungens* and *P. cf. cuspidata* fall in both categories).

Presence or absence of a central nodule was another special character used to divide *Pseudo-nitzschia* species into different groups: species with long and narrow valves and a central nodule were placed into the *delicatissima*-group, whereas species with long and broad valves without a central nodule were placed in the *seriata*-group. However, even combinations of morphological characters such as valve width, absence/presence of the central nodule, number of fibulae and striae per valve, number and structure of poroids, structure of girdle bands, and a.o, overlap in several species.

Although it is possible to divide *Pseudo-nitzschia* species into groups/complexes based on morphological valve features, the genetic investigations do not always support this arrangement. An increased number of *Pseudo-nitzschia* studies have uncovered a large intraspecific variation among the species, as well as the presence of cryptic (morphologically identical but genetically distinct), semi-cryptic (genetically distinct with subtle differences in morphology), and pseudo-cryptic species (divergence genetically with minor morphological differences).

Lundholm et al. (2002) found that *P. americana* (known before as *Nitzschia americana* Hasle), which morphologically resembles both *Pseudo-nitzschia* and *Fragilariopsis*, belongs to the genus *Pseudo-nitzschia*. After a detailed morphological examination of the short and wide *P. americana* and the two closely related species, *P. brasiliiana* and *P. lineata*, a new *americana*-group was established (Lundholm et al. 2002).

Morphological variation in *P. delicatissima* has been reported by Rivera already in 1985 (Rivera 1985) and during the past decade evidence of cryptic and semi-cryptic species diversity within the *delicatissima*-group has increased (Skov et al. 1999; Amato et al. 2007). A re-examination of the *delicatissima*-group based on morphological and molecular data, resulted in the description of the two new species: *P. decipiens* and *P. dolorosa* (Lundholm et al. 2006), later *P. aurenysensis* was added to the group (Quijano-Scheggia et al. 2009).

In the past the identity of *P. pseudodelicatissima* has caused uncertainty and the records of this species may actually correspond to *P. calliantha*. Based on morphological differences of valve structures and molecular data (phylogenetic analyses of the nuclear-encoded internal transcribed spacer 1 (ITS1), 5.8S, and ITS2 rDNA), Lundholm et al (2003) established the *P. pseudodelicatissima* /*cuspidata* complex with four members: *P. pseudodelicatissima*, *P. cuspidata*, *P. calliantha*, and *P. caciaantha*. The recently described *P. manii* from the Gulf of Naples, Italy was also assigned to this complex (Amato and Montresor 2008).

Lately, morphological and genetic variability was reported within *P. pungen*, leading to the establishment of three clades (based on rDNA) and the description of a new morphotype: *P. pungen* var. *aveirense* (Casteleyn et al. 2009; Churro et al. 2009).

The morphometric measurements of *Pseudo-nitzschia* species reported in previous studies are summarized in Tables 4.1 and 4.2. Morphological examinations of *Pseudo-nitzschia* found in the outer part of Oslofjorden revealed that the main valve features agree with the descriptions found in the identification literature (see Tables 3.3 and 3.4). However, some of the measurements (such as a width or length, density of fibula and striae) slightly differed from the literature descriptions. Only *P. cf. cuspidata*, had morphological features which did not comply with those reported in the literature: the proximal and distal mantle of the observed cells diverged from the original description (Lundholm et al. 2003). The observed morphometric differences in the remaining species reflect the morphological variability of the genus. A possible explanation may be that environmental factors such as temperature, salinity, and nutrients can affect the morphology of diatom frustules (Paasche 1975).

Table 4.1: Morphological features of *Pseudo-nitzschia delicatissima* group (valve width is ca 3 μm). Morphometric data in the table is based on Hasle et al 1996, Lundholm et Moestrub 2003.

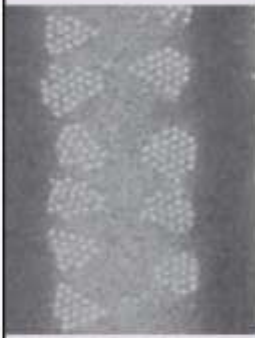
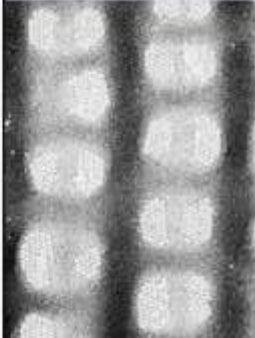
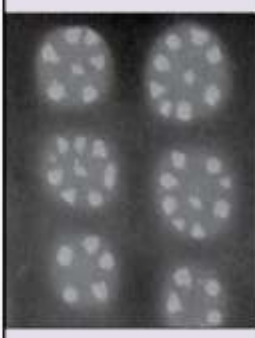

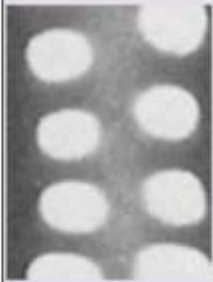
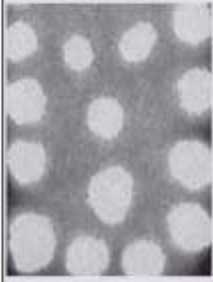
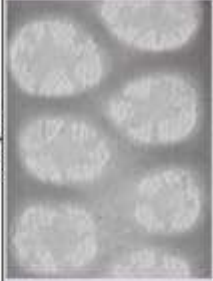


| Characters | <i>P. delicatissima</i> | <i>P. pseudodelicatissima</i> | <i>P. calliantha</i> | <i>P. cuspidata</i> |
|---|---|--|---|---|
| Valve shape | Linear, narrow, symmetric; cell ends are cut straight, slight sigmoid | Linear, narrow, lanceolate, symmetric; tapered towards pointed ends | Linear, lanceolate, symmetric; tapered towards pointed ends | Linear, lanceolate, symmetric; tapered from the middle towards pointed ends |
| Overlap of cells in chains | 1/7 – 1/10 | 1/5 – 1/6 | 1/5 – 1/7 | 1/5 – 1/6 |
| Apical axis (μm) | 40 – 78 | 54 – 87 | 41 – 98 | 30 – 90 |
| Transapical axis (μm) | 1.1 – 2.0 | 0.9 – 1.6 | 1.3 – 1.8 | 1.4 – 2.0 (3.9) |
| Central nodule | + | + | + | + |
| Striae in 10 μm | 37 – 40 | 32 – 44 | 39 – 44 | 35 – 44 |
| Interstriae in 10 μm | 36 – 41 | 36 – 43 | 34 – 39 | 29 – 39 (44) |
| Fibulae in 10 μm | Reg. spaced; 19 – 25 | Reg. spaced; 20 – 25 (28) | Reg. spaced; 15 – 22 | Reg. spaced; 11 – 16 (19-25) |
| Row of poroids (valve striae) | 2 | 1 | 1 | 1 |
| Poroids in 1 μm (valve striae) | 10 – 12; small | 5 – 6; oval / square | 4 – 6; round / square | 4 – 6; oval / square |
| Poroid type (hymenate velum) |  |  |  |  |

Table 4.1: Morphological features of *Pseudo-nitzschia seriata* and *P. americana* groups (valve width is more than 3 µm). Morphometric data in the table is based on Hasle et al. 1996) and Lundholm et al. 2002.

| Characters | <i>P. pungens</i> | <i>P. multiseries</i> | <i>P. fraudulenta</i> | <i>P. seriata</i> | <i>P. americana</i> |
|--------------------------------|---|---|--|---|---|
| Valve shape | Linear, lanceolate, symmetric; sharply pointed ends | Spindle, linear, lanceolate, symmetric; sharply pointed ends | Spindle shaped, symmetric; slightly rounded ends | Linear, lanceolate, asymmetric (longit.axis); slightly rounded end | Linear, lanceolate; broadly rounded ends |
| Overlap of cells in chains | 1/3 – 1/4 | 1/3 – 1/4 | 1/6 – 1/8 | 1/3 – 1/4 | ? |
| Apical axis (µm) | 74 – 174 | 68 – 140 | 50 – 119 | 91 – 160 | 16 – 42 |
| Transapical axis (µm) | 2.4 – 5.3 | 3.4 – 6.0 | 4.5 – 10 | 5.5 – 8.0 | 2.5 – 4.0 |
| Central nodule | - | - | + | - | - |
| Striae in 10 µm | 9 – 15 | 10 – 15 | 12 – 24 | 14 – 18 | 26 – 31 |
| Interstriae in 10 µm | 9 – 16 | 10 – 19 | 18 – 24 | 14 – 18 | 26 – 31 |
| Fibulae in 10 µm | Reg. spaced; 9 – 16 | Reg. spaced; 10 – 19 | Reg. spaced; 12 – 24 | Reg. spaced; 14 – 18 | Reg. spaced; 18 – 24 |
| Row of poroids (valve striae) | 2 (1) | (2) 3 – 4 | 2 – 3 | 3 – 5, often 2x2 rows | 2 (3) |
| Poroids in 1 µm (valve striae) | 3 – 4; round / oval | 4 – 6; small, round | 5 – 7; round, star-shaped | 7 – 8; small, round | 8 – 10; small, round |
| Poroid type (hymenate velum) |  |  |  |  |  |

4.3.2 Seasonal cycle

During the sampling period (June 2009-June 2010), species of the genus *Pseudo-nitzschia* were regular components of the marine phytoplankton in Outer Oslofjorden and were present in every sample collected, with densities ranging from 500 cells L⁻¹ in June 2010 to 1.61 million cells L⁻¹ in January 2010. The diversity and monthly composition of *Pseudo-nitzschia* species changed through the year and the number of species present in one sample varied from one in June 2010 to seven in June and October 2009.

Despite the fact that more than 30 species of the genus *Pseudo-nitzschia* are known worldwide, only ten species were observed and nine of them were identified in the TEM and SEM analyses of the present study; in alphabetical order: *Pseudo-nitzschia americana*, *P. calliantha*, *P. cf. cuspidata*, *P. delicatissima*, *P. fraudulenta*, *P. multiseriata*, *P. pseudo-delicatissima*, *P. pungens*, and *P. seriata*. Except for *P. americana*, all of the identified *Pseudo-nitzschia* species in this study are recorded as toxic in the literature (Bates and Trainer 2006; Moschandreou et al. 2010).

The diversity of the genus *Pseudo-nitzschia* in the outer part of Oslofjorden was slightly higher than that reported by Hasle et al. (1996) in a previous study from the Skagerrak and adjacent waters. Hasle et al. (1996) did not record *P. cf. cuspidata* and *P. pseudo-delicatissima* which appear to be recent additions to the Skagerrak phytoplankton community.

The results of the present investigation are in general agreement with the results of Hasle et al. (1996), a study of occurrence of the genus *Pseudo-nitzschia* in the Skagerrak and adjacent waters in the period from 1978 to 1993. However, in the study by Hasle et al. (1996), the *seriata*-group was prominent and the most abundant species was *P. pungens*, as opposed to the present study where the *delicatissima* – group dominated all samples. The bloom of *Pseudo-nitzschia* spp. in January 2010 was composed of *P. delicatissima* and *P. calliantha*, which were also the most frequently observed species during the sampling year.

According to Hasle (1996), *P. delicatissima* is a common species in Norwegian coastal waters and is regarded as autochthonous to the Skagerrak area. In the long-term records

of *P. delicatissima* by Hasle et al. (1996) it had a sporadic occurrence (see Table 7, Hasle et al. 1996); although in the 1990s it occurred mostly in the winter-spring periods. In the present study both *P. delicatissima* and *P. calliantha* occurred all year and were registered in nine out of eleven samples (see Table 3.1).

Recent investigations (Lundholm et al. 2003) have confirmed that the species previously identified as *P. pseudodelicatissima* from Norwegian waters is distinct from the type specimens of *P. pseudodelicatissima* and after re-examination it was confirmed to be *P. calliantha*. In August 1997 and September 2000, *P. calliantha* was a dominant species in the inner part of Oslofjorden and Drøbak, while from June to mid-October 1992 it had a massive occurrence in the Skagerrak (Thronsen et al. 2007). In this study, an unidentified *Pseudo-nitzschia* sp. was found in the same samples containing the *Pseudo-nitzschia pseudodelicatissima*; both species were rare and observed only in the samples collected in June 2009 and October 2009. The cells of *Pseudo-nitzschia* sp. were slightly aberrant in shape but the general morphological and morphometric parameters resembled *P. pseudodelicatissima*, except for the poroid structure; this dissimilarity may be explained as a result of different degrees of valve silicification (Hasle 1965). *Pseudo-nitzschia* cf. *cuspidata* was not reported by Hasle et al. (1996), but in the present study was detected twice: in late autumn and the beginning of winter. The initial description of *Pseudo-nitzschia cuspidata* was from an isolate collected near Las Palmas (Canary Islands).

Species from the *seriata*-group were less frequently observed during the sampling year (June 2009-June 2010).

Towards the end of the 1960s, *P. multiseriata* was the most abundant species of the genus in Oslofjorden and Skagerrak; it continued to be observed regularly in the 1970s and 1980s, mainly in the autumn and winter periods. For the past two decades the occurrence of *P. multiseriata* has declined, it has become less abundant and gradually replaced by *P. pungens* (Hasle et al. 1996). Findings by Lundholm et al. (2010) support the results of Hasle from the Skagerrak 1967-1968 (Hasle 1995). One of the hypotheses put forward to explain the seasonal shift in occurrence was a connection between growth rate and different temperature tolerance. Field and laboratory observations showed that *P. multiseriata* is capable of maintaining a higher growth rate at

temperatures of 5 °C-0 °C (Smith et al. 1993; Cho et al. 2001), while *P. pungens* stops growing at 10 °C (Cho et al. 2001) and occurs at seasons with higher temperatures than *P. multiseriata*, which has a broader temperature tolerance and was found in field samples at temperatures from 2 °C to 28 °C (Hasle 1965; Forbes and Denman 1991; Hasle et al. 1996). However, in the present study *P. pungens* and *P. multiseriata* were both observed in the samples collected in October and November 2009; *Pseudo-nitzschia pungens* was recorded during most of the year and at temperatures ranging from 6-16 °C with more frequent occurrences in the autumn sampling months. *P. multiseriata* was observed at temperatures varying from 8-12 °C.

Pseudo-nitzschia seriata is known as a cold-water species with a wide distribution mainly in the northern hemisphere (Hasle and Lundholm 2005). Previous studies have shown that this species is a typical winter-spring component of phytoplankton assemblages in the Skagerrak area. During this study the *P. seriata* species occurred sporadically in the summer, winter, and spring periods. It is difficult to conclude that this is a change in the seasonal distribution pattern of *P. seriata*; it may simply be a yearly variation and long-term observation is required.

Previously *P. fraudulenta* and *P. heimii* were reported as regular components of the phytoplankton of the Norwegian Sea and the North Atlantic (Hasle 1965) In the Skagerrak these species were sporadically observed and considered as allochthonous (introduced) in the fjords along the Norwegian west coast (Hasle et al. 1996). During this study, *P. heimii* was not detected, while the occurrence of *P. fraudulenta* was restricted to the summer-spring period.

Pseudo-nitzschia americana was the only member of the *americana*-group detected during the sampling period. This solitary species is often observed as an epiphyte on *Chaetoceros setae* in the Skagerrak area (Thronsen et al. 2007). During the sampling year it was detected twice, in December 2009 and January 2010, when *Chaetoceros* species were quite abundant (see Table 3.2).

In addition, it seems that the geographical distribution and occurrence frequency of toxic *Pseudo-nitzschia* species is changing worldwide (Hallegraeff 1993; Hasle 2002). Since 1900, the temperature in European waters has on average increased by ca. 1 °C, with a warming period especially after 1980s to the present day (Philippart 2007). The

increased temperature and nutrient loading has had an evident effect on phytoplankton (Edwards et al. 2006), therefore it could have affected the seasonal occurrence of several *Pseudo-nitzschia* species, such as *P. pseudodelicatissima*, *P. cf. cuspidata*, *P. fraudulenta*, *P. americana*, and *P. seriata*. Based on the literature, some of the identified species in the present study seem to be restricted to particular latitudinal zones or temperate regions, while others seem to have a cosmopolitan distribution, such as *P. pungens* (Casteleyn et al. 2008). Species of *P. americana*, *P. delicatissima*, *P. fraudulenta*, *P. multiseriata*, and *P. calliantha* are most probably also cosmopolitan, despite the paucity of observations from tropical and subtropical waters (Lundholm and Moestrup 2006).

More research is required to effectively elucidate whether an introduction of new species and seasonal changes in their occurrence have been observed in the investigated area or not. So far, no toxic outbreaks have been reported in Norwegian coastal waters. However, future outbreaks are possible due to continuously changing environmental conditions, making continuous monitoring of *Pseudo-nitzschia* species necessary. Furthermore, genetic examinations of the species, combined with domoic acid testing would be advisable.

4.4 Conclusions

The general pattern of the seasonal phytoplankton cycle (June 2009-June 2010) observed in the outer part of Oslofjorden was to a large extent in accordance with previous reports; however, the spring bloom observed in January 2010 was unusually early for the area. According to recent investigations, the abundance of dinoflagellates has decreased during autumn blooms in the Outer Oslofjorden, also in this study the number of the dinoflagellates were low during the autumn bloom in September 2009. The present study confirms the occurrence of *Prorocentrum gracile* in the outer part of Oslofjorden and it may be regarded as a new addition to the dinoflagellate community as it was also reported in 2008 when it was registered for the first time.

Compared to earlier observations some changes in the species composition of *Pseudo-nitzschia* in the outer part of Oslofjorden were observed. Whereas in earlier observations

the *seriata*-group dominated the samples and *P. pungens* was the most common species, in this study the *delicatissima*-group was dominating and the most frequently encountered species were *Pseudo-nitzschia calliantha* and *P. delicatissima*. *Pseudo-nitzschia pseudodelicatissima* and *P. cf. cuspidata* were reported for the first time, while the previously recorded *P. heimii* was not found. A *Pseudo-nitzschia* species that could not be assigned to any previously described species was observed on one occasion. Further investigation is needed to determine if this represent a species that is new to science. Eight potentially toxic *Pseudo-nitzschia* species were recorded: *Pseudo-nitzschia delicatissima*, *P. pseudodelicatissima*, *P. calliantha*, *P. cf. cuspidata*, *P. pungens*, *P. multiseries*, *P. fraudulenta* and *P. seriata*. Potentially toxic *Pseudo-nitzschia* species were recorded in all samples examined and may indicate that toxic representatives are present all year.

Appendix

1 Morphometric measurements of *Pseudo-nitzschia* species collected in the outer part of Oslofjord (June 2009-June 2010).

| Species | Apical axis (µm) | Trans-apical axis (µm) | Valve striae in 10 µm | Valve interstriae in 10 µm | Fibulae in 10 µm | Poroids in 10 µm (valve striae) | Row of poroids (valve striae) |
|-------------------------|------------------|------------------------|-----------------------|----------------------------|------------------|---------------------------------|-------------------------------|
| <i>P. delicatissima</i> | | | | | | | |
| 1 | 53.6 | 1.5 | 42 | 42 | 25 | 8 | 2 |
| 2 | 58.6 | 1.6 | 41 | 40 | 25 | 9 | 2 |
| 3 | 63.9 | 1.3 | 41 | 40 | 24 | 8 | 2 |
| 4 | 59.6 | 1.5 | 39 | 38 | 21 | 10 | 2 |
| 5 | 59.6 | 1.4 | 39 | 38 | 23 | 8 | 2 |
| 6 | 61.9 | 1.4 | 39 | 38 | 23 | 6 – 8 | 2 |
| 7 | 69.3 | 1.8 | 40 | 42 | 25 | 7 | 2 |
| 8 | 61.1 | 2.0 | 40 | 43 | 25 | 9 – 10 | 2 |
| 9 | 61.9 | 1.9 | 36 | 36 | 22 | 5 – 7 | 2 |
| 10 | 62.0 | 1.8 | 37 | 37 | 23 | 6 – 7 | 2 |
| 11 | 61.8 | 1.3 | 40 | 42 | 24 | 6 – 8 | 2 |
| 12 | 49.1 | 1.8 | 36 | 37 | 22 | 7 – 8 | 2 |
| 13 | 56.7 | 1.5 | 37 | 38 | 22 | 5 – 7 | 2 |
| 14 | 51.2 | 1.4 | 40 | 41 | 23 | 6 – 8 | 2 |
| 15 | 62.7 | 1.3 | 41 | 42 | 22 | 7 – 11 | 2 |
| 16 | 55.3 | 1.5 | 37 | 38 | 22 | 6 – 7 | 2 |
| 17 | 57.0 | 1.6 | 38 | 39 | 22 | 5 – 6 | 2 |
| 18 | 60.5 | 1.2 | 38 | 39 | 24 | 5 – 6 | 2 |
| 19 | 59.6 | 1.4 | 37 | 38 | 21 | 7 – 8 | 2 |
| 20 | 53.6 | 1.5 | 38 | 39 | 23 | 6 – 8 | 2 |
| 21 | 56.2 | 1.6 | 37 | 38 | 22 | 5 – 7 | 2 |

| | Apical axis (µm) | Trans-apical axis (µm) | Valve striae in 10 µm | Valve interstriae in 10 µm | Fibulae in 10 µm | Poroids in 10 µm (valve striae) | Row of poroids (valve striae) |
|---------------------------------------|------------------|------------------------|-----------------------|----------------------------|------------------|---------------------------------|-------------------------------|
| 22 | 58.6 | 1.4 | 38 | 39 | 23 | 8 | 2 |
| 23 | 57.2 | 1.6 | 40 | 40 | 23 | 7 – 8 | 2 |
| 24 | 55.3 | 1.3 | 41 | 41 | 23 | 7 – 8 | 2 |
| 25 | 60.7 | 1.2 | 37 | 37 | 23 | 8 | 2 |
| 26 | 58.1 | 1.7 | 38 | 39 | 24 | 8 – 9 | 2 |
| 27 | 59.1 | 1.3 | 38 | 39 | 24 | 8 – 9 | 2 |
| 28 | 53.8 | 1.4 | 40 | 41 | 23 | 8 | 2 |
| 29 | 53.3 | 1.2 | 38 | 39 | 22 | 8 – 9 | 2 |
| 30 | 55.1 | 1.3 | 40 | 41 | 22 | 8 | 2 |
| 31 | 58.6 | 1.6 | 38 | 39 | 23 | 8 – 9 | 2 |
| <i>P. pseudo delicatissima</i> | | | | | | | |
| 1 | 68.4 | 0.8 | 40 | 41 | 25 | 4 – 5 | 1 |
| 2 | 65.0 | 0.7 | 40 | 41 | 22 | 4 | 1 |
| 3 | 64.1 | 0.7 | 40 | 41 | 25 | 4 – 5 | 1 |
| 4 | 58.7 | 1.5 | 43 | 43 | 23 | 4 | 1 |
| 5 | 60.7 | 0.9 | 42 | 42 | 23 | 4 | 1 |
| 6 | 67.1 | 0.8 | 40 | 41 | 25 | 4 | 1 |
| 7 | 59.9 | 1.1 | 40 | 41 | 25 | 4 | 1 |
| <i>P. calliantha</i> | | | | | | | |
| 1 | 85.7 | 1.7 | 40 | 40 | 22 | 3-4 | 1 |
| 2 | 100.7 | 1.6 | 34 | 35 | 18 | 4 | 1 |
| 3 | 82.9 | 2.1 | 37 | 38 | 19 | 4 | 1 |
| 4 | 102.1 | 1.6 | 33 | 34 | 18 | 4 | 1 |
| 5 | 94.0 | 1.6 | 35 | 36 | 20 | 4 | 1 |
| 6 | 91.1 | 2.2 | 35 | 36 | 20 | 4 | 1 |
| 7 | 84.2 | 1.7 | 37 | 38 | 19 | 4 | 1 |
| 8 | 66.6 | 1.9 | 35 | 36 | 20 | 4 | 1 |
| 9 | 92.0 | 2.2 | 32 | 33 | 20 | 4 – 5 | 1 |
| 10 | 94.0 | 1.6 | 31 | 32 | 16 | 4 | 1 |

| Species | Apical axis (µm) | Trans-apical axis (µm) | Valve striae in 10 µm | Valve interstriae in 10 µm | Fibulae in 10 µm | Poroids in 10 µm (valve striae) | Row of poroids (valve striae) |
|------------------------------------|------------------|------------------------|-----------------------|----------------------------|------------------|---------------------------------|-------------------------------|
| 11 | 90.7 | 1.8 | 35 | 36 | 17 | 4 | 1 |
| 12 | 113.3 | 1.9 | 37 | 38 | 20 | 4 | 1 |
| 13 | 98.0 | 1.6 | 40 | 40 | 24 | 4 | 1 |
| 14 | 100.0 | 1.9 | 30 | 31 | 18 | 4 | 1 |
| 15 | 79.2 | 2.0 | 35 | 36 | 18 | 4 | 1 |
| 16 | 66.7 | 1.9 | 37 | 37 | 20 | 4 | 1 |
| 17 | 87.3 | 2.1 | 32 | 33 | 16 | 4 | 1 |
| 18 | 89.9 | 2.3 | 32 | 34 | 17 | 4 | 1 |
| 19 | 83,5 | 1,9 | 36 | 37 | 17 | 4 | 1 |
| 20 | 89.9 | 1.8 | 34 | 35 | 17 | 4 | 1 |
| 21 | 88.8 | 2.1 | 34 | 35 | 18 | 4 | 1 |
| 22 | 73.9 | 2.3 | 37 | 38 | 20 | 4 | 1 |
| 23 | 95.8 | 2.5 | 37 | 37 | 17 | 4 | 1 |
| 24 | 95.5 | 2.3 | 38 | 38 | 18 | 4 | 1 |
| 25 | 95.0 | 2.5 | 37 | 37 | 17 | 4 | 1 |
| 26 | 95.6 | 2.0 | 36 | 36 | 16 | 4 | 1 |
| 27 | 83 | 1.9 | 35 | 36 | 16 | 4 – 5 | 1 |
| 28 | 94,4 | 1.7 | 36 | 37 | 19 | 4 | 1 |
| <i>P. cf. cuspidata</i> | | | | | | | |
| 1 | 71.3 | 2.3 | 33 | 34 | 16 | 4 | 1 |
| 2 | 68.5 | 2.5 | 32 | 33 | 15 | 4 | 1 |
| 3 | 66.7 | 2.9 | 30 | 31 | 15 | 4 | 1 |
| 4 | 66.9 | 2.7 | 30 | 31 | 14 | 4 | 1 |
| 5 | 70.1 | 2.5 | 32 | 33 | 16 | 4 | 1 |
| 6 | 67.5 | 2.8 | 32 | 33 | 16 | 4 | 1 |
| <i>Pseudo-nitzschia</i> sp. | | | | | | | |
| 1 | 68.4 | 1.0 | 43 | 43 | 26 | 4 | 1 |
| 2 | 72.0 | 1.0 | 40 | 42 | 25 | 5 | 1 |
| 3 | 70.1 | 1.4 | 43 | 42 | 24 | 4 | 1 |
| 4 | 67.0 | 1.4 | 40 | 41 | 22 | 4 – 5 | 1 |

| Species | Apical axis (µm) | Trans-apical axis (µm) | Valve striae in 10 µm | Valve interstriae in 10 µm | Fibulae in 10 µm | Poroids in 10 µm (valve striae) | Row of poroids (valve striae) | |
|--------------------------|------------------|------------------------|-----------------------|----------------------------|------------------|---------------------------------|-------------------------------|---|
| | 5 | 65.5 | 1.2 | 41 | 42 | 22 | 4 | 1 |
| | 6 | 67.5 | 1.6 | 40 | 40 | 22 | 5 | 1 |
| <i>P. pungens</i> | | | | | | | | |
| | 1 | 82.1 | 2.5 | 12 | 12 | 12 | 3 – 4 | 2 |
| | 2 | 108.0 | 2.9 | 13 | 13 | 13 | 3 – 4 | 2 |
| | 3 | 97.9 | 3.0 | 13 | 13 | 13 | 3 | 2 |
| | 4 | 90.3 | 2.9 | 11 | 11 | 11 | 3 | 2 |
| | 5 | 116.0 | 2.8 | 12 | 12 | 12 | 3 | 2 |
| | 6 | 100.0 | 3.3 | 11 | 11 | 12 | 3 | 2 |
| | 7 | 90.9 | 3.8 | 10 | 11 | 11 | 3 | 2 |
| | 8 | 108.2 | 2.9 | 11 | 11 | 11 | 3 | 2 |
| | 9 | 110.0 | 3.4 | 10 | 11 | 12 | 3 | 2 |
| | 10 | 120.0 | 3.5 | 10 | 11 | 11 | 3 | 2 |
| | 11 | 124.0 | 4.2 | 12 | 12 | 12 | 1 – 3 | 2 |
| | 12 | 93.0 | 4.1 | 11 | 12 | 12 | 2 – 3 | 2 |
| | 13 | 100.3 | 3.3 | 11 | 12 | 13 | 3 | 2 |
| | 14 | 93.7 | 4.1 | 11 | 12 | 12 | 3 | 2 |
| | 15 | 105.7 | 3.2 | 12 | 12 | 12 | 3 | 2 |
| | 16 | 101.2 | 3.4 | 11 | 11 | 12 | 3 | 2 |
| | 17 | 92.8 | 2.9 | 12 | 12 | 12 | 2 – 3 | 2 |
| | 18 | 106.0 | 4.2 | 12 | 12 | 12 | 3 | 2 |
| | 19 | 102.4 | 3.7 | 12 | 12 | 12 | 3 | 2 |
| | 20 | 98.8 | 4.3 | 11 | 11 | 11 | 2 – 3 | 2 |
| | 21 | 91.5 | 3.8 | 11 | 11 | 11 | 2 – 3 | 2 |
| | 22 | 106.3 | 3.7 | 12 | 12 | 12 | 3 | 2 |
| | 23 | 89.8 | 3.2 | 12 | 12 | 12 | 3 | 2 |
| | 24 | 110.0 | 4.1 | 13 | 13 | 13 | 2 – 3 | 2 |
| | 25 | 85.6 | 3.1 | 11 | 12 | 12 | 3 | 2 |
| | 26 | 108.5 | 4.6 | 13 | 13 | 13 | 3 | 2 |

| Species | Apical axis (µm) | Trans-apical axis (µm) | Valve striae in 10 µm | Valve interstriae in 10 µm | Fibulae in 10 µm | Poroids in 10 µm (valve striae) | Row of poroids (valve striae) |
|-----------------------|------------------|------------------------|-----------------------|----------------------------|------------------|---------------------------------|-------------------------------|
| <i>P. multiseries</i> | | | | | | | |
| 1 | 90.9 | 5.8 | 12 | 12 | 12 | 3 – 4 | 4 |
| 2 | 85.7 | 4.9 | 12 | 12 | 12 | 5 – 6 | 4 – 5 |
| 3 | 100.0 | 5.3 | 12 | 12 | 12 | 4 – 6 | 3 – 5 |
| 4 | 97.2 | 5.0 | 11 | 11 | 11 | 6 | 4 |
| 5 | 104.0 | 5.5 | 12 | 12 | 12 | 5 – 6 | 3 – 4 |
| 6 | 89.1 | 4.9 | 11 | 11 | 11 | 6 | 4 |
| <i>P. fraudulenta</i> | | | | | | | |
| 1 | 69.3 | 6.1 | 24 | 25 | 20 | 6 | 2 – 3 |
| 2 | 63.9 | 5.4 | 22 | 22 | 20 | 6 | 2 – 3 |
| 3 | 82.2 | 4.9 | 24 | 25 | 21 | 5 | 2 – 3 |
| 4 | 80.1 | 5.0 | 20 | 25 | 20 | 5 | 2 – 3 |
| 5 | 87.8 | 5.2 | 23 | 24 | 24 | 4 – 5 | 2 – 3 |
| 6 | 90.0 | 4.6 | 23 | 24 | 22 | 5 – 7 | 2 |
| 7 | 67.5 | 4.5 | 22 | 22 | 20 | 5 – 6 | 2 – 3 |
| 8 | 92.0 | 5.2 | 20 | 22 | 20 | 5 | 2 – 3 |
| 9 | 80.0 | 4.2 | 23 | 24 | 22 | 5 – 6 | 2 – 3 |
| 10 | 82.8 | 5.9 | 18 | 19 | 19 | 5 – 6 | 2 – 3 |
| 11 | 80.4 | 5.8 | 23 | 23 | 22 | 5 – 6 | 2 – 3 |
| 12 | 75.5 | 5.8 | 22 | 22 | 20 | 6 | 2 – 3 |
| 13 | 90.7 | 4.6 | 22 | 23 | 22 | 6 | 2 – 3 |
| 14 | 88.9 | 5.1 | 23 | 24 | 24 | 5 | 2 – 3 |
| 15 | 93.3 | 5.4 | 20 | 22 | 20 | 5 – 6 | 2 – 3 |
| <i>P. seriata</i> | | | | | | | |
| 1 | 97.1 | 5.7 | 18 | 16 | 18 | 6 – 9 | 3 – 5 |
| 2 | 92.2 | 4.8 | 17 | 16 | 17 | 7 – 8 | 4 |
| 3 | 106.6 | 7.3 | 15 | 15 | 15 | 5 – 8 | 4 |
| 4 | 99.6 | 6.1 | 17 | 17 | 15 | 7 | 4 |
| 5 | 98.2 | 7.5 | 17 | 17 | 16 | 7 | 3 – 4 |
| 6 | 89.3 | 6.4 | 16 | 16 | 16 | 7 | 4 |

| Species | Apical axis (µm) | Trans-apical axis (µm) | Valve striae in 10 µm | Valve interstriae in 10 µm | Fibulae in 10 µm | Poroids in 10 µm (valve striae) | Row of poroids (valve striae) |
|----------------------------|------------------|------------------------|-----------------------|----------------------------|------------------|---------------------------------|-------------------------------|
| 7 | 95.9 | 5.8 | 16 | 16 | 16 | 8 – 9 | 4 |
| 8 | 100.2 | 6.1 | 16 | 16 | 16 | 7 | 4 |
| 9 | 92.3 | 6.4 | 17 | 17 | 17 | 7 | 3 – 5 |
| 10 | 105.0 | 6.5 | 17 | 17 | 17 | 6 | 3 – 4 |
| 11 | 90.8 | 5.7 | 15 | 15 | 15 | 7 | 3 – 4 |
| 12 | 97.3 | 5.4 | 16 | 16 | 15 | 6 – 7 | 4 |
| 13 | 101.3 | 7.2 | 16 | 16 | 15 | 7 – 8 | 3 – 4 |
| 14 | 93.0 | 6.5 | 17 | 16 | 17 | 6 – 7 | 3 – 4 |
| 15 | 91.7 | 5.6 | 17 | 17 | 17 | 5 – 7 | 3 – 5 |
| 16 | 98.3 | 6.1 | 18 | 18 | 17 | 5 – 8 | 3 – 4 |
| 17 | 92.2 | 5.3 | 16 | 16 | 16 | 6 – 7 | 4 |
| <i>P. americana</i> | | | | | | | |
| 1 | 21.8 | 3.4 | 25 | 26 | 19 | 6 | 2 |
| 2 | 25.1 | 3.3 | 28 | 28 | 20 | 5 – 6 | 2 |
| 3 | 27.0 | 3.4 | 25 | 25 | 19 | 6 | 2 |

Reference list

- Akima, H., A. Gerbhardt, T. Petzold and M. Maechler (2006). Akima: Linear or cubic spline interpolation for irregular gridded data.
- Alve, E. and J. Nagy (1990). "Main features of foraminiferal distribution reflecting estuarine hydrography in Oslo Fjord." *Marine Micropaleontology* **16**(3-4): 181-206.
- Amato, A., W. Kooistra, J. H. L. Ghiron, D. G. Mann, T. Proschold and M. Montresor (2007). "Reproductive isolation among sympatric cryptic species in marine diatoms." *Protist* **158**: 193-207.
- Amato, A. and M. Montresor (2008). "Morphology, phylogeny, and sexual cycle of *Pseudo-nitzschia mannii* sp nov (Bacillariophyceae): a pseudo-cryptic species within the *P. pseudodelicatissima* complex." *Phycologia* **47**(5): 487-497.
- Amzil, Z., J. Fresnel, D. Le Gal and C. Billard (2001). "Domoic acid accumulation in French shellfish in relation to toxic species of *Pseudo-nitzschia multiseries* and *P. pseudodelicatissima*." *Toxicon* **39**(8): 1245-1251.
- Anon. (1993). Den Norske Los. Farvannsbeskrivelse Svenskegrensen - Langesund. Gunnarshaug, Stavanger, Statents Kartverk. **2A**: 350.
- Anon. (1997). The Norwegian Sea Coastal water. Eutrophication-status and trends. Report from expert group for evaluation of eutrophication in fjords an coastal waters. State Pollution Control Authority (SFT). Norway: 90.
- Aure, J., D. S. Danielssen and J. Magnusson (2010). Langtransporterte tilførsler av næringsalter til Ytre Oslofjord 1996-2006. Fisken og havet. Rapport nr. 4-2010, Havforskningsinstituttet: 24.
- Aure, J., Sætre, R. (1979). Wind effects on the Skagerrak outflow. In: R. Sætre and M.Mork. The Norwegian Coastal Current. Bergen, Norway, University Press: 263-293.
- Baalsrud, K. and J. Magnusson (2002). Indre Oslofjord: natur og miljø. Oslo, Fagrådet for vann- og avløpsteknisk samarbeid i indre Oslofjord: 135.
- Bates, S. S., C. J. Bird, A. S. W. Defreitas, R. Foxall, M. Gilgan, L. A. Hanic, G. R. Johnson, A. W. McCulloch, P. Odense, R. Pocklington, M. A. Quilliam, P. G. Sim, J. C. Smith, D. V. S. Rao, E. C. D. Todd, J. A. Walter and J. L. C. Wright (1989). "Pennate diatom *Nitzschia pungens* as the primary source of Domoic Acid, a toxin in shellfish from Eastern Prince Edward Island, Canada." *Canadian Journal of Fisheries and Aquatic Sciences* **46**(7): 1203-1215.

- Bates, S. S. and V. L. Trainer (2006). The Ecology of Harmful Diatoms. Ecology of Harmful Algae. E. Granéli and J. T. Turner, Springer Berlin Heidelberg. **189**: 81-93.
- Braarud, T. (1945). A phytoplankton survey of the polluted waters of inner Oslo fjord. Oslo, Universitetsforlaget. **nr 28**: 142 s.
- Braarud, T., K. R. Gaarder and J. Grøntved (1953). The phytoplankton of the North Sea and adjacent waters in May 1948. Copenhagen, Le Conseil. **V. 133**: 87 s.
- Calado, A. J. and J. M. Huisman (2010). "Commentary: Gomez, F., Moreira, D., and Lopez-Garcia, P.(2010). *Neoceratium* gen. nov., a New Genus for All Marine Species Currently Assigned to *Ceratium* (Dinophyceae). Protist 161: 35-54." Protist **161**(4): 517-519.
- Casteleyn, G., N. G. Adams, P. Vanormelingen, A. E. Debeer, K. Sabbe and W. Vyverman (2009). "Natural Hybrids in the Marine Diatom *Pseudo-nitzschia pungens* (Bacillariophyceae): Genetic and Morphological Evidence." Protist **160**(2): 343-354.
- Casteleyn, G., V. A. Chepurnov, F. Leliaert, D. G. Mann, S. S. Bates, N. Lundholm, L. Rhodes, K. Sabbe and W. Vyverman (2008). "Pseudo-nitzschia pungens (Bacillariophyceae): A cosmopolitan diatom species?" Harmful Algae **7**(2): 241-257.
- Cho, E. S., Y. Kotaki and J. G. Park (2001). "The comparison between toxic *Pseudo-nitzschia multiseriis* (Hasle) Hasle and non-toxic *P. pungens* (Grunow) Hasle isolated from Jinhae Bay, Korea." Algae **16**(3): 275-285.
- Churro, C. I., C. C. Carreira, F. J. Rodrigues, S. C. Craveiro, A. J. Calado, G. Casteleyn and N. Lundholm (2009). "Diversity and abundance of potentially toxic *Pseudo-nitzschia* Peragallo in Aveiro Coastal lagoon, Portugal and description of a new variety, *P. pungens* var. *aveirensis* var. nov." Diatom Research **24**(1): 35-62.
- Cupp, E. E. (1943). Marine plankton diatoms of the West Coast of North America. Berkeley and Los Angeles, University of California Press. **5**: 237.
- Cusack, C. K., S. S. Bates, M. A. Quilliam, J. W. Patching and R. Raine (2002). "Confirmation of Domoic Acid production by *Pseudo-nitzschia australis* (Bacillariophyceae) isolated from Irish Waters." Journal of Phycology **38**(6): 1106-1112.
- Dahl, E. and M. Yndestad (1985). In: Toxic dinoflagellates. New York, Elsevier: pp. 495-500.
- DNV (2006). Overvåkning av eutrofitilstanden i Ytre Oslofjord. Femårsrapport 2001-2005, Den Norske Veritas; rapport nr. 2006-0831, rev.01: 127.
- Douglas, D. J., D. Landry and S. E. Douglas (1994). "Genetic relatedness of toxic and nontoxic isolates of the marine pennate diatom *Pseudo-nitzschia* (Bacillariophyceae): Phylogenetic analysis of 18S rRNA sequences." Natural Toxins **2**(4): 166-174.

- Dragsund, E., O. Aspholm, K. Tangen, S. M. Bakke, L. Heier and T. Jensen (2006).
 Overvåking av eutrofitilstanden i Ytre Oslofjord. Femårsrapport 2001-2005. nr. 2006-0831. Oslo, Det Norske Veritas AS: 127.
- Edvardsen, B. (1993). Toxicity of *Chrysochromulina* species (Prymnesiophyceae) to the Brine Shrimp, *Artemia-Salina*. Toxic Phytoplankton Blooms in the Sea. T. J. Smayda and Y. Shimizu. **3**: 681-686.
- Edwards, M., D. G. Johns, S. C. Leterme, E. Svendsen and A. J. Richardson (2006).
 "Regional climate change and harmful algal blooms in the northeast Atlantic."
 Limnology and Oceanography **51**(2): 820-829.
- Fehling, J., D. H. Green, K. Davidson, C. J. Bolch and S. S. Bates (2004). "Domoic Acid production by *Pseudo-nitzschia seriata* (Bacillariophyceae) in Scottish Waters." Journal of Phycology **40**(4): 622-630.
- Forbes, J. R. and K. L. Denman (1991). "Distribution of *Nitzschia pungens* in coastal waters of British Columbia." Canadian Journal of Fisheries and Aquatic Sciences **48**(6): 960-967.
- Fritz, L., M. A. Quilliam, J. L. C. Wright, A. M. Beale and T. M. Work (1992). "An outbreak of Domoic Acid poisoning attributed to the pennate diatom *Pseudo-nitzschia australis*." Journal of Phycology **28**(4): 439-442.
- Fryxell, G. A. and G. R. Hasle (2003). Taxonomy of harmful diatoms. In: Hallegraeff, G.M. et al. (Ed). Manual on harmful microalgae. Paris, UNESCO: 465-510.
- Gade, H. G. (1968). "Horizontal and vertical exchanges and diffusion in the water masses of the Oslo fjord." Helgoland Marine Research **17**(1): 462-475.
- Gentien, P. (1998). "Bloom dynamics and ecophysiology of the *Gymnodinium mikimotoi* species complex." NATO ASI Series Series G Ecological Sciences **41**: 155-173.
- Gomez, F., D. Moreira and P. Lopez-Garcia (2010). "*Neoceratium* gen. nov., a New Genus for All Marine Species Currently Assigned to *Ceratium* (Dinophyceae)." Protist **161**(1): 35-54.
- Hallegraeff, G. M. (1993). "A review of harmful algal blooms and their apparent global increase." Phycologia **32**(2): 79-99.
- Hardy, A. C. and E. R. Gunther (1935). The plankton of the South Georgia whaling grounds and adjacent waters, 1926-1927. Cambridge, The University press. **11**: 456.
- Hasle, G. (1978). "Settling: the inverted-microscope method." Monographs on oceanographic methodology **6**: 88-96.
- Hasle, G. R. (1965). *Nitzschia* and *Flagilariopsis* species studied in the light and electron microscopes Vol II. The group *Pseudo-nitzschia*. Oslo, Universitetsforl. **no. 18**: 45 s., 17 pl.

- Hasle, G. R. (1994). "*Pseudo-nitzschia* as a genus distinct from *Nitzschia* (Bacillariophyceae)." *Journal of Phycology* **30**(6): 1036-1039.
- Hasle, G. R. (1995). "*Pseudo-nitzschia pungens* and *P. multiseriata* (Bacillariophyceae) - Nomenclatural history, morphology, and distribution." *Journal of Phycology* **31**(3): 428-435.
- Hasle, G. R. (2002). "Are most of the domoic acid-producing species of the diatom genus *Pseudo-nitzschia* cosmopolites?" *Harmful Algae* **1**(2): 137-146.
- Hasle, G. R., C. B. Lange and E. E. Syvertsen (1996). "A review of *Pseudo-nitzschia*, with special reference to the Skagerrak, North Atlantic, and adjacent waters." *Helgolander Meeresuntersuchungen* **50**(2): 131-175.
- Hasle, G. R. and N. Lundholm (2005). "*Pseudo-nitzschia seriata* f. *obtusa* (Bacillariophyceae) raised in rank based on morphological, phylogenetic and distributional data." *Phycologia* **44**(6): 608-619.
- Hasle, G. R. and E. E. Syvertsen (1997). Marine diatoms. In: Tomas C. R.: Identifying marine diatoms and dinoflagellates. San Diego, Academic Press: 5–385.
- Heck, K. L., G. Vanbelle and D. Simberloff (1975). "Explicit calculation of rarefaction diversity measurement and determination of sufficient sample size " *Ecology* **56**(6): 1459-1461.
- Hoppenrath, M., M. Elbrächter and G. Drebes (2009). Marine phytoplankton : selected microphytoplankton species from the North Sea around Helgoland and Sylt. Stittgart, E. Schweizerbart'sche Verlagsbuch.: 264.
- Hui, J. A. (1996). "Diatoms from the surface sediments of the Skagerrak and the Kattegat and their relationship to the spatial changes of environmental variables." *Journal of Biogeography* **23**(2): 129-137.
- Johnsen, T. M., W. Eikrem, C. D. Olseng, K. E. Tollefsen and V. Bjerknes (2010). "*Prymnesium parvum*: the Norwegian experience." *Journal of the American Water Resources Association* **46**(1): 6-13.
- Jones, K. J., P. Ayres, A. M. Bullock, R. J. Roberts and P. Tett (1982). "A red tide of *Gyrodinium aureolum* in sea lochs of the Firth of Clyde and associated mortality of pond-reared salmon." *Journal of the Marine Biological Association of the United Kingdom* **62**(4): 771-782.
- Karlson, B., C. K. Cusack and E. Bresnan (2010). IOC Manual and Guides. Microscopic and molecular methods for quantitative phytoplankton analysis. 55. UNESCO. Paris: 110.
- Kautsky, H., W. Appel and H. Amann (1960). "Chlorophyll fluorescence and Kohlensäureassimilation .13. Die fluoreszenzkurve und die Photochemie der pflanze." *Biochemische Zeitschrift* **332**(3): 277-292.

- Kirk, J. T. O. (1994). *Light and Photosynthesis in Aquatic Ecosystems*. Cambridge, Cambridge University Press.
- Lundholm, N., P. Andersen, K. Jorgensen, B. R. Thorbjornsen, A. Cembella and B. Krock (2005). "Domoic acid in Danish blue mussels due to a bloom of *Pseudo-nitzschia seriata*." *Harmful Algae News* **29**: 8-10.
- Lundholm, N., G. R. Hasle, G. A. Fryxell and P. E. Hargraves (2002). "Morphology, phylogeny and taxonomy of species within the *Pseudo-nitzschia americana* complex (Bacillariophyceae) with descriptions of two new species, *Pseudo-nitzschia brasiliiana* and *Pseudo-nitzschia linea*." *Phycologia* **41**(5): 480-497.
- Lundholm, N. and O. Moestrup (2002). "The marine diatom *Pseudo-nitzschia galaxiae* sp nov (Bacillariophyceae): morphology and phylogenetic relationships." *Phycologia* **41**(6): 594-605.
- Lundholm, N., O. Moestrup, G. R. Hasle and K. Hoef-Emden (2003). "A study of the *Pseudo-nitzschia pseudodelicatissima/cuspidata* complex (Bacillariophyceae): What is *P. pseudodelicatissima*?" *Journal of Phycology* **39**(4): 797-813.
- Lundholm, N., O. Moestrup, Y. Kotaki, K. Hoef-Emden, C. Scholin and P. Miller (2006). "Inter- and intraspecific variation of the *Pseudo-nitzschia delicatissima* complex (Bacillariophyceae) illustrated by rRNA probes, morphological data and phylogenetic analyses." *Journal of Phycology* **42**(2): 464-481.
- Lundholm, N., O. Moestrup, C. Scholin and P. Miller (2003). "Genetic variation of *Pseudo-nitzschia* cf. *delicatissima* studied using molecular probes." *Journal of Eukaryotic Microbiology* **50**(2): 40A.
- Lundholm, N. and Ø. Moestrup (2006). *The Biogeography of Harmful Algae. Ecology of Harmful Algae*. E. Granéli and J. T. Turner, Springer Berlin Heidelberg. **189**: 23-35.
- Lundholm, N. and Ø. Moestrup. (2007). "IOC Reference List of Toxic *Pseudo-nitzschia* species." from www.bi.kv.dk/IOC/group1.asp.
- Mann, K. H. and J. R. N. Lazier (1991). *Dynamics of marine ecosystems: biological-physical interactions in the oceans*. Boston, Blackwell Scientific Publications: XI, 466.
- Martin, J. L., K. Haya, L. E. Burrige and D. J. Wildish (1990). "*Nitzschia pseudodelicatissima* - a source of Domoic Acid in the Bay of Fundy, eastern Canada." *Marine Ecology-Progress Series* **67**(2): 177-182.
- Moschandreu, K. K., D. Papaefthimiou, P. Katikou, E. Kalopesa, A. Panou and G. Nikolaidis (2010). "Morphology, phylogeny and toxin analysis of *Pseudo-nitzschia pseudodelicatissima* (Bacillariophyceae) isolated from the Thermaikos Gulf, Greece." *Phycologia* **49**(3): 260-273.
- Naustvoll, L., E. Gustad and M. Kleiven (2011) "Overvåkning av mikroalger langs norskysten." *Kyst, Havforsningsrapporten*, 47-50.

- Nezan, E., E. Antoine, L. Fiant, Z. Amzil and C. Billard (2006). " Identification of *Pseudonitzschia australis* and *P. multiseriis* in the Bay of Seine. Was there a relation to presence of domoic acid in king scallops in autumn 2004? ." *Harmful Algae News* **31**: 1-3.
- Oksanen Jari, F. Guillaume Blanchet, Roeland Kindt, Pierre Legendre, R. B. O'Hara, Gavin L. Simpson, Peter Solymos, M. H. H. Stevens and H. Wagner (2010). *vegan*: Community Ecology Package. R package version 1.17-5. <http://CRAN.R-project.org/package=vegan>
- Paasche, E. (1975). "The influence of salinity on the growth of some plankton diatoms from brackish water." *Norwegian Journal of Botany* **22**(3): 209-215.
- Philippart, C. J. M. (2007). "Impacts of climate change on European marine and coastal environments." European Science Foundation. Marine Board Position Paper 9: 83.
- Proshkina-Lavrenko, A. I. (1955). *Diamtomplankton of the Black Sea*. Moskva-Leningrad, Akademy Nauk SSSR.
- Quijano-Scheggia, I. S., E. Garces, N. Lundholm, O. Moestrup, K. Andree and J. Campi (2009). "Morphology, physiology, molecular phylogeny and sexual compatibility of the cryptic *Pseudo-nitzschia delicatissima* complex (Bacillariophyta), including the description of *P. arenysensis* sp nov." *Phycologia* **48**(6): 492-509.
- Rhodes, L. L. (1998). "Identification of potentially toxic *Pseudo-nitzschia* (Bacillariophyceae) in New Zealand coastal waters, using lectins." *New Zealand Journal of Marine and Freshwater Research* **32**(4): 537-544.
- Rivera, R. P. (1985). "Las especies del genero *Nitzschia* Hassall, seccion *Pseudonitzschia* (Bacillariophyceae), en las aguas marinas chilenas." *Gayana Botanica* **42**: 9-38.
- Round, F. E., R. M. Crawford and D. G. Mann (1990). *The diatoms: biology & morphology of the genera*. Cambridge, Cambridge University Press: 747.
- Scholin, C. A., F. Gulland, G. J. Doucette, S. Benson, M. Busman, F. P. Chavez, J. Cordaro, R. DeLong, A. De Vogelaere, J. Harvey, M. Haulena, K. Lefebvre, T. Lipscomb, S. Loscutoff, L. J. Lowenstine, R. Marin, P. E. Miller, W. A. McLellan, P. D. R. Moeller, C. L. Powell, T. Rowles, P. Silvagni, M. Silver, T. Spraker, V. Trainer and F. M. Van Dolah (2000). "Mortality of sea lions along the central California coast linked to a toxic diatom bloom." *Nature* **403**(6765): 80-84.
- Sierra Beltran, A., M. Palafox-Uribe, J. Grajales-Montiel, A. Cruz-Villacorta and J. L. Ochoa (1997). "Sea bird mortality at Cabo San Lucas, Mexico: evidence that toxic diatom blooms are spreading." *Toxicon* **35**(3): 447-453.
- Skov, J., N. Lundholm, O. Moestrup and J. Larsen (1999). "Potentially Toxic Phytoplankton. 4. The diatom genus *Pseudo-nitzschia* (Diatomophyceae/Bacillariophyceae)." *ICES Identification Leaflets for Plankton* **185**: 1-8.

- Smith, J. C., R. Cormier, J. Worms, C. J. Bird, M. A. Quilliam, R. Pocklington, R. Angus and L. Hanic (1990). Toxic blooms of the domoic acid containing diatom *Nitzschia-pungens* in the Cardigan River Prince Edward Island Canada in 1988: 227-232.
- Smith, J. C., J. L. McLachlan, P. G. Cormier, K. E. Pauley and N. Bouchard (1993). "Growth and domoic acid production and retention by *Nitzschia-pungens* forma *multiseries* at low-temperatures." Toxic Phytoplankton Blooms in the Sea **3**: 631-636.
- Svansson, A. (1975). Physical and chemical oceanography of Skagerrak and Kattegat, Fishery board of Sweden. Institute for Marine research. Report nr. 1: 88.
- Sætre, R. (2007). The Norwegian coastal current: oceanography and climate. Trondheim, Institute of Marine Research: 159.
- Tangen, K. and E. Dahl (1999). Harmful phytoplankton in Norwegian waters - an overview. Proceeding International Seminar on Application of Seawatch Indonesia Information System for Indonesian Marine Resources Development, BPPT Jakarta.
- Thronsen, J. (1978). Preservation and storage. In: Sournia A (ed.): Phytoplankton manual. UNESCO Monogr. Oceanogr. Method. **UNESCO. 6::** 69-74.
- Thronsen, J., G. R. Hasle and K. Tangen (2007). Phytoplankton of Norwegian Coastal Waters. Oslo, Almatel Forlag AS: 343.
- Tomas, C. R., Ed. (1996). Identifying marine diatoms and dinoflagellates. San Diego, Calif., Academic Press, Inc. 598.
- Tomas, C. R., Ed. (1997). Identifying marine phytoplankton. San Diego Academic Press. 858.
- Trainer, V. L., B. M. Hickey and R. A. Horner (2002). "Biological and Physical Dynamics of Domoic Acid Production off the Washington Coast." Limnology and Oceanography **47(5)**: 1438-1446.
- Underdal, B., O. M. Skulberg, E. Dahl and T. Aune (1989). "Disastrous bloom of *Chrysochromulina polylepis* (Prymnesiophyceae) in Norwegian Coastal Waters 1988 - mortality in marine biota." Ambio **18(5)**: 265-270.
- Utermöhl, H. (1958). "Zur vervollkommnung der quantitativen phytoplankton-methodik. Mitt. Int. Ver. Theo. Angew." Limnologia **9**: 1-38.
- Vrieling, E. G., R. P. T. Koeman, C. A. Scholin, P. Scheerman, L. Peperzak, M. Veenhuis and W. W. C. Gieskes (1996). "Identification of a domoic acid-producing *Pseudo-nitzschia* species (Bacillariophyceae) in the Dutch Wadden sea with electron microscopy and molecular probes." European Journal of Phycology **31(4)**: 333-340.
- Walday, M., J. Gitmark, L. Naustvoll, K. Horling, J. R. Selvik and S. Kai (2010). Overvåkning av Ytre Oslofjord 2009. Årsrapport, NIVA, Havforskningsinstituttet, Fagrådet for Ytre Oslofjord, Klima og forurensningsdirektoratet: 58.

Wiull, G. (1948). The phytoplankton of the Oslo fjord in the spring of 1938. Oslo, Nytt magasin for naturvidenskapene: 23.

Wright, J. L. C., R. K. Boyd, A. S. W. Defreitas, M. Falk, R. A. Foxall, W. D. Jamieson, M. V. Laycock, A. W. McCulloch, A. G. McInnes, P. Odense, V. P. Pathak, M. A. Quilliam, M. A. Ragan, P. G. Sim, P. Thibault, J. A. Walter, M. Gilgan, D. J. A. Richard and D. Dewar (1989). "Identification of domoic acid, a neuroexcitatory amino-acid, in toxic mussels from eastern Prince-Edward-Island." Canadian Journal of Chemistry-*Revue Canadienne De Chimie* **67**(3): 481-490.

Internet websites:

<http://algeinfo.imr.no/>

<http://www.bvuf.se>

<http://www.thefullwiki.org/>

<http://www.marinespecies.org/HAB/>

http://www.smhi.se/oceanografi/oce_info_data/plankton_checklist/ssshome.htm